

# **Molecular characterization of the UV-response in *Caenorhabditis elegans***

Inaugural-Dissertation

zur

Erlangung des Doktorgrades

der Mathematisch-Naturwissenschaftlichen Fakultät

der Universität zu Köln

vorgelegt von

Stefanie Wolters

aus Leverkusen

Köln, 2013

Referee / Gutachter: Dr. Björn Schumacher

Institut für Genetik, Universität zu Köln

Referee / Gutachter: Prof. Dr. Thorsten Hoppe

Institut für Genetik, Universität zu Köln

Chairman / Vorsitzender: Prof. Dr. Günter Schwarz

Institut für Biochemie, Universität zu Köln

Tag der mündlichen Prüfung: 17. Oktober 2013

The work described in this dissertation was conducted from May 2009 to August 2013 under supervision of Dr. Björn Schumacher at the Institute for Genetics, University of Cologne, Zùlpicher StraÙe 47a, D-50674 Cologne, Germany.

Die Arbeiten, die in dieser Dissertation beschrieben sind, wurden durchgeföhrt zwischen Mai 2009 und August 2013 unter der Anleitung von Dr. Björn Schumacher am Institut für Genetik der Universität zu Köln, Zùlpicher StraÙe 47a, D-50674 Köln, Deutschland.

Parts of this work have been published:

Teile dieser Arbeit wurden bereits veröffentlicht:

Stefanie Wolters and Björn Schumacher

**Genome maintenance and transcription integrity in aging and disease**

Front. Genet., 25 Februar 2013 | doi: 10.3389/fgene.2013.00019

Parts of this work have been submitted for publication:

Teile dieser Arbeit wurden als Manuskript eingereicht:

Stefanie Wolters, Maria A. Ermolaeva, Jeremy S. Bickel, Jaclyn M. Fingerhut, Jayshree Khanikar, Raymond C. Chan and Björn Schumacher

**BRC-1/BRD-1 inactivation suppresses genome instability during replication blockage in *C. elegans smc-5* mutants**

Genetics, 2014

# Table of Contents

<b>I</b>	<b>SUMMARY</b> .....	<b>6</b>
<b>II</b>	<b>INTRODUCTION</b> .....	<b>8</b>
2.1	<i>C. ELEGANS AS A MODEL ORGANISM FOR STUDIES ON DNA REPAIR</i> .....	9
2.2	DOUBLE STRAND BREAK REPAIR.....	13
2.2.1	<i>Homologous Recombination Repair</i> .....	15
2.2.2	<i>Non-Homologous End Joining</i> .....	17
2.3	INTERSTRAND CROSSLINK REPAIR .....	18
2.4	NUCLEOTIDE EXCISION REPAIR.....	18
2.5	TRANSLSION SYNTHESIS.....	21
<b>III</b>	<b>BRC-1/BRD-1 INACTIVATION SUPPRESSES GENOME INSTABILITY DURING REPLICATION BLOCKAGE IN SMC-5 MUTANTS</b> .....	<b>23</b>
3.1	INTRODUCTION.....	23
3.1.1	<i>Discovery of a novel radiation-sensitive gene</i> .....	23
3.1.2	<i>The Smc family</i> .....	23
3.1.3	<i>The subunits of the Smc5/6 complex</i> .....	24
3.1.4	<i>Characteristics of the Smc5/6 complex</i> .....	25
3.2	RESULTS .....	27
3.2.1	<i>Screening for UV-sensitive alleles in L1 larvae</i> .....	27
3.2.2	<i>Identification of a novel xpg-1 allele is a proof of concept for the screening method</i> .....	30
3.2.3	<i>smc-5 is required for resistance to UV-induced DNA lesions in the C. elegans germline</i> .....	31
3.2.4	<i>smc-5 is dispensable for the repair of UV-induced lesions</i> .....	36
3.2.5	<i>SMC-5 functions in parallel to POLH-1-mediated TLS</i> .....	38
3.2.6	<i>SMC-5 is required when replication fork progression is impaired</i> .....	42
3.2.7	<i>BRC-1/BRD-1 mutations suppress defects in smc-5 activity</i> .....	44
3.2.8	<i>Rescue of defects of the smc-5 mutant by suppression of BRC-1/BRD-1 complex is partially mediated by POLH-1</i> .....	45
3.3	DISCUSSION .....	49
3.3.1	<i>Landscape of EMS-induced mutations</i> .....	49
3.3.2	<i>The ATPase domain of SMC-5 is essential for UV-resistance</i> .....	49
3.3.3	<i>The mutagenicity of DNA repair pathways</i> .....	50
3.3.4	<i>Restoring replication stress resistance in the absence of SMC-5/6 complex</i> .....	53
<b>IV</b>	<b>ROLE OF MICRORNAS IN THE UV-RESPONSE OF YOUNG C. ELEGANS LARVAE</b> .....	<b>57</b>

4.1	INTRODUCTION .....	57
4.1.1	<i>miRNA synthesis</i> .....	58
4.1.2	<i>miRNA maturation</i> .....	58
4.1.3	<i>Posttranscriptional gene silencing</i> .....	60
4.1.4	<i>miRNA classification</i> .....	61
4.1.5	<i>Studying miRNAs</i> .....	62
4.1.6	<i>Aim of the study</i> .....	65
4.2	RESULTS .....	66
4.2.1	<i>Establishment of a deep sequencing approach to analyze the miRNA profile upon UV irradiation</i> .....	66
4.2.2	<i>Sequencing reveals regulation of small RNAs after irradiation with UV light.</i> .....	68
4.2.3	<i>Investigation of UV-dose-dependency and timing of the miRNA regulation.</i> .....	72
4.2.4	<i>let-7 and lin-4, mediators of larval transitions, are differentially expressed after UV irradiation.</i> .....	74
4.2.5	<i>mRNA target prediction of miRNAs with altered expression after UV irradiation.</i> .....	81
4.3	DISCUSSION .....	84
4.3.1	<i>Establishment of sequencing-based screening for UV-regulated miRNAs</i> .....	84
4.3.2	<i>lin-4 expression is repressed upon UV irradiation independently from DAF-16.</i> .....	84
4.3.3	<i>miRNAs associated with L1 diapause state are induced upon UV-treatment.</i> .....	85
4.3.4	<i>Small RNA sequencing indicates UV-dependent regulation of a set of miRNAs</i> .....	87
4.3.5	<i>let-7 is downregulated in response to UV irradiation</i> .....	88
4.3.6	<i>UV-responsive miRNAs are predicted to fine-tune growth, development and MAPK signaling</i> .....	90
<b>V</b>	<b>MATERIAL &amp; METHODS</b> .....	<b>92</b>
5.1	<i>C. ELEGANS CULTURE MAINTENANCE</i> .....	92
5.2	SYNCHRONIZING WORMS.....	93
5.3	GENOTYPING OF WORM STRAINS.....	93
5.4	QPCR EXPRESSION ANALYSIS .....	95
5.4.1	<i>RNA preparation</i> .....	95
5.4.2	<i>Quantitative real-time PCR</i> .....	95
5.5	ISOLATION OF GENOMIC DNA .....	100
5.6	GFP REPORTER STRAIN ANALYSIS.....	101
5.7	IMMUNOSTAINING AND MICROSCOPY.....	101
5.8	DEVELOPMENTAL STAGING ASSAY.....	101
5.9	SCREENING FOR NOVEL UV-SENSITIVE <i>C. ELEGANS</i> STRAINS .....	102
5.9.1	<i>EMS mutagenesis</i> .....	102
5.9.2	<i>Screening and selection of worms</i> .....	102
5.9.3	<i>SNP mapping of novel UV-sensitive alleles (Davis et al. 2005)</i> .....	102

5.9.4	<i>Whole genome sequencing</i> .....	104
5.10	EGG-LAYING AND HATCHING RATE .....	104
5.11	GERMLINE DEVELOPMENT ASSAY .....	104
5.12	HU TREATMENT.....	104
5.13	RNAI-MEDIATED GENE KNOCKDOWN .....	105
5.14	GENERATION OF MALES FOR CROSSING .....	105
5.15	SMALL RNA SEQUENCING AND BIOINFORMATICAL ANALYSIS .....	106
5.15.1	<i>small RNA sequencing</i> .....	106
5.15.2	<i>Data analysis</i> .....	106
5.16	CPD REPAIR ASSAY USING SLOTBLOT .....	106
5.17	ANTIBODIES USED .....	107
5.18	GROWTH MEDIA & SOLUTIONS .....	107
5.18.1	<i>Single worm lysis buffer</i> .....	107
5.18.2	<i>M9 buffer</i> .....	107
5.18.3	<i>NGM plates</i> .....	108
5.18.4	<i>RNAi plates</i> .....	108
5.18.5	<i>2x Freezing buffer</i> .....	108
5.18.6	<i>2x Bleaching solution</i> .....	108
5.18.7	<i>LB</i> .....	109
5.18.8	<i>LB-agar plates</i> .....	109
5.18.9	<i>PBS</i> .....	109
5.18.10	<i>50x TAE</i> .....	109
5.18.11	<i>TE buffer</i> .....	109
5.18.12	<i>0.5M EDTA</i> .....	110
<b>VI</b>	<b>LIST OF ABBREVIATIONS</b> .....	<b>110</b>
<b>VII</b>	<b>ACKNOWLEDGEMENTS</b> .....	<b>113</b>
<b>VIII</b>	<b>REFERENCES</b> .....	<b>113</b>

## I Summary

The Structural Maintenance of Chromosomes (SMC) proteins form distinct complexes that maintain genome stability during chromosome segregation, homologous recombination (HR), and DNA replication. Using a forward genetic screen, we identified two alleles of *smc-5* that exacerbate UV-sensitivity in *C. elegans*. Germ cells of *smc-5* defective animals show reduced proliferation, sensitivity to perturbed replication and accumulation of RAD-51 foci that indicate the activation of HR. Mutations in the translesion synthesis polymerase *polh-1* act synergistically with *smc-5* mutations in provoking genome instability after UV-induced DNA damage. In contrast, the DNA damage accumulation and UV-sensitivity in *smc-5* mutant strains are suppressed by mutations in the *C. elegans* BRCA1/BARD1 homologues, *brc-1* and *brd-1*. We propose that SMC-5/6 promotes replication fork stability and facilitates recombination-dependent repair when the BRC-1/BRD-1 complex initiates HR at stalled replication forks. Our data suggest that BRC-1/BRD-1 can both, promote and antagonize genome stability depending on whether HR is initiated during DSB repair or during replication stalling.

In addition, we characterized the pool of small regulatory RNAs that respond to UV irradiation in young *C. elegans*. Deep sequencing identified miRNAs that were regulated differentially after treatment with UV light and revealed novel miRNAs. We validated upregulation of *mir-2214\**, *mir-235*, *mir-71* and *mir-238* as well as suppression of *mir-1830*, *let-7*, *mir-2211*, *mir-48* and *lin-4*. However, analysis of mutants and GFP-reporter strains indicated that *lin-4* and *let-7* are dispensable for resistance to UV and that promoter activity is not changed after irradiation. Combining literature research and bioinformatical approaches we found that UV-regulated miRNAs are associated with growth and development. Also, we provide evidence that miRNAs alter MAPK kinase signaling, control nucleotide excision repair and the proteasome in response to UV irradiation.

## I Zusammenfassung

Proteine der Familie “Structural Maintenance of Chromosomes” formen spezifische Komplexe, welche während der Segregation von Chromosomen, Homologer Rekombination (HR) und DNA Replikation für genomische Stabilität essentiell sind. Mit Hilfe eines genetischen Screenings haben wir zwei neue Allele von *smc-5* entdeckt, die *C. elegans* sensitiv gegenüber UV-Bestrahlung machen. Die Keimzellen dieser *smc-5*-Mutanten weisen verringerte Proliferationsraten, Sensitivität gegenüber Replikationsstörungen, sowie eine erhöhte Anzahl von RAD-51 foci auf, welche auf die Aktivierung von HR hinweisen. UV-induzierte Läsionen der DNA können von der DNA Polymerase POLH-1 überlesen werden. Die Kombination von Mutationen in *polh-1* mit *smc-5* Mutationen wirkt sich synergistisch auf genomische Instabilität in Folge von UV-induzierten DNA-Schäden aus. Im Gegensatz dazu unterdrücken Mutationen der *C. elegans* Homologe des BRCA1/BARD1 Komplex, *brc-1* und *brd-1*, die Akkumulation von DNA Schäden sowie die UV-Sensitivität von *smc-5* Mutanten. Unsere Daten deuten darauf hin, dass der SMC-5/6 Komplex die Stabilität von Replikationsgabeln sichert und Rekombinations-abhängige Reparaturmechanismen fördert, wenn BRC-1/BRD-1 HR an blockierten Replikationsgabeln induziert.

Weiterhin haben wir die Gruppe der kleinen regulatorischen RNAs charakterisiert, welche nach UV-Bestrahlung differentielle Expression in jungen *C. elegans* Larven aufweisen. Mittels Deep-Sequencing konnten wir nicht nur Regulation von miRNAs feststellen, sondern waren auch in der Lage bislang unbekannte miRNAs zu identifizieren. In diesem Zusammenhang haben wir die Hochregulation von *mir-2214\**, *mir-235*, *mir-71* und *mir-238* sowie die Suppression von *mir-1830*, *let-7*, *mir-2211*, *mir-48* and *lin-4* validieren können. Nichtsdestotrotz konnten wir keine Abhängigkeit der UV-Resistenz von *let-7* oder *lin-4* feststellen. Ebenso haben wir auch keine Veränderung der Promotor-Aktivität, durch die Nutzung von Fluoreszenz-Reportern beider Gene feststellen können. Literaturrecherche in Verbindung mit bioinformatischer Analyse zeigte, dass miRNAs, welche nach UV-Bestrahlung veränderte Expression aufweisen, in Verbindung mit Wachstum und Entwicklungsprozessen stehen. Weiterhin deuten unsere Daten darauf hin, dass der MAPK Signalweg, die Nukleotid Exzisions Reparatur und das Proteasom unter der Kontrolle der UV-regulierten miRNAs stehen.

## II Introduction

**(modified from Wolters and Schumacher 2013)**

It was estimated that DNA damage occurs on the order of tens of thousands per genome on a daily basis (Lindahl and Nyberg 1972). Genotoxic insults can arise from a large variety of endogenous and exogenous sources (Figure II.1). Cellular metabolism can produce reactive oxygen species (ROS) and alkylating agents, while cells can be exposed to ultraviolet (UV) light, ionizing radiation (IR), and a variety of genotoxic chemicals (Loeb and Harris 2008). The type of lesion can vary widely and depends on the source of DNA damage. For example, ROS induces oxidative base modifications, IR typically leads to single- and double-strand breaks (SSB and DSB, respectively), DNA alkylation can lead to adduct and interstrand crosslink (ICL) formation, and UV light triggers the formation of thymidine dimers (Hurley 2002). The toxicity of DNA damage depends on the structural changes they inflict as well as the characteristics of the cell they occur in. Proliferating cells have a different repertoire of DNA repair pathways than quiescent cells and, therefore, the same lesion might have different effects in different tissues. In cycling cells, for instance, a single DSB is sufficient to impair chromosome segregation during mitosis and ICLs lead to replication fork collapse. For these reasons even a small number of DSBs and ICLs can be cytotoxic. In contrast, oxidative base modifications are generally less obstructive, while UV-induced cyclobutane pyrimidine dimers (CPDs) can be read through by specialized DNA polymerases and thus, can persist through replication, but pose an obstacle to transcription and lead to stalling of RNA polymerases (RNAPs).

Despite the toxic potential of DNA breaks, they are also needed for normal developmental and metabolic processes. Induction of DSBs is the basis for diversity of the immune system during V(D)J recombination in lymphocytes and allows generation of a enormous variety of antigen receptors (Bednarski and Sleckman 2012). Moreover, programmed DSBs and subsequent strand invasion into homologous sequences are the foundation for recombination to ensure biological diversity and are required for proper chromosome segregation during meiosis (Lemmens and Tijsterman 2011). Nevertheless, even deliberately introduced lesions are obstructive to cells if not sealed correctly.

Given the frequency and impact of DNA damage, highly sophisticated DNA repair systems have evolved. These systems recognize specific types of lesions and induce DNA damage signaling.

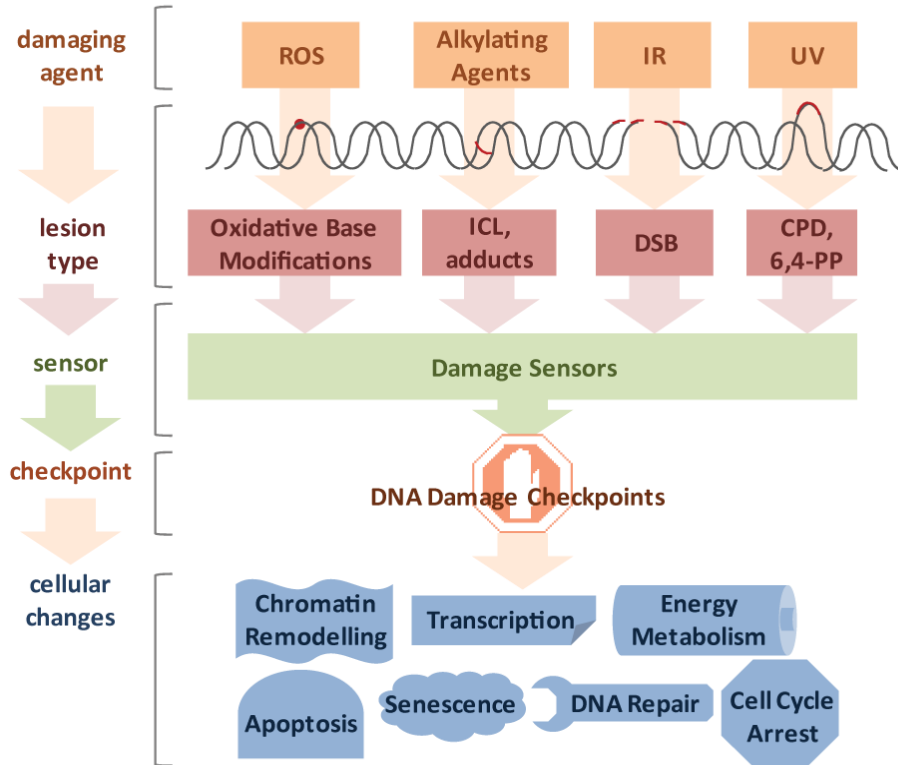


**Figure II.1. Diverse lesion types trigger DNA damage responses.**

DNA damage can be caused by various genotoxic agents, such as reactive oxygen species (ROS) produced during cellular metabolism, alkylating agents that find application in cancer therapy, ionizing irradiation (IR), which is used for radio therapy, or ultraviolet (UV) irradiation presenting a daily threat as it is contained in sunlight. The inflicted lesions are just as diverse, since ROS usually lead to base modifications; alkylating agents form adducts, while bifunctional alkylating agents crosslink DNA to form interstrand crosslinks (ICLs). IR typically induces double-strand breaks (DSBs), and UV light triggers the formation of cyclobutane pyrimidine dimers (CPDs) and 6,4-photoproducts (6,4-PPs). Cells have a repertoire to sense the different lesions and subsequently activate DNA damage checkpoint proteins. Ultimately, cells respond to the DNA damage by chromatin remodeling, modified transcription, fine-tuning of energy metabolism, cell cycle arrest, activation of DNA repair pathways and, in the case of irreparable damage load, induction of senescence or apoptosis.

(taken from Wolters and Schumacher, 2013)

Failure of DNA repair has been associated with severe disorders in humans, often associated with occurrence of cancer and/or premature aging.

## 2.1 *C. elegans* as a model organism for studies on DNA repair

*C. elegans* is especially suitable for characterization of DNA repair pathways because it is susceptible to genetic manipulation, has a short life cycle and produces self-fertilized progeny. Moreover, it is a multicellular organism that can also reproduce sexually, therefore being a good model for genetic experiments. Furthermore the whole genome is sequenced and the major DNA

repair machineries found in mammals are conserved (Boulton et al. 2002). A large number of mutant strains are available through well organized online databases (e. g. [www.wormbase.org](http://www.wormbase.org) and Caenorhabditis Genetics Center at the University of Minnesota). *In vivo* observation of fluorescence-tagged proteins and phenotypical analysis of germ cells is facilitated by transparency of the nematode. The developmental program of *C. elegans* is well characterized and invariable in the course of events (Goenzyz and Rose 2005). There are two sexes of *C. elegans*, hermaphrodites with XX genotype and males with XO genotype. Although the general body plan is the same for both sexes they can be easily distinguished by behavior and appearance (Herman 2006). Usually *C. elegans* are self-fertilizing hermaphrodites but under unfavorable conditions or by chance they might lose an X chromosome by non-disjunction mutation and produce males (0.1% in wildtype worms at standard laboratory conditions). Therefore increased abundance of males (referred to as *High Incidence of Males (him)* phenotype) is indicative of genomic instability of a worm strain and often seen for DNA repair mutants (e.g. *brc-1* mutant) (Lemmens and Tijsterman 2011).

In the fertilized embryo asynchronous cell divisions determine the cell fate. Already the first division gives rise to the germline precursor P1. At L1 stage, primordial germ cells Z2 and Z3, as well as somatic germline precursors Z1 and Z4 are formed. Before the end of L1 stage Z1 and Z4 give rise to two DTCs that provide the signal for proliferation of the germ cells (Hubbard and Greenstein 2005). When the egg is laid it contains already a majority of the cells that make up the adult animal (Clejan, Boerckel, and Ahmed 2006). An adult hermaphrodite has 959 somatic cells that are mainly post-mitotic (Herman 2006). In contrast, germ cells continue to divide throughout adulthood.

During lifecycle *C. elegans* passes through four larval stages (L1, L2, L3 and L4), each of them ending with molting to enter the next stage (Figure II.2 A) (Altun and Hall 2006). Within three days under optimal conditions it develops from egg to a reproducing adult. The total lifespan is about three weeks but could be much longer under unfavorable conditions when worms enter diapauses stage (Figure II.2 A). If worms hatch in the absence of food they arrest at L1 stage but resume development once food is available again. In the laboratory this feature of *C. elegans* is used to obtain synchronous populations. However, in response to stress, like high population density, starvation or high temperatures, worms enter dauer stage (P. J. Hu 2007). The decision for this alternative second molt occurs late in the L1 larval stage and is communicated via

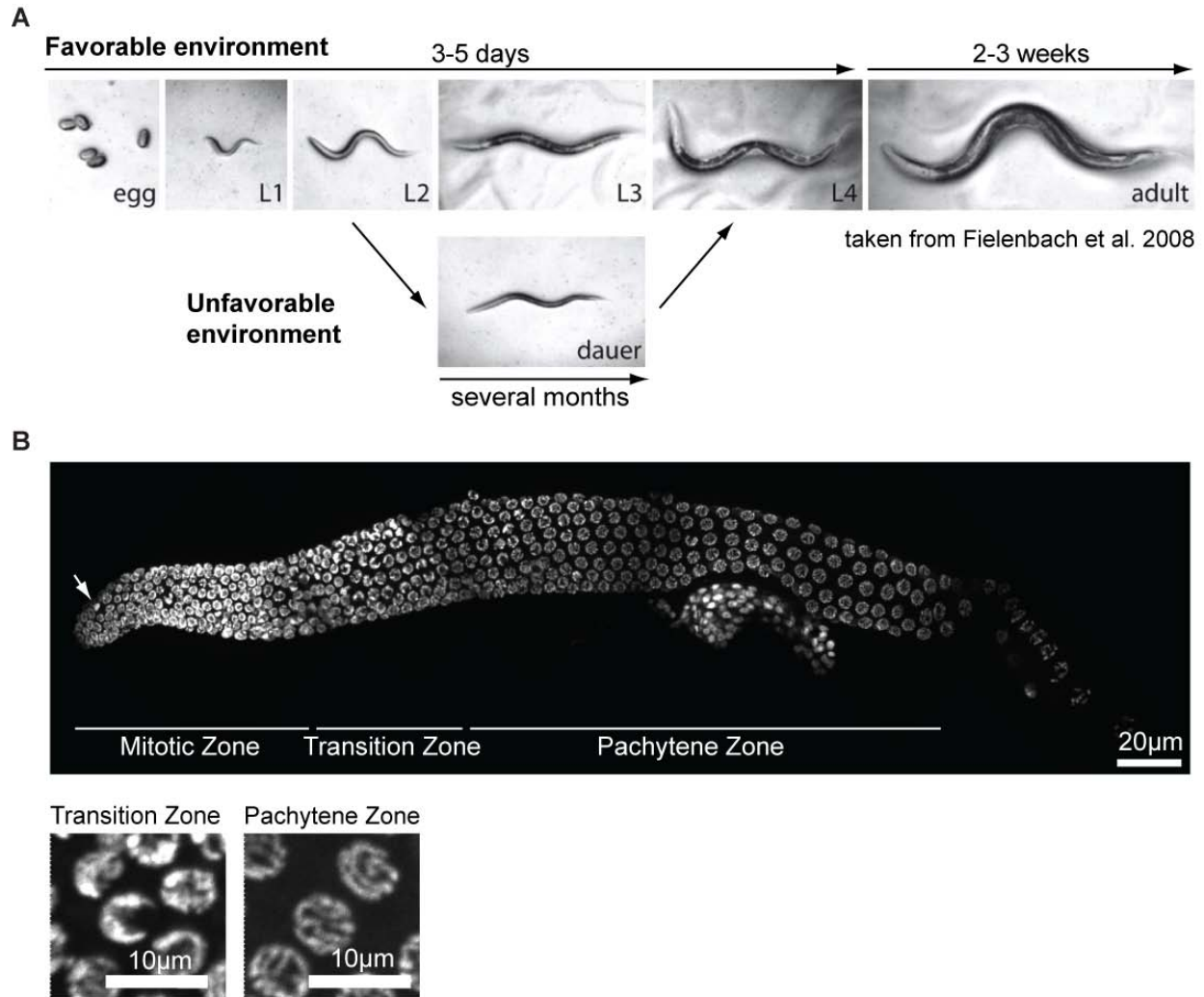


**Figure II.2 The model organism *Caenorhabditis elegans*.**

**A** *C. elegans* life cycle. In favorable environments worms develop from egg to reproducing adults within 3-5 days depending on the temperature. The adult lifespan is about 2-3 weeks. Under unfavorable conditions worms develop into an alternative larval stage called dauer. In this state they can outlast for several months and resume development once environmental conditions improve.

**B** DAPI staining of dissected hermaphrodite germline. The germline of *C. elegans* is a polar organ with mitotic cells at the distal end and nuclei progressing through meiosis towards the proximal end. Cells of each zone can be easily identified by their characteristic shape. While nuclei of the mitotic region have a uniform round shape with exception of few mitotic figures (indicated by an arrow), transition zone cells are crescent shaped. Once cells enter pachytene region, the DNA forms long strings followed by condensation into six bivalents at diplotene and diakinesis.

pheromones. Dauer stage worms differ from normal L3 larvae in their morphology (Figure II.2 A), metabolism and transcriptome and are highly stress-resistant to various kinds of agents and

conditions. Under current investigation is a third diapauses state, the adult reproductive diapauses, that enables fully developed worms to survive stressful conditions, for instance starvation or hypoxia, and delay reproduction (Angelo and Van Gilst 2009; Leiser et al. 2013).

The reproductive system of *C. elegans* consists of two U-shaped tubes at which proximal end oocytes get fertilized by passing the spermatheca and finally eggs are laid through the vulva at the ventral midline of the worms' body (Greenstein 2005; Altun and Hall 2006). Germ cells are organized in a syncytium where nuclei with incomplete borders are connected through an inner canal. The germline is a convenient organ to study DNA damage pathways because of its spatial separation of mitotic and meiotic cells (Figure II.2 B). Proliferation is mediated by the somatic distal tip cell (DTC) that determines a stem cell niche at the distal end of the gonad arm by secretion of pro-mitotic molecules (Kimble and Crittenden 2005). Through continuous proliferation at the distal end of the germline, nuclei move out of the area of influence of the DTC. This transition zone is marked by DNA condensation giving rise to crescent-shaped 4',6-diamidino-2-phenylindole (DAPI)-stained structures and entry into meiosis (Figure II.2 B) (leptotene and zygotene stage of prophase I). Nuclei at pachytene stage of meiosis have characteristic "bowl of spaghetti" morphology (Lints and Hall 2009). Cells in this region induce DSBs using topoisomerase VI-related *spo-11* to activate homologous recombination (HR) repair. One DSB per chromosome is repaired by crossover formation to ensure proper chromosome segregation in subsequent steps of meiosis and may lead to recombination of sequence information from the two homologous chromosomes. To maintain tissue homeostasis, cells at pachytene stage near the loop region undergo programmed cell death. In 1999 Gumienny et al. estimated that about one half of all germ cells die, possibly to nurse the surviving cells by providing cytoplasmic components (Gumienny, Lambie, Hartweg, Horvitz, & Hengartner, 1999). Corpses can be identified using DIC microscopy by their typical round and detached shape. In addition to tissue homeostasis, apoptosis of germ cells is also utilized to eliminate damaged cells, for instance upon DNA damage. Unlike pachytene cells, cells of the mitotic region are not capable of apoptosis but arrest cell cycle when encountering damaging insults (Stergiou, Doukoumetzidis, Sandoel, & Hengartner, 2007). DAPI staining of mitotic nuclei easily identifies arrested nuclei because in comparison to cycling cells they are heavily enlarged (Gartner, MacQueen, and Villeneuve 2004). In contrast, worms defective for checkpoint response do not arrest germ cells. In the loop region, nuclei enter diplotene stage where

chromosomes condense and then continue to diakinesis (Figure II.2 B). Here, the chromosomes are most condensed and form six discrete bivalents. In parallel the cytoplasmatic volume increases and oocyte maturation is completed before oocytes enter into the spermatheca. During accumulation of cytoplasm, oocytes are equipped with maternal molecules, which is why homozygous progeny of a heterozygous mother may show a less pronounced phenotype than expected (Hubbard and Greenstein 2005). After fertilization the embryo enters the uterus and is laid.

## 2.2 Double Strand Break Repair

As the presence of a DSB poses a major obstacle for further cell division a sophisticated network of DNA damage response (DDR) signaling is ignited (Ciccia and Elledge 2010). Genetic experiments that were performed in yeast nearly 25 years ago established that DNA damage checkpoints transiently halt cell cycle progression in the presence of genotoxic stress to assure that the repair is completed before cell division (Weinert and Hartwell 1989; Rowley, Hudson, and Young 1992). The recognition that DDR defects are causal for cancer development has sparked major research efforts employing model systems from yeast to mammals. The DNA damage checkpoint mechanisms turned out to be highly conserved throughout evolution. For instance, *C. elegans* has been used intensively for characterization and identification of known and new DSB-responsive molecules (Lemmens and Tijsterman 2011). Cells, however, not only respond by transient cell cycle arrest but also by inducing cellular senescence, thus permanently withdrawing from cell division. Dependent on the circumstances cells induce apoptosis upon DNA damage and, thus, no longer pose a threat to the organism (Harper and Elledge 2007). Intriguingly, the DDR not only impacts on regulators of cellular proliferation and cell death but impinges on a variety of cellular processes such as transcription, DNA repair, respiration, energy metabolism, chromatin remodeling, and others (Figure II.1) (Jackson and Bartek 2009).

In human cells the initial recognition of DSBs involves binding of the trimeric Mre11-Rad50-Nbs1 (MRN) complex to the broken DNA ends (Figure II.3) (Bartek and Lukas 2007). The MRN complex activates the PI3 kinase-like kinase ataxia telangiectasia mutated (ATM), which in turn phosphorylates a plethora of targets (Shiloh 2003). ATM targets include Mediator of DNA Damage Checkpoint 1 (MDC1) as well as the checkpoint kinase CHK2, which in turn activates p53. p53 then induces cell cycle arrest and, amid severe damage, apoptosis.

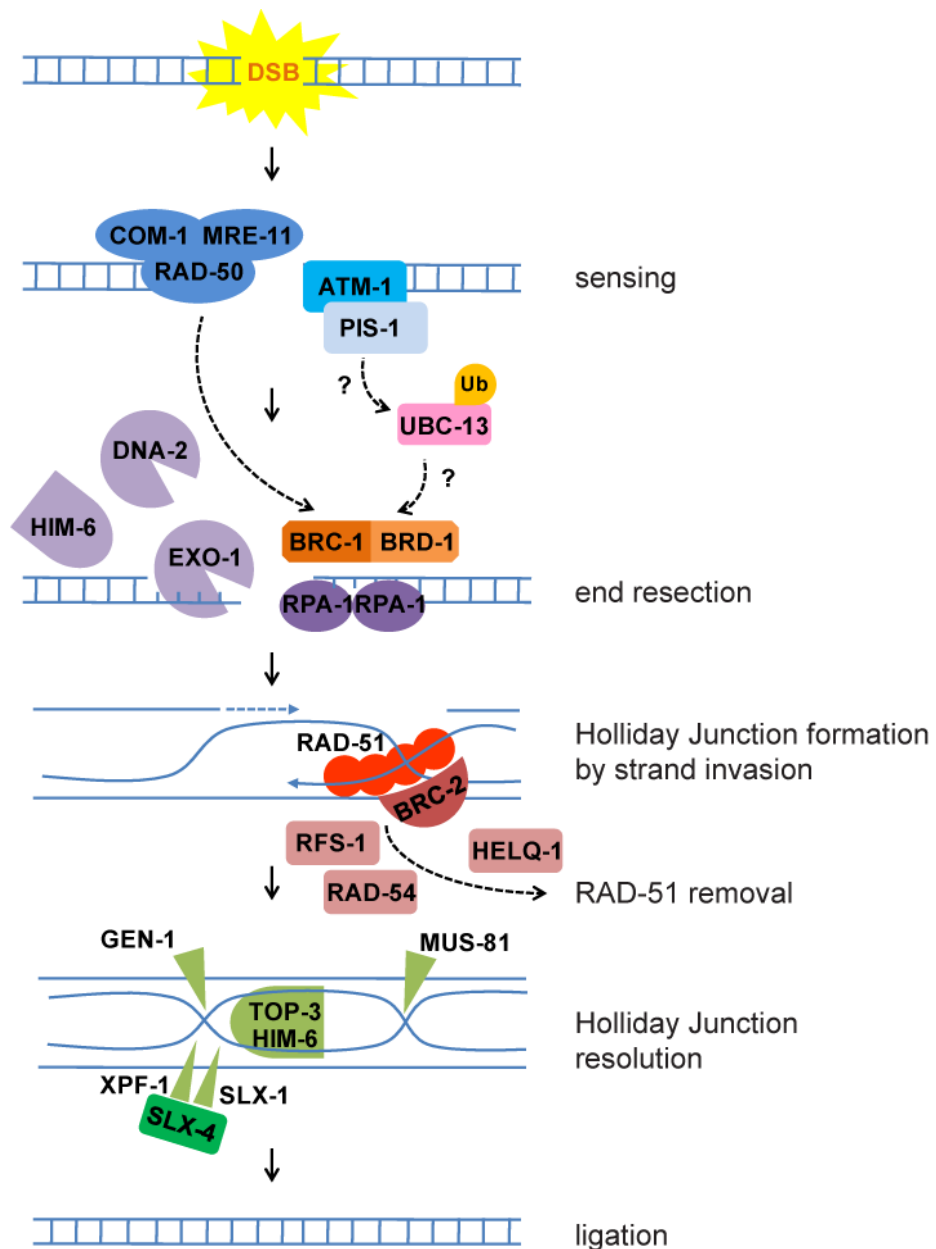


**Figure II.3 Homologous Recombination in *C. elegans*.**

DSBs are sensed by ATM kinase and MRN complex comprised of MRE-11, RAD-50 and COM-1, homolog of human NBS1. Subsequently, a number of repair factors are recruited and phosphorylated by ATM including MDC1 (the ortholog of which is PIS-1 in *C. elegans*). Studies in cell culture suggest that ubiquitination events mediated by UBC-13 lead to recruitment of BRC-1. BRC-1/BRD-1 mediates end resection together with the MRN complex, the nucleases EXO-1 and DNA-2, and the homolog of RecQ helicase, HIM-6. The single stranded DNA ends are protected by RPA-1. Next RAD-51, stabilized by BRC-2, induces strand invasion to a homologous DNA sequence. After induction of double Holliday Junction, RAD-51 is removed with the help of RFS-1, RAD-54 and HELQ-1. Holliday Junction resolution requires nucleases GEN-1, MUS-81 and SLX-4 that serves as a scaffold for SLX-1 and XPF-1. Furthermore helicase/topoisomerase complex HIM-6/TOP-3 promote dissolution. Finally the nicks are sealed to restore the intact DNA strands.

These key factors are highly conserved in *C. elegans*, like for example *cep-1* homologue of p53. While DNA damage checkpoint signaling halts the cell cycle, at least two distinct DSB repair machineries are activated depending on the phase of the cell cycle (Chapman, Taylor, and Boulton 2012). In S/G2 phase HR uses the sister chromatid as template for accurate repair, while during G1 non-homologous end joining (NHEJ) ligates the broken ends after end resection. Thereby NHEJ comprises a fast and efficient but error prone DNA repair method. However, for large parts of the genome the NHEJ-induced errors can be tolerated when genes are not affected. Since NHEJ is utilized when no sister chromatid is available, it is thought to function mainly in non-proliferating cells, like neurons (Jeppesen, Bohr, and Stevnsner 2011).

### **2.2.1 Homologous Recombination Repair**

After sensing of a DNA DSB by MRN complex and MDC1 phosphorylation by ATM, MDC1 recruits additional repair factors (Figure II.3). A well-known factor of HR repair is breast cancer type 1 susceptibility protein (BRCA1). Its recruitment requires ubiquitination events at the site of DSBs mediated by UBC13 E2, RNF8 and RNF168 E3 enzymes. Subsequently RAP80 binds to the ubiquitin chains and recruits BRCA1 (Huen, Sy, and Chen 2010; Rosen 2013). In how far these events are conserved in *C. elegans* should be studied in future because this organism lacks obvious homologues of RNF8 and RAP80. However, BRCA1 forms a heterodimer with BRCA1-associated RING domain protein 1 (BARD1). The RING domain classifies BRCA1 as an E3 ubiquitin ligase which enzymatic activity is potentiated by binding to BARD1 (Xia et al. 2003). Ubiquitination is a highly dynamic posttranslational modification of proteins to control diverse cellular processes, such as protein degradation, signal transduction and DNA repair (Fournane et al. 2012; Pinder, Attwood, and Dellaire 2013). Protein modification by ubiquitin requires at least three enzymes called E1, E2 and E3. First, E1 activates ubiquitin moieties, which are then transferred to E2 and finally, ubiquitin is conjugated to a lysine residue of the target protein with the help of an E3 ligase. BRCA1 has been shown to bind different E2 ubiquitin ligases through its RING domain (Christensen, Brzovic, and Klevit 2007). H2AX, H2A, CtIP and topoisomerase IIA (Lou, Minter-Dykhouse, and Chen 2005) are targets of BRCA1 in human cells, however, the functions of most of these interactions remain elusive (Huen, Sy, and Chen 2010). At its C-terminus BRCA1 has conserved BRCT, phosphopeptide-

binding domains. Interaction of BRCA1 with a number of DNA damage response factors is mediated through its BRCT domains. By binding different subsets of cofactors BRCA1 forms at least four distinct protein complexes that fulfill different functions (Huen, Sy, and Chen 2010; Rosen 2013). By now BRCA1 has been implicated in several processes during DNA repair. Through interaction with CtIP and the MRN complex BRCA1 promotes end resection at the site of a DSB (Figure II.3). The formation of single stranded stretches is crucial to make the DNA ends accessible and find a homologous template for repair (Lemmens and Tijsterman 2011). The 5'-3' DNA degradation is mediated redundantly by several genes in addition to BRCA1 complex. Experiments in yeast identified Mre11, Rad50, Exo1, Dna2 and Sgs1 (Bloom Syndrome helicase) (Huertas, 2010; Manfrini, Guerini, Citterio, Lucchini, & Longhese, 2010) as such resection factors. However, resection needs to be controlled. Therefore BRCA1 interaction with MRN is linked to the cell-cycle to ensure that end resection is only executed in S-phase in the presence of a homologous template. The DNA single stranded stretches are protected by replication protein A (RPA) until RAD51 protein forms nucleofilaments along the DNA to induce strand invasion. Nucleofilament formation and removal of RPA are mediated by BRCA2 (Martin et al. 2005; Petalcorin et al. 2007; Ward et al. 2007). Through strand exchange two Holliday Junctions are formed by invasion of the broken 3' end into the donor DNA to prime DNA synthesis. In *C. elegans* RAD-51 is removed from double stranded DNA redundantly by *helq-1* and *rfs-1* (Ward et al. 2010) (Figure II.3). Furthermore it was suggested that RAD-54 is important for nucleofilament removal because RAD-51 persists on the DNA in *C. elegans rad-54* mutants (Mets and Meyer 2009). Resolution of the Holliday Junction relies on a number of nucleases that are conserved from *C. elegans* to human, namely *gen-1* (Bailly et al. 2010), *mus-81* (Oh et al. 2008; Lemmens and Tijsterman 2011), *slx-4* that serves as a scaffold protein to direct *slx-1* and *xpf-1* nucleases and a helicase-topoisomerase complex (Saito et al. 2009) (Figure II.3). To facilitate homology search during HR, cohesins keep sister chromatids in close proximity to each other. Alternatively, the homologous chromosome may be used as template for repair. During meiosis DNA DSBs are intended because they are prerequisite for crossover formation and correct chromosome segregation. Outside meiosis crossovers are usually suppressed during HR repair of DSBs.

In the last few years HR has also been proven to be important to overcome replication fork barriers. During replication DNA polymerase may stall at obstacles arising from DNA secondary

structures (e.g. quadruplex DNA), protein-DNA complexes, intersections with other replication forks or the transcription machinery. Exogenous sources of replication fork stalling are DNA damage as well as inhibition of replication by nucleotide depletion (e.g. by hydroxyurea (HU) treatment). To cope with this potentially toxic insult the nascent strand needs to be protected, the fork needs to be stabilized and finally restarted, all of which is mediated by HR (Lambert et al. 2005). It was shown that BRCA1 and BRCA2 form foci specifically in S-phase in response to HU and UV irradiation (J. Chen et al. 1998). These foci colocalize with RAD51 (Huen, Sy, and Chen 2010) and can be easily detected by immunofluorescence or fluorescence-tagging of repair proteins. This is because DNA damage response signal spreads up to 1Mb up- and downstream to the initial DSB and forms therefore huge complexes at the site of damage (Costes et al. 2010). Nevertheless, excessive end resection and exaggerated spreading of the DNA damage response must be avoided. While BRCA1 complex has been shown to be important for end resection induction by RNF8 and RNF168 ubiquitination events, it also restricts resection via BRCC36 deubiquitination (Coleman and Greenberg 2011; Shao et al. 2009; J. Wu et al. 2012; Bartocci and Denchi 2013).

In parallel to DNA repair, cell cycle must be stopped transiently to give time for repair. It was suggested that BRCA1 triggers G2-M checkpoint through its promotion of DNA end resection. Furthermore it delays the onset of mitosis upon DSB recognition by control of intra-S checkpoint (B Xu, Kim St, and Kastan 2001; Bo Xu et al. 2002).

Taken together, HR is an error-free repair process of DSBs that is utilized in S- or G2-cell cycle phase when a homologous sequence is available and BRCA1 plays a crucial role in orchestrating HR at different steps.

### **2.2.2 Non-Homologous End Joining**

When no homologous chromosome is available, error-prone NHEJ is utilized to repair DSBs instead of HR. In *C. elegans* CKU-70/CKU-80 heterodimer senses DSBs, protects the broken ends and recruits LIG-4 ligase for sealing of the gap (Clejan, Boerckel, and Ahmed 2006; Lemmens and Tijsterman 2011).

Surprisingly, although HR and NHEJ are specifically repairing DSBs of the DNA, it was shown that they are not acting redundantly and may not compensate for each other in *C. elegans* (Clejan, Boerckel, and Ahmed 2006). While HR is primarily utilized during the fast

proliferations in young embryos and in the germline, NHEJ is important only later during embryogenesis and in non-dividing somatic cells. Therefore, knockdown of HR by *rad-54* or *rad-51* RNAi elicits germline radiation sensitivity whereas mutations in NHEJ factors, like *cku-80* and *lig-4*, do not. In contrast, NHEJ mutants display somatic defects and slow growth upon IR that are not found in HR-deficient worms. Moreover, genomic instability in the absence of RAD-54 in worms was shown to be partially rescued by *lig-4* mutation (Ryu, Kang, and Koo 2013), which could be explained by the variability in end resection, nucleotide addition and ligation process producing different NHEJ products even when starting from identical substrates (Lieber 2010).

Hallmarks of NHEJ deficiency in human are not only hypersensitivity to IR but also immunodeficiency as it is crucial for V(D)J recombination and class switch recombination (Lieber 2010).

### **2.3 Interstrand Crosslink Repair**

Like DSB repair, the employment of removal mechanisms of ICLs alters depending on cell cycle stage. During G1 the excision repair cross-complementation group 1–xeroderma pigmentosum group F (ERCC1–XPF) endonuclease initiates the ICL removal (Deans and West 2011). When ICLs are encountered by the replication fork a Fanconi anemia (FA) protein complex comprised of FANCA, -B, -C, -E, -F, -G, -L, and -M mono-ubiquitylates FANCD2 that interacts with DSB repair proteins including BRCA1, FANCD1/BRCA2, FANCI, and the MRN complex (Kee and D’Andrea 2010). BRCA1/FANCD2 and RAD51/FANCD2 complexes accumulate at the site of damage and form foci during S-phase of cell cycle. Subsequent repair is thought to be achieved by HR pathway (Taniguchi et al. 2002).

### **2.4 Nucleotide Excision Repair**

Different types of helix distorting lesions, like those inflicted by UV radiation of the sunlight, chemotherapeutics or cigarette smoke, can be removed by nucleotide excision repair (NER) (Lans and Vermeulen 2011). Mutations in NER underlie a variety of skin cancer predisposing and degenerative disorders (Cleaver, Lam, and Revet 2009). Mutations that affect the two distinct branches of NER are linked either to cancer susceptibility or to premature aging. Defects

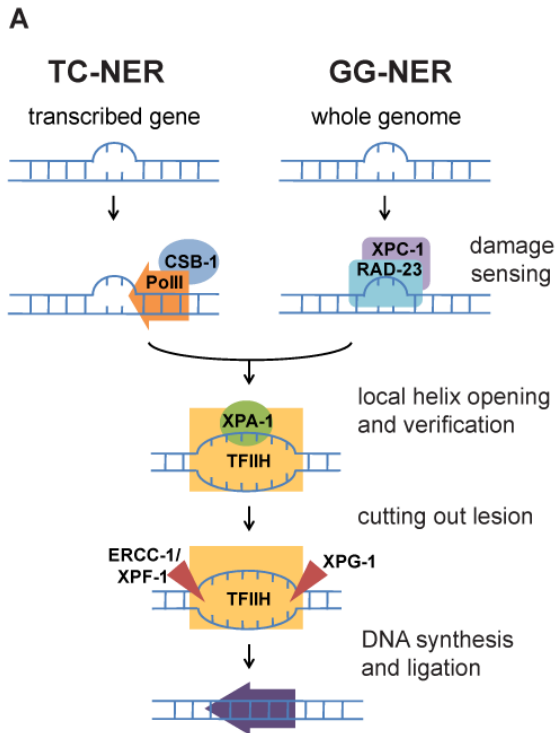


**Figure II.4 Mutations in GG-NER and TC-NER lead to embryonic lethality and developmental arrest, respectively.**

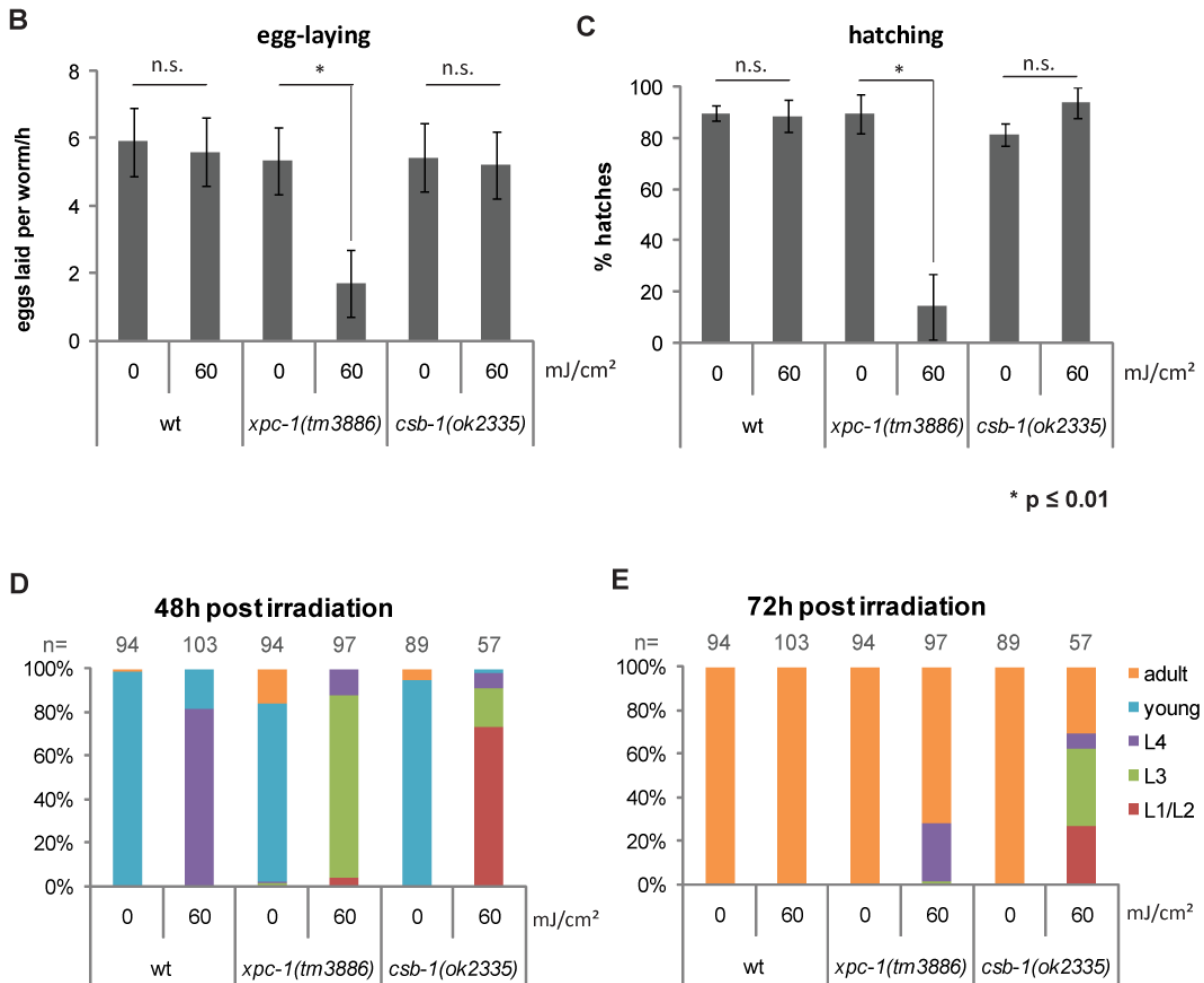
**A** NER pathway. After sensing transcription stalling by CSB-1 or bulky lesion sensing elsewhere in the genome by RAD-23/XPC-1, the helix is locally opened by TFIIH and the lesion is validated by XPA-1. The endonucleases ERCC-1/XPC-1 and XPG-1 cut the damaged strand to release an oligonucleotide containing the lesion. The DNA is restored by gap filling and ligation with the help of the replication machinery.

**B** Average number of eggs laid per hour, 24h post irradiation of L4 larvae.

**C** Percentage of worms hatched from eggs quantified in B.

**B and C** Error bars indicate standard deviation between three independent replicates. Asterisks denote p value  $\leq 0.01$  calculated applying two-tailed students T-Test.

**D and E** Percentage of larval stages 48h and 72h after irradiation at L1 stage, respectively. Number of worms used (n) for analysis is indicated at the top of the columns.



in the global genome (GG-)NER branch cause the skin cancer susceptibility syndrome Xeroderma pigmentosum (XP), while mutations affecting the transcription-coupled (TC-)NER branch lead to progeroid syndromes such as Cockayne syndrome (CS) that is characterized by postnatal growth retardation and accelerated aging but not cancer (Alan R Lehmann 2003). Hence, even in the absence of exogenous DNA damage NER is important for normal development, growth and tissue maintenance. The two branches of NER differ in their recognition of the lesion but funnel into the same pathway for processing and removal of the damage. The CSB protein is associated with RNAPII and, upon stalling at a lesion, recruits CSA and activates TC-NER. Outside of actively transcribed genes the UV-DDB ubiquitin complex and the trimeric XPC/hHR23/Centrin complex scan for lesions disrupting the helical structure known as GG-NER. Upon lesion sensing, the NER machinery is recruited including XPA and the 10-subunit transcription factor II H (TFIIH) that comprises XPB, XPD, and TTDA (p8). TFIIH locally unwinds the DNA and recruits XPG to the 3' side of the lesion, which in turn stabilizes binding of the XPF-ERCC1 heterodimer (also called XFE) 5' to the lesion. Both, XFE and XPG, are endonucleases that incise the damaged strand 25–30 nucleotides apart. The single-stranded stretch is coated by RPA before the gap is filled by DNA polymerases  $\delta$  and  $\epsilon$  that are recruited through RFC and PCNA. Finally, the nick is sealed by DNA ligase.

In *C. elegans* NER has been extensively studied and revealed conservation of most of the NER genes, such as *csb-1*, *rad-23/xpc-1* homologues of the mammalian TC-NER and GG-NER factors, respectively (Figure II.4A) (Lans et al. 2010; Lans and Vermeulen 2011). Although it remains unclear in how far *C. elegans* is exposed to UV light as a genotoxin in its natural habitat (Félix and Duveau 2012; Barriere and Felix 2006), worms might be exposed to normally occurring DNA damaging chemicals. Therefore, *C. elegans* relies on NER to repair these lesions. For examination of helix-distorting lesions in the laboratory, however, it is convenient to use UV irradiation of worms. UV light is divided into three wavelength ranges: UVA (320–400 nm), UVB (290–320 nm) and UVC (<290 nm). Sunlight filtered through the ozone layer is mostly composed of UVA and UVB. While it has been shown that UVC and UVB can induce CPDs and 6,4-photoproducts (6,4-PPs) directly by photoreaction of the DNA, UVA has also been implicated in radiation-mediated oxidative DNA damage (Ravanat, Douki, and Cadet 2001). Both types of DNA damage lead to bulky lesions in the DNA and a disruption of the helical structure. In the absence of helix-distorting lesion, *C. elegans* strains deficient in any of the NER

factors are phenotypically wildtype-like. However, upon UVB-irradiation, hallmarks of GG-NER and TC-NER deficiency are embryonic lethality (Figure II.4B and C) and developmental arrest (Figure II.4D and E), respectively. This suggests that GG-NER is acting mainly in the germline whereas TC-NER is employed in somatic cells. Worms mutant for factors of the common NER pathway or TC- and GG-NER double mutants arrest already at UV doses that do not harm mutants for TC-NER or GG-NER only. Hence, both pathways act synergistically, and soma and germline cells depend on the other NER branch if one is not functional (Lans et al. 2010; Lans and Vermeulen 2011).

## 2.5 Translesion synthesis

Alternatively to NER and HR, lesions in proliferating cells may be overcome by replicating over the damage to avoid replication fork stalling. Translesion polymerases are characterized by a more open active site compared to high fidelity DNA polymerases and therefore, are able to read over DNA lesions. Known translesion polymerases in vertebrates are Pol $\eta$ , Pol $\kappa$ , Pol $\iota$  and Rev1, of the Y-family of polymerases and Pol $\zeta$ , B-family member. The structure of the active site confers the lesion specificity of the different polymerases but is also the cause for the lack of proofreading activity. Because of this translesion synthesis (TLS) is considered as an error-prone DNA damage response. Pol $\eta$  is mutated in Xeroderma Pigmentosum Variant (XPV) disorder (Masutani et al. 1999) which is characterized by increased susceptibility to UV-induced carcinogenesis like NER-deficient patients (Alan R Lehmann et al. 2007). In line with the disease pattern, Pol $\eta$  is specific for UV-induced CPDs as well as some other lesions (Roerink et al. 2012). The *C. elegans* homologue of Pol $\eta$ , *polh-1* is crucial during the first rapid divisions in the embryo upon fertilization (Ohkumo et al. 2006; Roerink et al. 2012). While in the absence of DNA damaging insults, *polh-1* mutant worms are wildtype-like, embryos are extremely UV sensitive as measured by survival of progeny from UV-treated L4 larvae (Roerink et al. 2012). The early divisions of the *C. elegans* are fixed in their spatiotemporal progression and any deviation or delay from this pattern may be detrimental to the embryo. Therefore, it is very important to strictly control this process and prevent any delay. It was shown that embryos silence the checkpoint response with the help of POLH-1 by reading over lesions (Holway et al. 2006). In contrast to *polh-1* embryonic sensitivity, worms defective for *xpa-1*, an essential component of NER pathway (Figure II.4 A), are not sensitive. However, development of L1

larvae and also germ cell maturation mainly relies on NER whereas *polh-1* is dispensable (Roerink et al. 2012). Double mutants compromised for *xpa-1* and *polh-1* are even more sensitive to DNA damage than the respective single mutants, suggesting that they are acting in parallel pathways. Upon stalling of the replication fork at a lesion, TLS is mainly promoted by two posttranslational modification events. Mono-ubiquitination of PCNA homologue, PCN-1, (Alan R Lehmann et al. 2007) induces polymerase switching and POLH-1 is protected from degradation by SUMOylation (Kim and Michael 2008). In addition to UV- and cisplatin-sensitivity, it was reported that *polh-1* deficient worms are as sensitive to IR as *brc-1* (ortholog of human BRCA1) mutants. Yet, evidence is accumulating that sensitivity to IR is not caused by *polh-1* acting in HR, as suggested earlier, but is rather a consequence of IR-induced lesions other than DSB (McIlwraith et al. 2005; Alan R Lehmann et al. 2007).

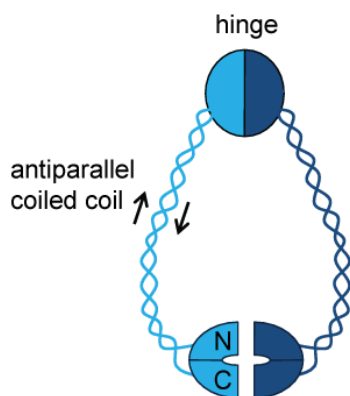
### III BRC-1/BRD-1 inactivation suppresses genome instability during replication blockage in *smc-5* mutants

(modified from Wolters et al. 2013, under review at Genetics)

#### 3.1 Introduction

##### 3.1.1 Discovery of a novel radiation-sensitive gene

In the 1970s several radiation-sensitive (rad) mutant *Schizosaccharomyces pombe* (*S. pombe*) were isolated and UV- as well as IR-sensitivity was characterized (Nasim and Smith 1975). The *S. pombe rad18-X* mutant was described to be a Structural Maintenance of Chromosomes (SMC) family member judged from its sequence motifs (A R Lehmann et al. 1995). Later, rad18 was renamed to smc6. Structurally smc6 comprises an ATP-binding domain at its N- and C-terminus and disruption of the N-terminus leads to dysfunction of the protein. Moreover, the protein harbors two extended coiled coil domains which are separated by a hinge in the middle (Figure III.1) (Fousteri and Lehmann 2000; T. Hirano 2006). The protein folds back in an antiparallel coiled coil that brings together the ATPase domains on the N- and C-terminus. The hinge domain is the interacting motif for heterodimerization of Smc6 with Smc5. Mutations impairing either Smc6 or Smc5 are thought to disrupt the functionality of Smc5/6 complex and, hence, elicit the same phenotypes.



modified from Hirano et al. 2006.

**Figure III.1 Basic architecture of SMC complexes.**

Each SMC binding partner of a heterodimer folds back in a coiled coil bringing together the N- and the C-terminus. Thereby an ATP-binding head region is formed. The hinge domain is the interacting motif with the other SMC subunit. Non-SMC subunits mainly bind to the head region to close the ring formation.

##### 3.1.2 The Smc family

Like Smc5/6 also the other SMC family members form heterodimers, which are Smc2 and Smc4, and Smc1 and Smc3, commonly known as condensin and cohesin, respectively (T. Hirano 2006;

N. Wu and Yu 2012). Furthermore, all three complexes are associated with non-Smc elements (Nse). Cohesin has a well-established role in sister-chromatid cohesion by embracing the sister chromatids inside its ring (M. Hirano and Hirano 2006; Sun et al. 2009). It is loaded during telophase and G1 phase before the onset of replication. Chromatids are released by cleavage of cohesin employing separase at meta-anaphase transition. Similar to Smc5/6, cohesin-defective yeast was reported to be sensitive to killing by UV irradiation and IR. Based on this observation, further studies suggested implications of cohesin in DSB repair. Here, cohesin is important to keep sister chromatids in close proximity as a prerequisite for strand invasion and intra-S as well as G2/M checkpoint activation upon DNA damage (N. Wu and Yu 2012).

The third SMC complex, condensin, functions in chromosome organization and condensation. In human two condensin complexes differing in their subunit composition have been reported. While condensin I was shown to be linked to single strand break DNA repair, condensin II has a role in DSB repair by HR. *C. elegans* encodes an additional condensin-like SMC complex important for dosage compensation (N. Wu and Yu 2012).

### **3.1.3 The subunits of the Smc5/6 complex**

In yeast the Smc5/6 complex is associated with at least six Nse proteins and so far only four were found in human (reviewed in De Piccoli, Torres-Rosell, and Aragón 2009).

Nse1 resembles structurally an ubiquitin ligase due to its RING finger motif. The enzymatic action of this protein, however, remains to be shown. Nevertheless, *S. cerevisiae* carrying a mutation in Nse1 display growth defects and human Nse1 was reported to be ubiquitinated *in vivo*. Furthermore Nse1 interacts with Nse3, forming a subcomplex together with Nse4 (Palecek et al. 2006).

Nse2 is also known as Mms21 and confers DNA damage resistance in *S. cerevisiae* through its action as a SUMO E3 ligase (X. Zhao and Blobel 2005). Deficiency for this enzymatic function lead to MMS-, UV- and bleomycin- (inducing DNA damage similar to IR) sensitivity as well as defects in nucleolar organization and telomere integrity. Also in human MMS21 was shown to be important for DDR and prevention of inappropriate apoptosis induction (Potts and Yu 2005). Targets of Mms21 SUMO ligase are Smc5 and Yku70, NHEJ factor, as indicated in yeast (X. Zhao and Blobel 2005) as well as SMC6 in human (Potts and Yu 2005).

Nse3 is structurally related to the MAGE (melanoma antigen gene) family of proteins and leads to MMS sensitivity in human cells carrying MAGEG1, homologue of Nse3, mutation (Taylor et al. 2008). In *Drosophila*, mutation of *MAGE* sensitizes to IR, HU and MMS comparable to *Smc5* and *Smc6* mutations (X. Li et al. 2013). Furthermore, it was reported that dysfunctional MAGE leads to pupal lethality upon treatment with ATR and ATM kinase inhibitor, caffeine.

Nse4 belongs to the kleisin superfamily that are characterized by interaction with SMC proteins to form ring-like structures (Schleiffer et al. 2003). In particular, Nse4 was shown to bridge *Smc5* and *Smc6* to form a ring (Palecek et al. 2006).

Finally, Nse5 and Nse6, which are reported to be yeast-specific, were also found to interact with *Smc5/6* and, like Nse4, might join the arms of the *Smc5/6* complex (Palecek et al. 2006).

### **3.1.4 Characteristics of the *Smc5/6* complex**

The initial publication about *rad18* (*smc6*) by Lehmann et al. reported that this novel protein acts in parallel to *rad13*, the homologue of NER factor XPG, and is epistatic with the *RAD51* homologue, *rhp51* (A R Lehmann et al. 1995). Furthermore the authors noted that *rad18* is important for replication. Concerning the radiation sensitivity, it was suggested that *smc6* could act by promoting *Rhp51* strand invasion or hold together the ends of a DNA DSB (Fousteri and Lehmann 2000). Further evidence for *smc6* acting in HR came from the finding that *smc6* is also epistatic with *mus81* endonuclease (Sheedy et al. 2005). Another allele of *smc6* was identified later in a screen for DNA damage checkpoint-defective strains, namely *rad18-74* (Verkade et al. 1999). The point-mutation found in this strain affected the C-terminal ATP-binding domain and conferred Methyl methanesulfonate (MMS)- and HU-sensitivity. In particular, G2 checkpoint was not triggered in response to IR, MMS or UV-mimetic 4-NQO agent treatment in the *rad18-74* mutant strain in contrast to wildtype *S. pombe*. While *chk1* phosphorylation kinetics after IR and UV irradiation were normal at the beginning, *rad18-74* mutants were unable to maintain *chk1* activation in the presence of DNA damage. Genetic analysis of *rad18* revealed that overexpression of *brc1*, containing a BRCT domain, suppressed *rad18-74* and *rad18-X* UV-, MMS-, 4-NQO and HU-sensitivity (Verkade et al. 1999; Sheedy et al. 2005). In contrast, *brc-1Δ* was found to be synthetically lethal with *rad18-74* (Sheedy et al. 2005). *S. pombe* BRC1 is the homologue of human PAXIP1 (also known as PTIP), which is implicated in NHEJ-mediated V(D)J recombination of T-killer cells (Callen et al. 2012). In line with its role in NHEJ, PAXIP1

has been shown to interact with 53BP1 (Cho et al. 2007). After testing a number of other DNA repair and HR factors it was hypothesized that *smc6-74* mutants might accumulate aberrant DNA structures that rely on recombination for resolution. Furthermore Sheedy et al. stated that this recombination is mediated by Brc1, Slx1 (homologue of human endonuclease SLX1), Rhp18 (homologue of human RAD18) and Mus81 (homologue of human endonuclease MUS81). Consistent with a role in HR, temperature sensitive *smc6-9* mutant *S. cerevisiae* were found to arrest in G2/M induced by Rad53 (Chk2) activation (Torres-Rosell et al. 2005). The same was true for a mutant of the binding partner of *smc6*, *smc5*. 2D gel electrophoresis revealed that *smc5* and *smc6* mutants accumulate X-shaped DNA structures that are likely HR repair intermediates. A fraction of these intermediates could be still resolved in *smc6* mutants with the help of SGS1 RecQ helicase and TOP3 topoisomerase III (Torres-Rosell et al. 2005). Studies using HU to induce replication stress illustrated that spatiotemporal recruitment of repair factors, like Rad22 (homologue of human RAD52) and Rhp51 (homologue of human RAD51) does not differ from wildtype in *smc6* defective *S. cerevisiae*. Taken together this indicates that Smc5/6 is dispensable for HR factor recruitment but is essential for Holliday Junction resolution (Ampatzidou et al. 2006). Yeast two-hybrid screen and co-immunoprecipitation experiments identified helicase Mph1, FANCM homologue, as direct binding partner of Smc5/6 complex. Mph1 does not only dissociate DNA D-loops which are precursor structures of double Holliday Junctions (Y.-H. Chen et al. 2009) but also supports lagging-strand synthesis by Okazaki fragment processing (Kang et al. 2009).

Although initially identified in yeast, Smc5/6 is conserved up to human. In 2010 the first study about SMC-5/6 in a multicellular organism, *C. elegans*, was published. In contrast to defects of Smc5/6 in yeast, *C. elegans* mutant for either of the proteins are viable (Bickel et al. 2010). Nevertheless, worms displayed some degree of genomic instability as seen by chromatin bridges in intestinal cells as well as transgenerational sterility due to defects in the germ cells. Similar to the yeast mutants, also *C. elegans smc-5* and *smc-6* mutants were sensitive to IR and displayed two times more germ cell corpses (Bickel et al. 2010). Moreover it was found that SMC-5/6 defective *C. elegans* accumulate RAD-51 foci in meiotic germ cells at mid-pachytene that could be rescued by mutating *spo-11* meiotic recombination initiator. Genetic analysis revealed that SMC-5/6 has some role in promoting inter-sister recombination repair in *C. elegans*.

## 3.2 Results

### 3.2.1 Screening for UV-sensitive alleles in L1 larvae.

We sought to identify new genes involved in the response to UV-induced DNA damage. We employed a forward ethyl methanesulfonate (EMS) mutagenesis screen in *C. elegans* to recover mutant worms that are hypersensitive to UVB-irradiation (Figure III.2 A). EMS as a mutagen has been used for a long time and is an established tool. First it was employed in 1959 (Loveless and Stock) for examination of the effect of alkylating agents. In 1974 it was established for the nematode model system as a tool for mutagenesis by Sydney Brenner (S. Brenner 1974). Generally EMS has a tendency to make GC to AT transitions, which is an advantage because exons are GC rich compared to the rest of the *C. elegans* genome (Flibotte et al. 2010). By screening over 2,500 worms, five strains could be identified displaying UV-sensitivity. This was confirmed by repetition of the experiment using a synchronized L1 larvae population and treatment with UV light. While two strains arrested at L1 stage upon irradiation, three strains were sterile in adulthood. The novel strains and the respective alleles were named BJS1(*sbj1*), BJS2(*sbj2*), BJS3(*sbj3*), BJS4(*sbj4*) and BJS19(*sbj19*). In the next step we backcrossed the strains to N2 wildtype worms to outcross mutations not linked to the UV-specific phenotype. Since those strains were indistinguishable from wildtype worms when not treated with UV-radiation, we had to screen the F2 generation of the crossed P0 worms for UV-sensitivity. This was done similarly to the initial screening method by irradiation of the F3 generation while single F2 worms were kept in liquid culture backup plates.

In parallel, the mutation was mapped to the chromosome by single nucleotide polymorphism (SNP) mapping technique (Davis et al. 2005). After several rounds of backcrossing, Solexa whole-genome sequencing was performed. The sequencing data were analyzed using the ‘Mapping and Assembly with Qualities’ (MAQ) Gene mapping software with the *C. elegans* genomic sequence version WS201 from [www.wormbase.org](http://www.wormbase.org) as reference. The data were processed using standard settings for MAQ Gene software. Overall around 1,900 to 2,000 mutations were found in each of the mutants. However, all five strains sequenced had 1,013 mutations in common with each other. Most likely these aberrations display differences between the wildtype strain in our laboratory compared to the wormbase reference and are not induced by EMS. Therefore, these variations were not taken into account for further analysis.

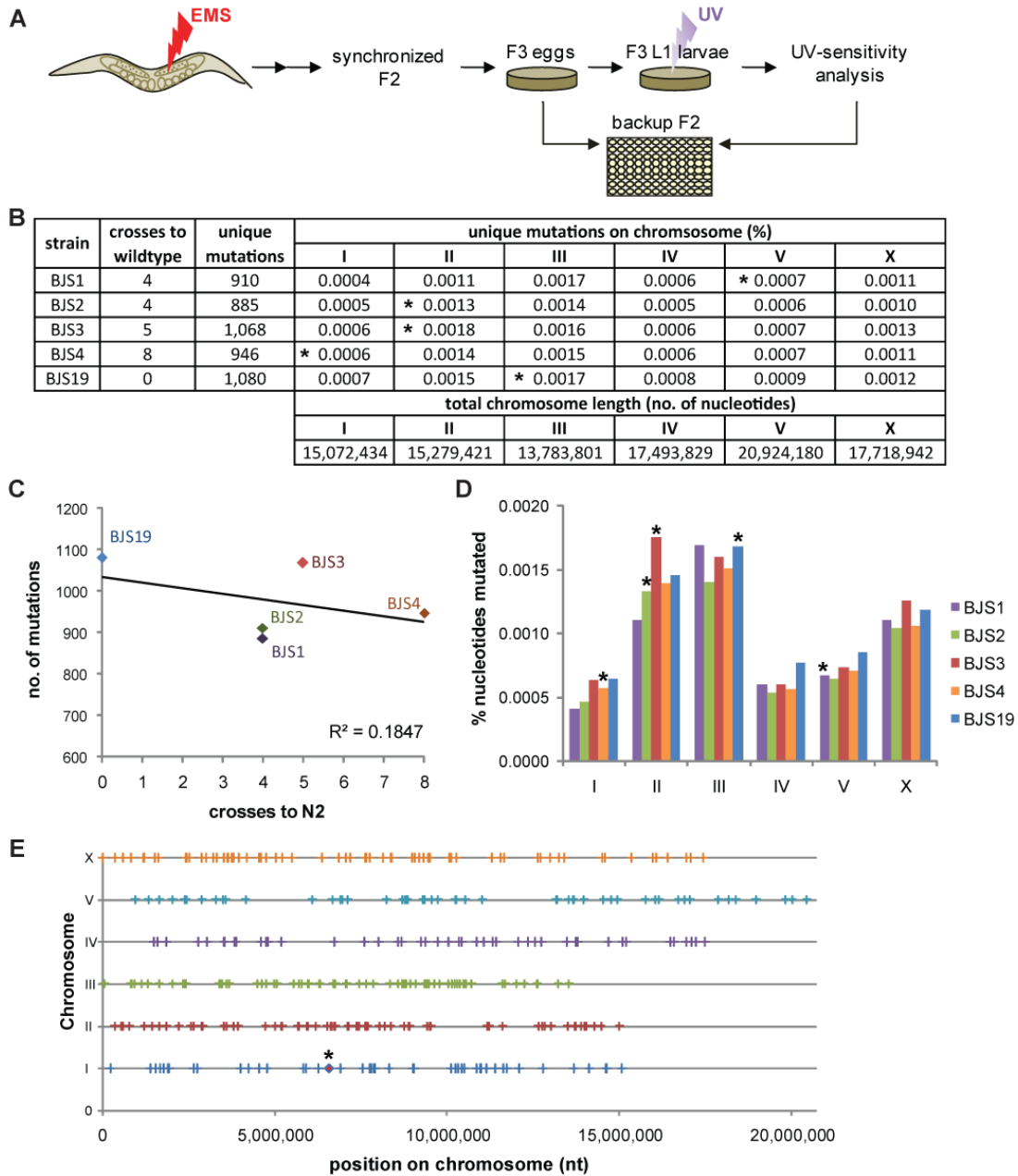


### Figure III.2 EMS-based forward genetic screening.

**A** Worms were mutagenized with EMS and F2 generation synchronized. After egg-laying for 2-3h, F2 adults were backed up in 96-well plate liquid culture. F3 larvae were irradiated with 60mJ/cm<sup>2</sup> UV light and screened for impaired development and reproduction 48h later. The phenotypes were confirmed using the worms from the 96-well backup plate.

**B** Table showing the number of mutations found in five worm strains using whole-genome sequencing and MAQ gene analysis (Bigelow et al. 2009). **C.** *elegans* genomic sequence version WS201 from www.wormbase.org served as reference. The number of 'unique mutations' represents mutations not common to all five strains to account for differences of the wildtype used here and the wormbase reference. The chromosome linked to the mutation conferring UV-sensitivity is marked with an asterisks (\*). BJS1, BJS2 and BJS19 were identified by Dr. Maria A. Ermolaeva.

**C** Graph displays the relationship between the number of mutations in a given worm strain and the number of crosses to N2 wildtype worms. The linear regression line ( $y = -13.591x + 1034.9$ ) and R<sup>2</sup> are shown.

**D** Percentage of nucleotides mutated on the six chromosomes of *C. elegans* in the five sequenced candidate strains. The chromosome linked to the mutation conferring UV-sensitivity is marked with an asterisks (\*).

**E** Distribution of mutations in BJS4 strain. Plus-signs denote mutations solely found in BJS4 and not in any other of the four strains. The mutation linked to the UV-sensitivity phenotype is marked with an asterisks (\*).

Interestingly, the number of crosses to wildtype N2 worms does not correlate with the number of mutations found (Figure III.2C). While BJS1 and BJS2 were backcrossed four times and have 910 and 885 mutations, respectively (Figure III.2C), the eight times backcrossed strain BJS4 has a similar frequency of mutations. Nonetheless, we could observe that backcrossed worms looked less sick than their not backcrossed ancestors. Especially the vulva perturbation phenotype that was seen in almost 100% of non-backcrossed BJS3 was hardly found in the five times backcrossed strain.

Furthermore, it was expected that the number of mutations on the chromosome linked to the mutation of interest was bigger compared to the other chromosomes (Zuryn et al. 2010). The chromosome linked to the mutation was selected during backcrossing and therefore, mutations on this chromosome might remain while the other chromosomes recombine and get exchanged during the crosses. Based on this idea, Zuryn and coworkers developed a method for directly mapping a mutation to a chromosome by whole-genome sequencing (Zuryn et al. 2010). For mapping of the mutation, the region on one chromosome is determined that contains the most mutations compared to the rest of the backcrossed genome. At least in our case this was not possible, because even after outcrossing eight times, mutations seemed to be randomly distributed throughout the genome (Figure III.2 B and D). Interestingly, the proportion of mutations found on the individual chromosomes differed much, e. g. only about 0.0005% of the nucleotides were mutated on chromosome I and IV, whereas about 0.0015% were mutated on chromosome II and III. This pattern was found for all five strains sequenced (Figure III.2 B and D). Nevertheless, none of the strains showed a remarkable increased number of mutations on the chromosome linked to (Figure III.2 D). Moreover, for instance BJS4 that was backcrossed eight times to wildtype, showed a rather random distribution of mutations all over its genome and along the six chromosomes (Figure III.2 E). Hence, a high-density cluster of mutations positioned around the actual mutation could not be found. This discrepancy might be due to a higher EMS concentration of 50mM that was used by Zuryn *et al.* in comparison to 30mM used in our study. Therefore, such a low concentration of EMS might be insufficient to induce enough mutations to identify the location of the actual mutation. This comparable low concentration of 30mM EMS was chosen to avoid a high load of mutations leading to the probability that an observed phenotype is induced by several mutations simultaneously. Phenotypes caused by

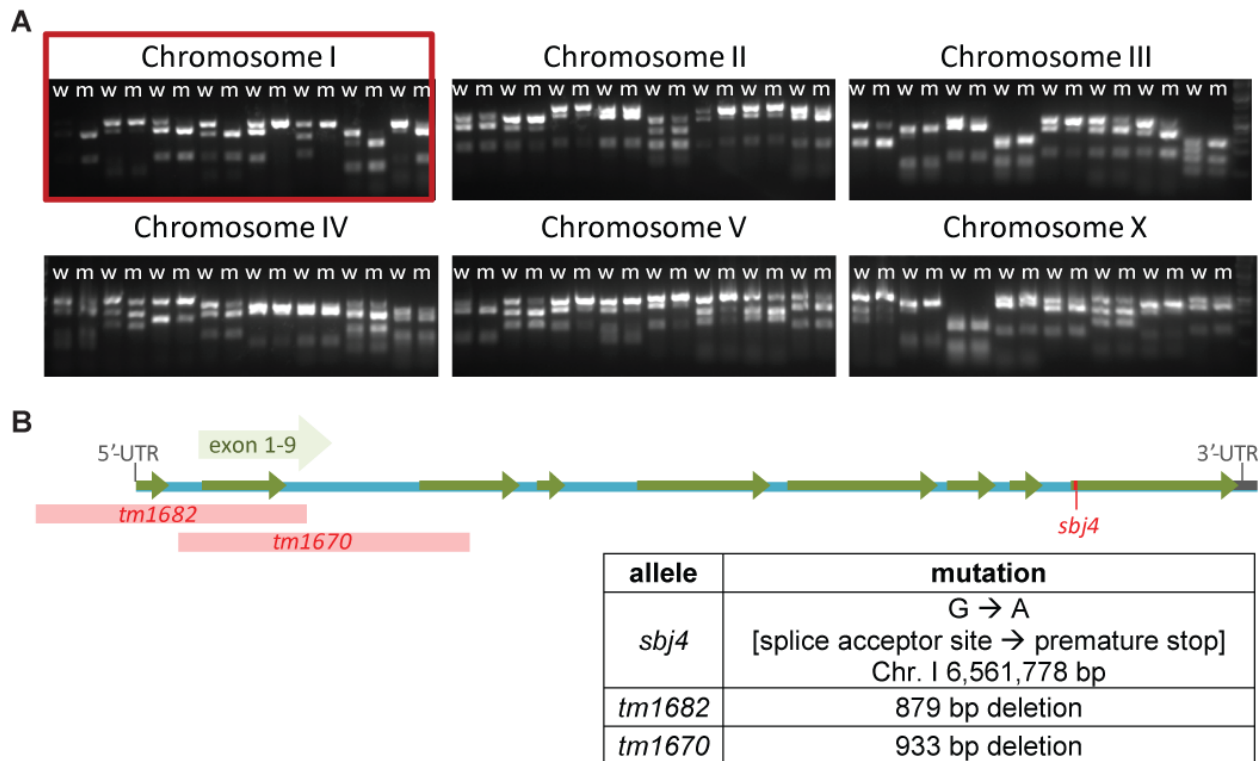


**Figure III.3 *sbj4* is a novel allele of *xpg-1*.**

**A** SNP mapping of BJS4 according to Davis et al. 2005. Gel electrophoresis pictures of *Dra*I-restricted SNP PCR products are shown. Lanes of worms displaying wildtype phenotype are denoted with 'w', bands of UV-sensitive worms are denoted with 'm'. All lanes show bands indicating Hawaiian and Bristol SNPs except for chromosome I where several 'm'-bands lack Hawaiian SNPs resulting from absence of recombination at this region. The expected sizes of fragments can be found in the report by Davis et al. 2005.

**B** Scheme of *xpg-1* genomic region (chromosome I: 6,558,700 - 6,562,392bp) with exon location. *tm1682*, *tm1670* and *sbj4* alleles are indicated. *sbj4* is a Guanine to Adenine nonsense mutation changing a splice acceptor site into a stop-codon.

multiple mutations are very difficult to analyze and moreover, the phenotype might be lost during outcrossing.

### 3.2.2 Identification of a novel *xpg-1* allele is a proof of concept for the screening method.

By SNP mapping we could show that the UV-sensitivity-inducing mutation of BJS4 is linked to chromosome I (Figure III.3 A). Whole-genome sequencing revealed 87 mutations on chromosome I of BJS4 that were not common to the other strains. All mutations thought to be redundant, including silent or non-genic mutations, variations of SNPs, mutations in the 3'-UTR or in the 5'-UTR, were discarded. After this selection, step seven mutations were still left: one

inframe, three missense, one read-through, one non-coding RNA mutation and a mutation in a splice acceptor site. This splice acceptor site mutation is located between the eighth intron and the ninth exon of the *xpg-1* gene (Figure III.3 B). Knowing that *xpg-1* mutant *C. elegans* are highly sensitive to UV irradiation, this gene was a good candidate gene causing the UV-sensitivity of BJS4 (Lans et al. 2010). BJS4 as well as strains carrying either *xpg-1(tm1682)* or *xpg-1(tm1670)* deletion mutations arrested in their development upon irradiation with 60mJ/cm<sup>2</sup> UV at L1 stage. To confirm that BJS4 is actually affected by its mutation in the *xpg-1* we performed non-complementation test. BJS4 was crossed to each of the deletion mutants and the heterozygous F1 generation was irradiated at L1 larval stage with UVB. 100% of F1 worms arrested, showing that the deletion strains of *xpg-1* could not complement for the BJS4 mutation. Thus, we identified a new point mutation allele of the NER endonuclease *xpg-1* (Figure III.3 B), providing a proof of principle that our screening strategy was effective at discovering mutations in DNA repair genes.

### **3.2.3 *smc-5* is required for resistance to UV-induced DNA lesions in the *C. elegans* germline**

Two isolated mutant strains, BJS2 and BJS3, displayed hypersensitivity to UV irradiation specifically in the germline reminiscent of the phenotypes of GG-NER *xpc-1* and *rad-23* mutants (Lans et al. 2010). Non-complementation analysis for UV-radiation sensitivity indicated that the mutations are allelic. Subsequent SNP mapping (Figure III.4 A) and whole genome sequencing revealed two different mutations in *smc-5* (Figure III.4 B). The *sbj2* allele has a missense mutation in the highly conserved ABC transporter signature motif of *smc-5* (Figure III.4 B and C). Previous studies in yeast indicate that the ATPase activity of the Smc5/6 complex is essential for its function (Verkade et al. 1999; Fousteri and Lehmann 2000). Nevertheless, the *sbj2* allele does not reduce the steady state levels of *smc-5* mRNA (Figure III.5 A). The *sbj3* allele which introduces a premature stop-codon (Figure III.4 B) and the *smc-5(ok2421)* deletion mutation (Knockout Consortium allele) which truncates the carboxyl terminal half of the wildtype SMC-5 protein, both reduce the *smc-5* mRNA levels by approximately five-fold (Figure III.5 A). Consistent with a previous report (Bickel et al. 2010) we found that SMC-6, the binding partner of SMC-5, colocalizes with DNA in the germline utilizing immunofluorescence staining (Figure III.5 B). SMC-6 staining was specific, since it was not found in the *smc-6(ok3294)* mutant.

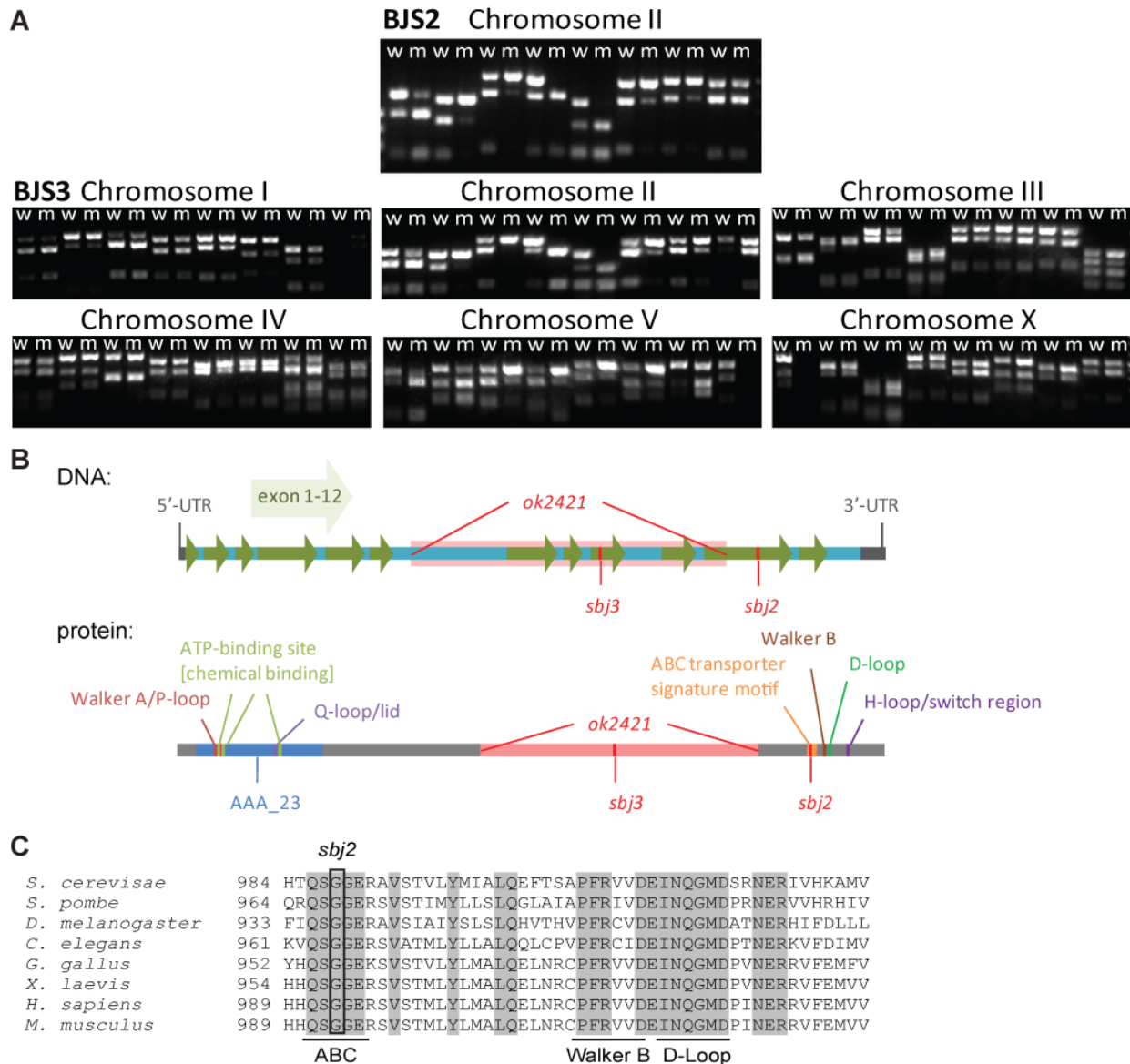


**Figure III.4 Screening for UV-sensitive mutants identified two novel alleles of *smc-5*.**

**A** SNP mapping of BJS2 and BJS3 according to Davis et al. 2005. Gel electrophoresis pictures of *Dra*I-restricted SNP PCR products are shown. Lanes of worms displaying wildtype phenotype are denoted with 'w', bands of UV-sensitive worms are denoted with 'm'. All lanes show bands indicating Hawaiian and Bristol SNPs except for chromosome II where several 'm'-bands lack Hawaiian SNPs resulting from absence of recombination at this region. The expected sizes of fragments can be found in the report by Davis et al. 2005.

**B** Scheme of *smc-5* genomic region (chromosome II: 5,062,121bp – 5,067,121bp) with exon location. *sbj2*, *sbj3* and *ok2421* alleles are indicated. *sbj2* is a Guanine to Adenine missense mutation changing Glycine to Arginine and *sbj3* is a Cytosine to Thymine mutation transforming Glutamine into a stop-codon (upper picture). Scheme of SMC-5 protein with annotation of functional domains and *sbj2*, *sbj3* and *ok2421* alleles. All domains indicated are conserved motifs forming an ATPase domain (lower picture).

**C** Alignment of carboxyl-terminal regions of SMC-5 homologs highlighting *sbj2* allele that changes a Glycine (G) of a conserved ABC signature motif into an Arginine (R).

Furthermore, colocalization of SMC-6 with DNA is dependent on its binding partner SMC-5 as seen by mislocalization in *smc-5(ok2421)* and *smc-5(sbj3)* (Figure III.5 B). However, *smc-5(sbj2)* mutants not only retained mRNA expression levels of *smc-5* (Figure III.5 B) but also were able to recruit SMC-6 to the DNA (Figure III.5 C). This shows that the ATPase ABC transporter motif of SMC-5 is important for conferring UV-resistance in *C. elegans* but is dispensable for SMC-5/6 complex formation on the DNA. Work from Raymond Chan's laboratory indicate that SMC-5/6 accumulates already in the primordial germ cells in late embryos indicating that it might already fulfill functions at this early step of development (unpublished data).

To document and measure the UV-sensitivity of SMC-5/6 complex mutants, we defined three categories reflecting the integrity of germline (Figure III.6 A). The first group are worms with a normally developed germline which can be easily recognized by DIC microscopy. Worms with a misshapen germline, disrupting the normal order of oocytes like pearls on a string, were assigned as a second group. The third group are worms where no developed germline is detectable using a stereomicroscope. Similar to *sbj2* and *sbj3*, we found that the *smc-5(ok2421)* mutation also confers UV hypersensitivity (Figure III.6 A). This phenotype was not complemented in the F1 progeny from crosses between strains carrying either of the two new *smc-5* alleles and the *smc-5* deletion mutant strain. These results reassure that the UV hypersensitivity is caused by a defect in the *smc-5* gene. In line with SMC-5 functionality depending on binding partner SMC-6, *smc-6(ok3294)* mutants failed to develop a germline as well, when treated with UV irradiation at L1 stage (Figure III.6 A). Reduced egg-laying activity and ensuing embryonic lethality are typically observed in animals with defective DNA repair in the germ cells following irradiation at the L4 stage (Gartner, MacQueen, and Villeneuve 2004). Consistently, UV treatment of *smc-5(ok2421)* mutants at the L4 stage resulted in reduced egg-laying activity and increased embryonic lethality similar to *xpc-1* mutants (Figure III.6 B and C). Unlike the rapidly proliferating cells of the embryo and the germline, somatic tissues were only moderately delayed, with ~70% of *smc-5(ok2421)* mutant worms treated with a UV dose of 60mJ/cm<sup>2</sup> reaching adulthood within three days (Figure III.7 C). L1 stage hermaphrodites contain already 558 of the 959 cells of the adult animal. Hence, the majority of cell divisions is already finished and growth is conferred by cellular expansion rather than proliferation (McIlwraith et al. 2005; Clejan, Boerckel, and

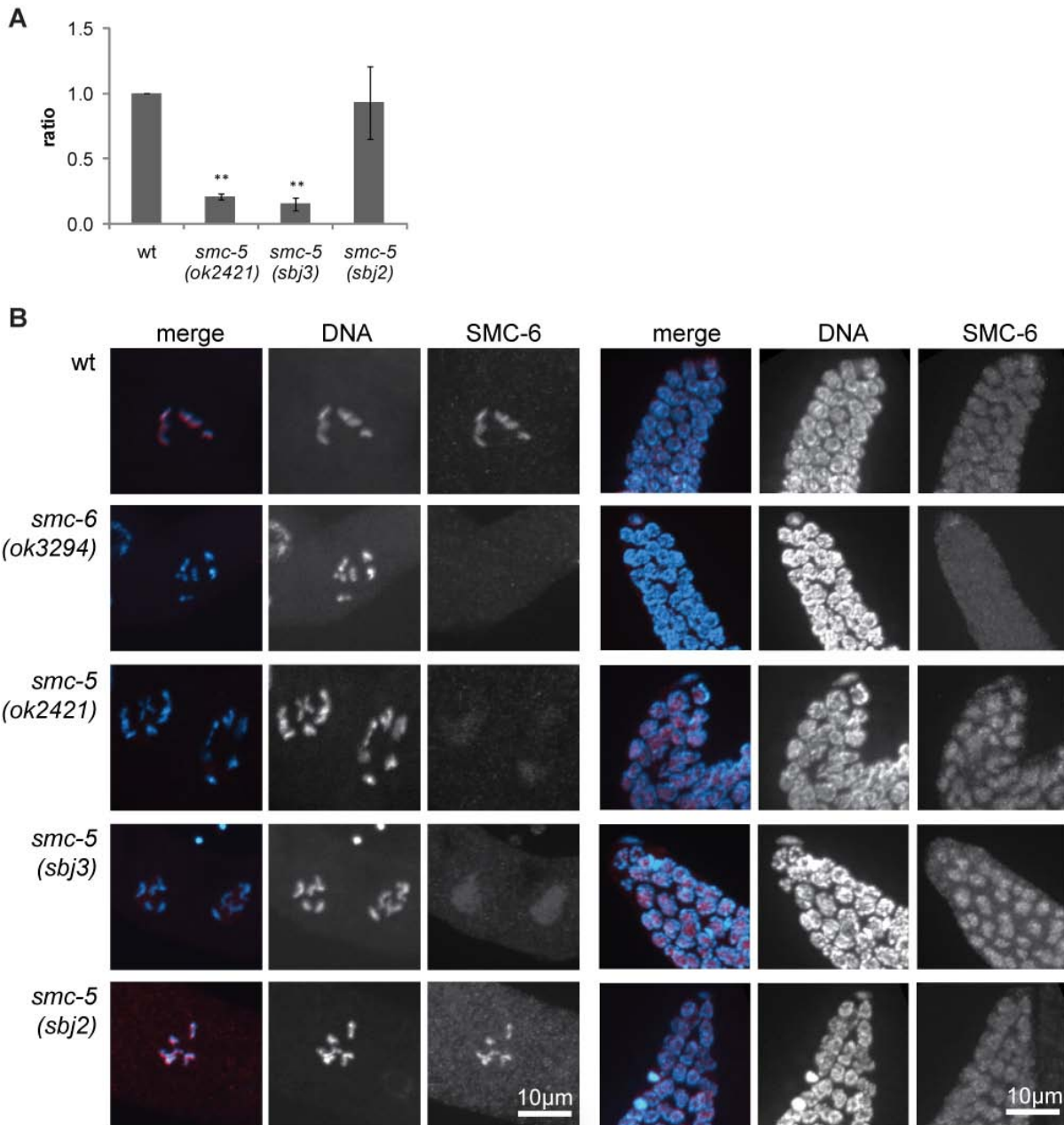


**Figure III.5 *smc-5* alleles *ok2421* and *sbj3* impair *smc-5* mRNA levels and SMC-6 localization but *sbj2* does not.**

**A** RT qPCR of *smc-5* using populations of mixed stages of the indicated genotypes. Error bars represent standard deviation between three biological replicates. *smc-5* mRNA levels were significantly reduced in *smc-5(ok2421)* and *(sbj3)* but not *(sbj2)* alleles. Double-asterisks (\*\*) denote p value >0.0001 calculated applying two-tailed students T-Test.

**B** Immunofluorescence of SMC-6 (red) and DAPI (blue) staining of isolated germlines. Micrographs on the left side show nuclei at diakinesis stage of meiosis. Micrographs on right side display the distal part of the germline comprised of mitotic cells.

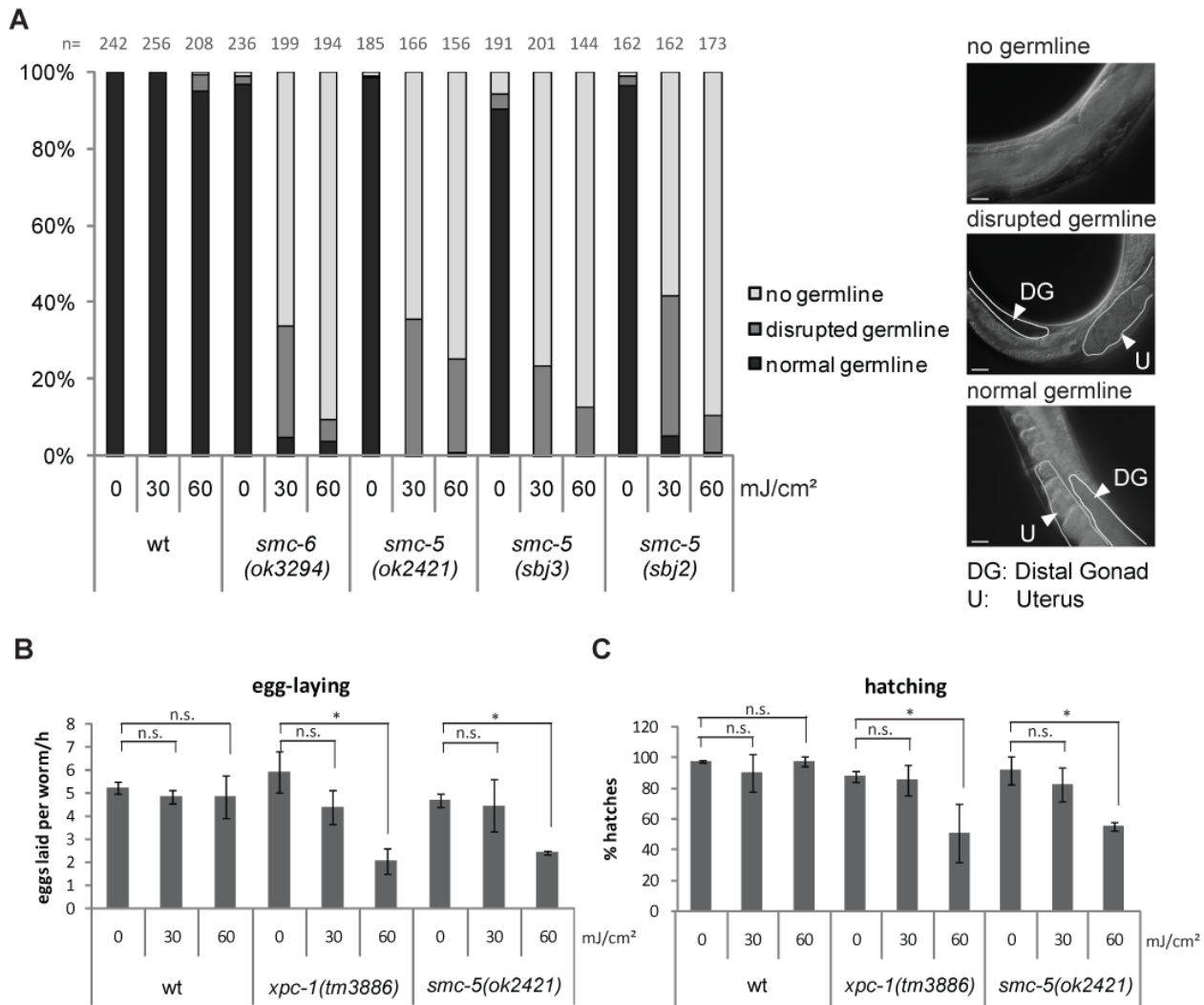


**Figure III.6 *smc-5* mutants display germline defects upon UV irradiation.**

**A** Quantification of a representative experiment examining germline development of worms three days after mock or UVB-irradiation at the L1 stage. Worms were grouped into categories of 'normal', 'disrupted' and 'no germline'. Representative DIC micrographs from each of the three categories show the middle part of *smc-5(ok2421)* adult worms with the germline and uterus outlined. Scale bar = 20  $\mu$ m.

**B** Average number of eggs laid per hour, 24h post irradiation of L4 larvae.

**C** Percentage of worms hatched from eggs quantified in Figure III.6 B.

Ahmed 2006). Taken together, the data showing defects in embryos and germ cells indicate the SMC-5/6 complex is required for UV-resistance in proliferating cells.

### 3.2.4 *smc-5* is dispensable for the repair of UV-induced lesions

Given the similarity of UV-induced defects of *smc-5* mutants compared to GG-NER mutants (Figure III.6 B and C), we tested whether SMC-5 is needed for the repair of UV-induced DNA lesions. The *smc-5(ok2421)* mutants showed equivalent capacity to remove CPD lesions compared to wildtype, while *xpc-1* mutants that are defective in GG-NER failed to remove CPDs after UV irradiation (Figure III.7 A). This suggests that SMC-5 does not mediate DNA damage tolerance through direct repair of DNA lesions. To further test this prediction, we examined the genetic interactions between the *smc-5(ok2421)* deletion mutant and loss-of-function mutations in the GG- and the TC- branches of the NER pathway. If SMC-5 functions in parallel to DNA repair to promote tolerance to UV-induced damage, then the combination of the *smc-5(ok2421)* null mutant with null mutations in the NER pathway should enhance the UV-damage tolerance defect. In agreement with this prediction, the UV-induced germline development defects seen in the single mutants of *smc-5(ok2421)* and *xpc-1(tm3886)* are enhanced in the *smc-5(ok2421);xpc-1(tm3886)* double mutant (Figure III.7 B). Combining the *smc-5(ok2421)* mutation with the GG-NER *xpc-1* mutant or the TC-NER *csb-1* mutant also enhances UV-induced delay in somatic development compared to the single mutants (Figure III.7 C), indicating that SMC-5 functions in parallel to both branches of the NER pathway in the soma. Importantly, the *smc-5(ok2421)* mutant showed higher UV-sensitivity in the germline than in the soma, with 100% of animals exhibiting germline defects (Figure III.6 A) compared to ~30% of animals with somatic developmental delay (Figure III.7 C) after 60mJ/cm<sup>2</sup> UV treatment. Together, these findings indicate that SMC-5 is required for an additional DNA damage tolerance mechanism other than NER-mediated DNA repair.

The *smc-5* and *smc-6* mutant strains exhibit several defects suggestive of impaired DNA replication. The three *smc-5* mutant strains and the *smc-6(ok3294)* strain all exhibited ectopic RAD-51 foci in the mitotic germline in adults (Figure III.8 A) (Bickel et al. 2010). Unlike the meiotic RAD-51 foci defect previously reported for *smc-5* and *smc-6* mutants (Bickel et al., 2010), the RAD-51 foci in the mitotic germline do not require SPO-11, a nuclease (unpublished data by Raymond Chan).

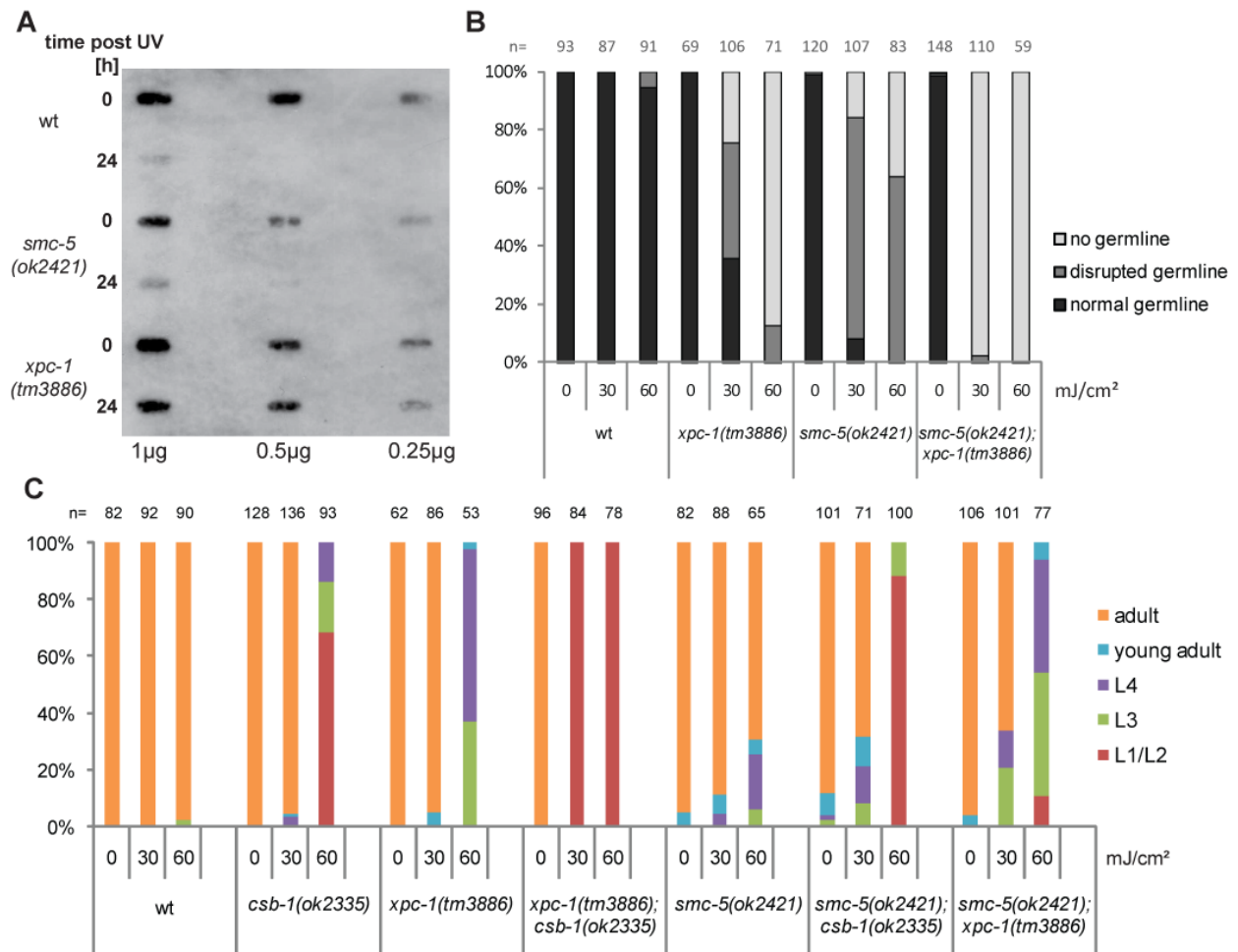


**Figure III.7 *smc-5* acts in parallel to NER in genome maintenance upon UV-irradiation.**

**A** Slot blot stained with CPD-specific antibody of whole genomic DNA from young adult worms immediately [0h] or one day after [24h] irradiation with 60mJ/cm<sup>2</sup> UV light. From left to right decreasing amounts of DNA were blotted on the membrane.

**B** Germline development quantification of worms three days after irradiation with UVB at L1 stage or untreated control worms. Worms were categorized into groups of ‘normal’, ‘disrupted’ and ‘no germline’ by inspection on a dissection microscope. Shown is one representative experiment.

**C** Percentage of larval stages 72h after UVB-irradiation at L1 larval stage of the indicated genotypes.

The aberrant accumulation of RAD-51 foci in *smc-5* and *smc-6* mutants could be indicative of DSB in the mitotic germ cells. Therefore, we were interested whether DNA damage checkpoint signalling was activated. In response to replication fork stalling, cells phosphorylate CHK-1 to induce cell cycle arrest (H. Zhao and Piwnica-Worms 2001; S.-J. Lee et al. 2010). To test for CHK-1 activation, we stained isolated germlines using antibodies specific for phosphorylated CHK-1. Despite RAD-51 foci formation, CHK-1 phosphorylation in *smc-5(ok2421)* mutant germ cells was not detectable in the absence of an exogenous genotoxic insult (Figure III.8 B). However, upon UV irradiation, CHK-1 phosphorylation was readily detectable in *smc-5(ok2421)*

mutant animals. The *smc-5(ok2421)* mutant worms showed CHK-1 activation similar to wildtype in response to UV treatment, suggesting that DNA damage checkpoint activation was functional in *smc-5(ok2421)* mutant worms but not triggered by the RAD-51-loaded structures.

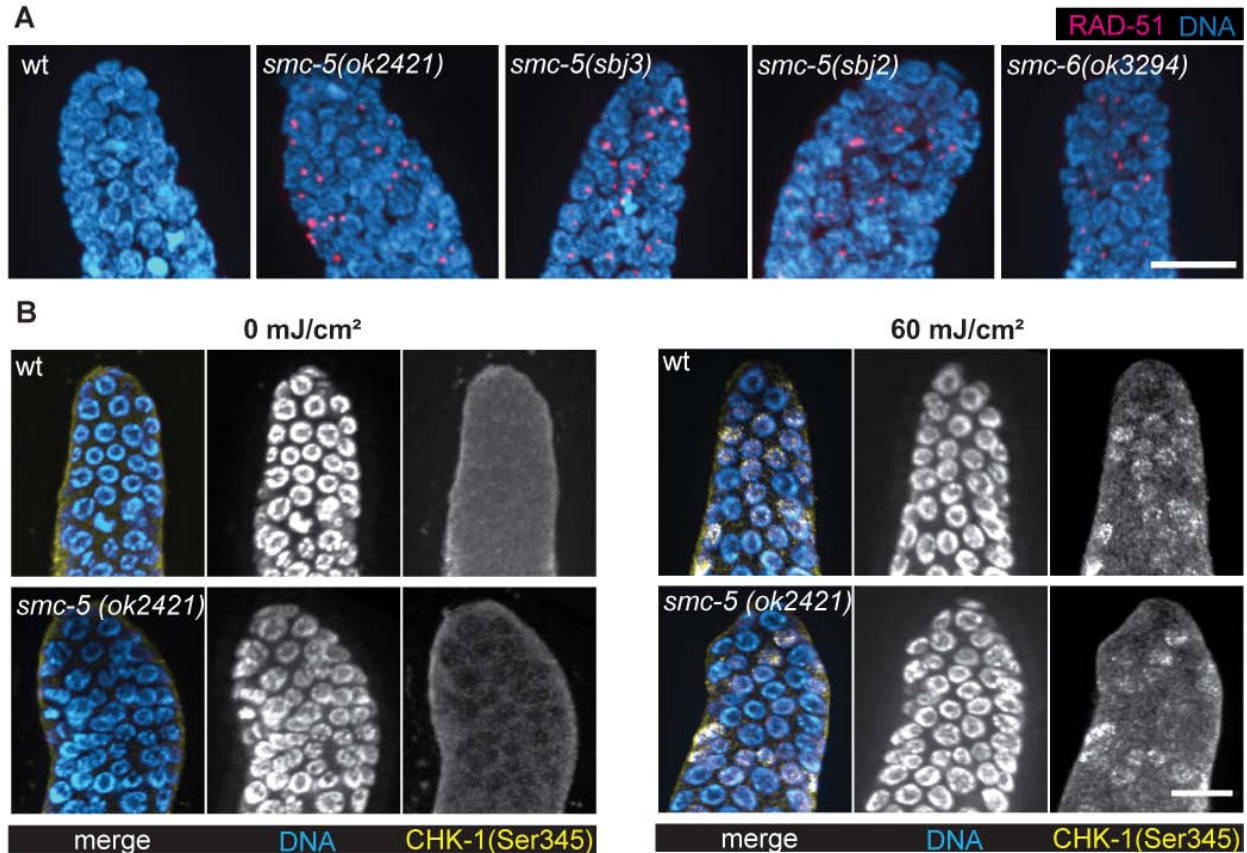


**Figure III.8 Replicating germ cells accumulate RAD-51 foci but do not activate CHK-1 in the absence of SMC-5.**

**A** Representative images showing RAD-51-specific and DAPI staining of mitotic zone germline of the indicated genotypes. Scale bar = 10 µm.

**B** Immunostaining of Serine 345-phosphorylated CHK-1 and DAPI staining of DNA in the proliferative zone of germline in young adult worms. Germlines were dissected 30min after irradiation with 60mJ/cm<sup>2</sup> UVB. Untreated samples were collected in parallel. Representative images are shown. Scale bar = 10µm.

### 3.2.5 SMC-5 functions in parallel to POLH-1-mediated TLS

We hypothesized that RAD-51 accumulation could be caused by replication-blocking lesions as reported earlier (Ward et al. 2007). During DNA replication, TLS DNA polymerases can incorporate nucleotides at sites of UV-induced lesions preventing replication fork collapse and disruption of the DNA. POLH-1, the *C. elegans* homologue of TLS polymerase Polη, covers lesions induced by UV irradiation, especially during the fast embryonic cell divisions (Roerink et

al. 2012; Holway et al. 2006). We explored the genetic interactions of *polh-1* with *smc-5* utilizing two alleles of *polh-1*: the previously described *ok3317* deletion allele (Roerink et al. 2012) and the premature stop allele *mn156*. The *mn156* allele was initially identified as *rad-2* in a screen for radiation-sensitive mutants in *C. elegans* (Hartman and Herman 1982). A non-complementation test analyzing egg-laying and hatching rate between *polh-1(ok3317)* and *rad-2(mn156)*, as well as sequencing of the *polh-1* locus identified *rad-2* as *polh-1* and *mn156* as a nonsense mutation in *polh-1* (Figure III.9).

Given the high UV-sensitivity of *polh-1* mutants, less than one-tenth the UV dose used in NER or the *smc-5* mutant analysis was applied. Interestingly, irradiating L1 larvae of the *smc-5(ok2421);polh-1(mn156)* and *smc-5(ok2421);polh-1(ok3317)* double mutant strains with a UV-dose of 2-3mJ/cm<sup>2</sup> constricted germline development. This dose showed no or hardly any effect on germline development in *smc-5* and *polh-1* single mutants, respectively (Figure III.10 A). Notably, some *smc-5; polh-1* double mutants displayed synthetic somatic defects upon UV irradiation characterized by a reduction in size, altered pigmentation and general impression of disruption of tissues (Figure III.10 B).

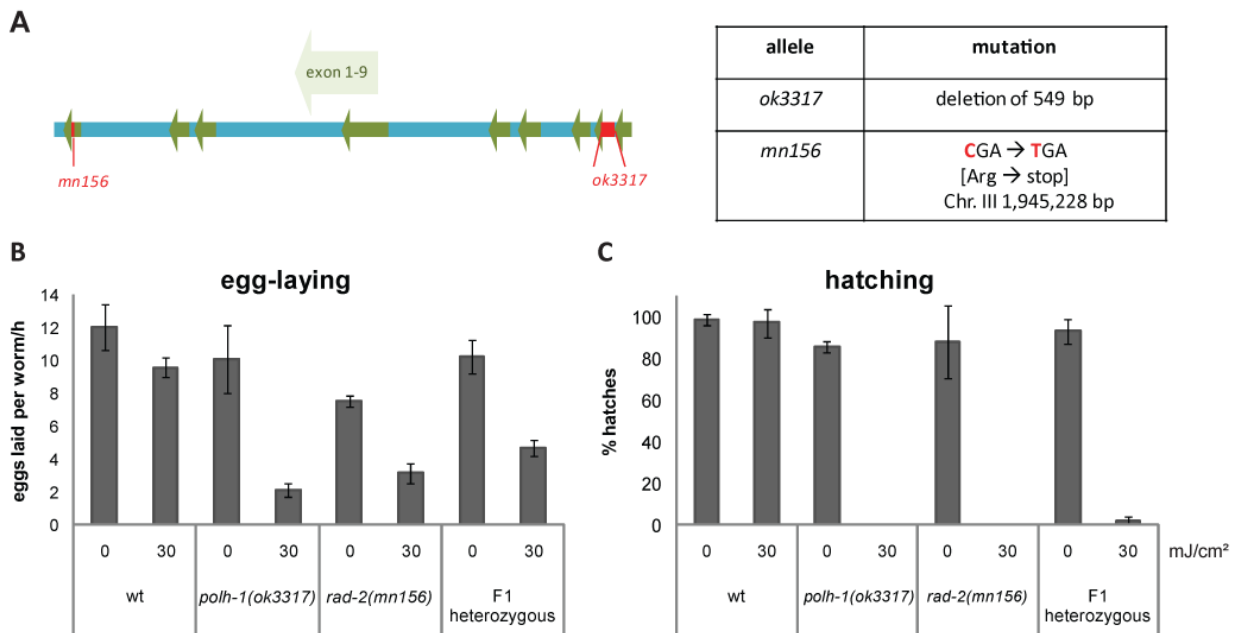


**Figure III.9 *mn156* is a nonsense mutation in *polh-1*.**

**A** Genomic locus of *polh-1* (III: 1,945,111bp – 1,950,257bp) with exon location and annotation of *mn156* and *ok3317* alleles.

**B** Eggs laid 24h post irradiation at L4 stage. Shown are averages between three replicates of three worms. Error bars indicate standard deviation between the replicates.

**C** Percentage of hatches two days after egg-laying shown in Figure III.9B. Displayed are averages between three replicates of three worms. Error bars indicate standard deviation between the independent replicates

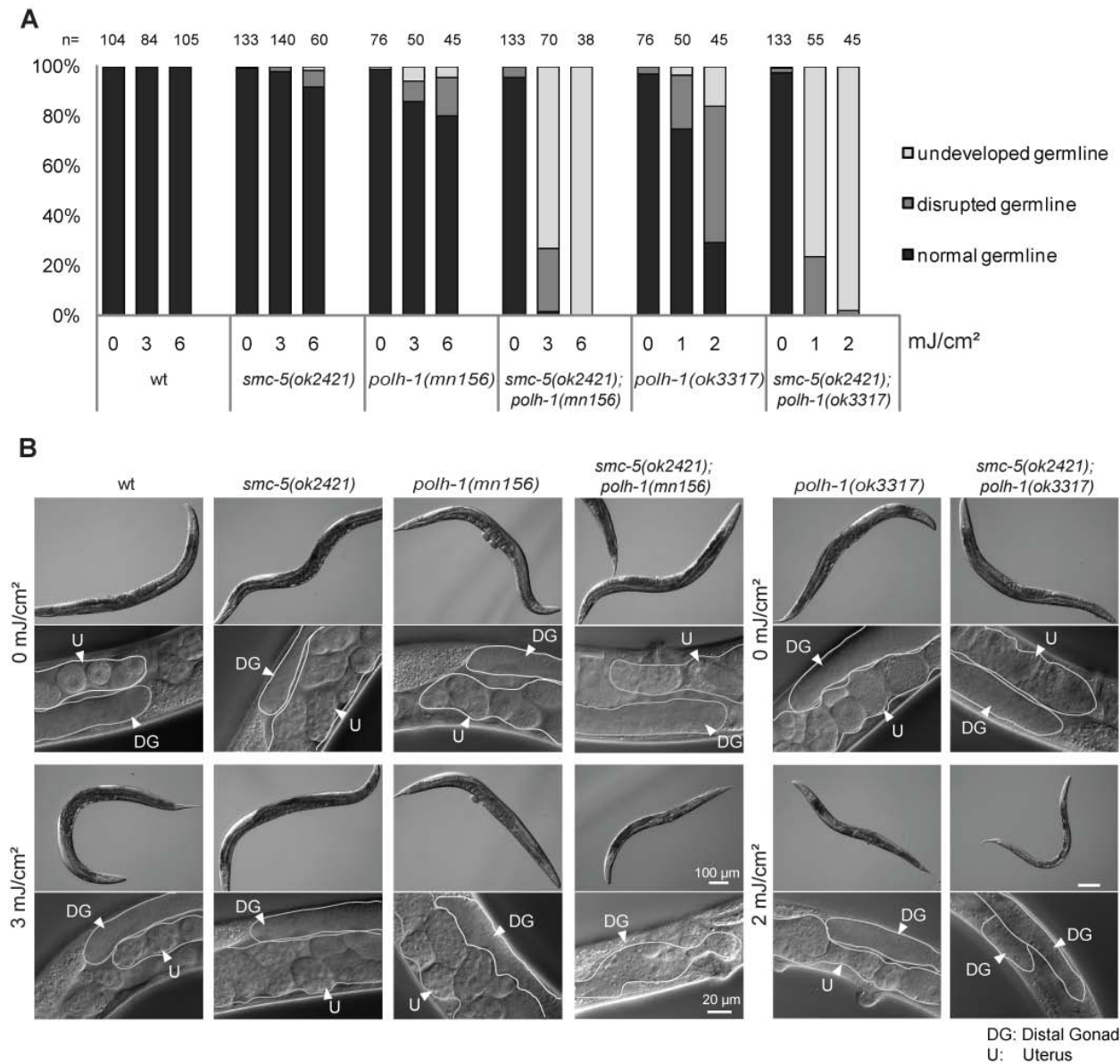


**Figure III.10 *smc-5* and *polh-1* act in parallel pathways to overcome UV-induced lesions in mitotic germ cells.**

**A** Germline development quantification of worms three days after irradiation with UVB at L1 stage or untreated control worms. Worms were categorized into groups of ‘normal’, ‘disrupted’ and ‘no germline’ using a dissection microscope. Shown is one representative experiment.

**B** DIC images of whole worms and magnified view on the middle part of the body 72h after L1 stage. Synchronized worms were irradiated at L1 larval stage and kept at 20 °C until reaching adulthood. Scale bar 100 µm (upper panels) and 20 µm (lower panels).

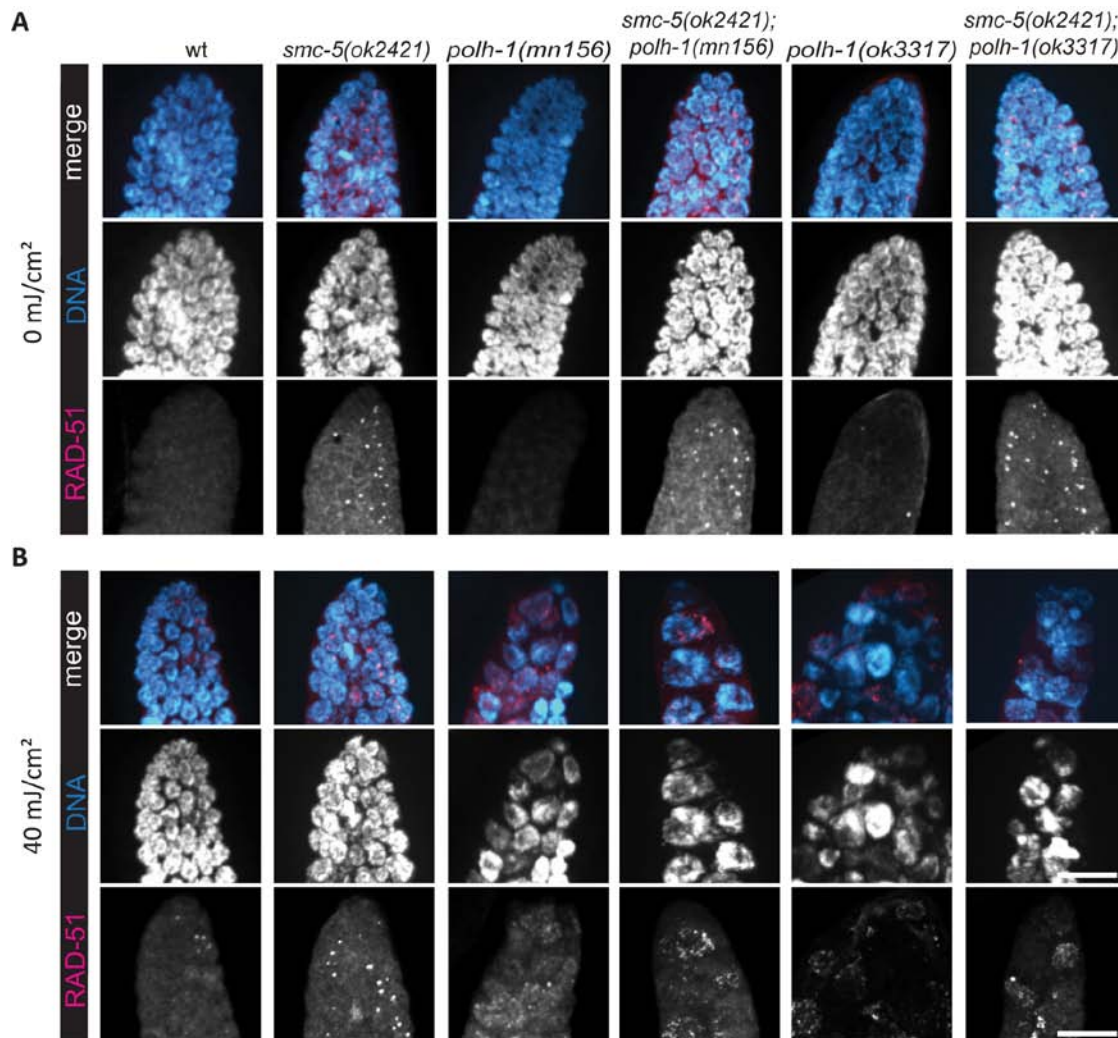


**Figure III.11 *polh-1* mutant germ cells arrest upon UV irradiation and display DNA bridges.**

**A and B** RAD-51-specific and DAPI staining of mitotic germ cells. Young adults were dissected 24h after UVB irradiation (**B**) and untreated controls were dissected in parallel (**A**). Representative images in extended view of stack spanning the whole germline are shown. Scale bar = 10  $\mu$ m.

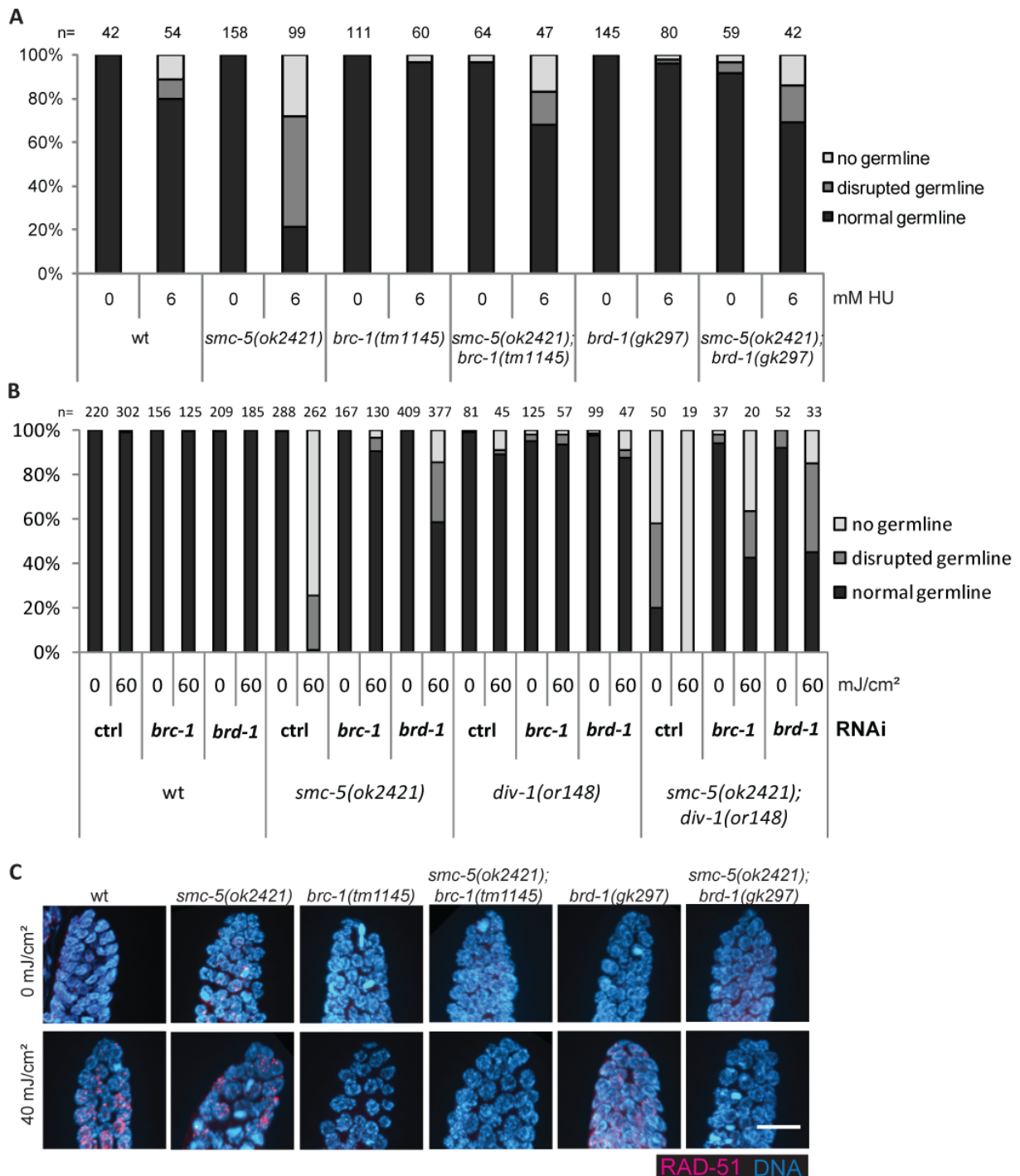
In response to UV-induced DNA damage, cells in the mitotic germline of adult worms respond with rapid RAD-51 foci formation and transient cell cycle arrest that becomes evident as a drop in cell number and enlargement of the nucleoplasm (Ward et al. 2007). To further characterize the role of *polh-1* and *smc-5* in the DNA damage response, we followed the persistence of RAD-51 foci and cell cycle arrest in the adult germline. We treated animals with UV irradiation at the L4 stage and assessed the level of UV-sensitivity in the young adult germline 24h later. RAD-51 is loaded on DNA following UV treatment as seen by a dense RAD-51 foci dotted pattern 5h after UV irradiation in wildtype germ cells (Figure III.12 C). Within 24 hours, the number of RAD-51 foci was restored to the level seen in untreated worms of the same genotype

for both, wildtype and *smc-5* mutants (Figure III.11). In contrast, cells in the mitotic region of *polh-1* mutants retained RAD-51 foci 24h post-treatment, with some cells displaying extensive RAD-51 staining, indicative of high loads of unprocessed DNA breaks. The size of the germ cells increased upon UV treatment in *polh-1* mutants, indicative of cell cycle arrest in the mitotic germline and DNA bridges point at erroneous mitosis (Figure III.11 B).

Taken together we found that the UV-sensitivity of worms with defective SMC-5/6 complex is typically indicated by defects in germ cell proliferation (Figure III.6 A and III.10 A); however, when TLS is also impaired, as in *smc-5;polh-1* double mutants, UV lesions compromise somatic growth, too (Figure III.10 B). Moreover, *smc-5;polh-1* double mutant worms show germline defects at UV doses that do not impair germline development in *smc-5* single mutant worms, providing evidence that POLH-1 is particularly required for bypassing UV lesions when forks stall in the absence of SMC-5 (Figure III.10 and Figure III.11). These observations indicate that *smc-5* and *polh-1* are functioning in parallel in the germline as well as in somatic development to confer UV resistance.

### **3.2.6 SMC-5 is required when replication fork progression is impaired**

To further characterize the role of SMC-5/6 complex at replication forks, we applied pharmacological and genetic assays to assess replication-associated phenotypes. Studies in budding and fission yeast have implicated Smc5/6 complex in promoting the progression of replication forks via various mechanisms such as restart of stalled forks, maintenance of stalled replication forks and altering DNA topology conducive to processivity of the replication fork (Branzei et al. 2006; Irmisch et al. 2009; Kegel et al. 2011). Because the *C. elegans smc-5* and *smc-6* mutant germ cells are capable of mitotic cell division, we posit that the worm SMC-5/6 complex is not essential for, but may enhance, the progression of the replication fork, in particular in the presence of fork blocking lesions like those induced by UV light. If the complex is actually needed for replication fork stabilization, then replication fork barriers should enhance the defects of worms with defective SMC-5/6 complex. Indeed, we found that decrease of the dNTP pool by HU treatment was efficient in inducing germline depletion in *smc-5(ok2421)* mutants (Figure III.12 A). While only about 20% of wildtype worms were impaired in germline development and 80% did not show any defects at all, only 20% of *smc-5(ok2421)* mutant worms were capable developing a normal germline (Figure III.12 A).



Furthermore we and Raymond Chan's group could show that *smc-5* mutants display chromatin bridges in gut cells and in mitotic cells of the germline.

In a separate assay, we examined genetic interactions between *smc-5* and *div-1*, which encodes the B subunit of DNA polymerase  $\alpha$ -primase (Encalada et al. 2000). Disruption in DIV-1 primase activity is expected to impede the progression of DNA replication forks. The temperature-sensitive *div-1(or148)* mutants developed germlines normally at a semi-permissive temperature and did not develop germline defects upon UV irradiation (Figure III.12 B). In contrast, *smc-5(ok2421);div-1(or148)* double mutants developed no or only disrupted germlines even in the absence of exogenous DNA damage. Moreover, upon UV treatment, when roughly 20% of *smc-5(ok2421)* mutant worms were still capable of forming disrupted germlines, double mutant worms completely lacked germlines (Figure III.12 B). The enhancement of the germ cell proliferation defect in *smc-5(ok2421);div-1(or148)* mutants is consistent with a role for SMC-5/6 complex in DNA replication. Together the enhanced cellular defects conferred on the *smc-5* and *smc-6* mutants by genetic and pharmacological means impairing DNA replication, demonstrate hypersensitivity of the *smc-5* and *smc-6* mutants to DNA replication stress.

### **3.2.7 BRC-1/BRD-1 mutations suppress defects in *smc-5* activity**

The accumulation of RAD-51 foci in the germlines of *smc-5* mutant worms and the synthetic interaction of *smc-5* with *polh-1* in response to UV suggests that HR is initiated at sites of stalled replication but cannot be completed in the absence of a functional SMC-5/6 complex. Indeed, SMC-5 has been implicated in HR, and *smc-5* mutant strains are sensitive to IR-induced DSBs (Bickel et al. 2010). BRCA1 has been suggested to promote postreplicative repair upon replication fork stalling in mammalian cells (Pathania et al. 2011). In *C. elegans* the BRCA1/BARD1 complex, comprised of BRC-1 and BRD-1, is required for repair of DSBs following IR treatment (Boulton et al. 2004). Moreover, in recombination-dependent repair of DSBs during meiosis, *smc-5* is epistatic with *brc-1*, as demonstrated by chromosomal fragmentation in oocytes (Bickel et al. 2010). To test whether *brc-1* and *brd-1* genetically interact with *smc-5* in response to replication stress, we analysed the HU sensitivity of *smc-5;brc-1* and *smc-5;brd-1* double mutants employing deletion alleles of *brc-1* and *brd-1*. The *brc-1(tm1145)* and *brd-1(gk297)* single mutant worms showed similar HU resistance as wildtype

animals. Likewise, knockdown of *brc-1* and *brd-1* did not alter resistance to UV irradiation (Figure III.12 B), suggesting that the BRC-1/BRD-1 complex is not needed to overcome deleterious effects of HU and UV light in *C. elegans* germ cells. Surprisingly, the loss of *brc-1* and *brd-1* by genetic mutations and RNAi strongly suppressed the HU- as well as the UV-sensitivity of *smc-5(ok2421)* mutant worms (Figure III.12 A and B). The same was true for UV-sensitivity of *smc-6(ok3294)* mutant animals. To explore how BRC-1/BRD-1 affects genome stability in *smc-5* mutant worms following UV damage, we assessed RAD-51 foci formation in adult germlines 5h after mock and 40mJ/cm<sup>2</sup> UV treatment. While RAD-51 foci were only detected in wildtype germ cells after UV irradiation, *smc-5(ok2421)* mutant germ cells exhibited RAD-51 foci without UV and increased RAD-51 focal staining after UV irradiation (Figure III.12 C). By contrast to both, wildtype and *smc-5* mutant germ cells, the *brc-1* and *brd-1* single mutant germ cells had substantially less RAD-51 staining following UV irradiation (Figure III.12 C, lower panels). Strikingly, both *smc-5;brc-1* and *smc-5;brd-1* double mutant worms had decreased RAD-51 foci formation compared to *smc-5* mutant worms in absence and presence of UV treatment (Figure III.12 C). Thus, UV-sensitivity and endogenous genome instability resulting from a dysfunctional SMC-5/6 complex, as well as RAD-51 foci formation in *smc-5* mutants or upon UV treatment are dependent on BRC-1/BRD-1.

### **3.2.8 Rescue of defects of the *smc-5* mutant by suppression of BRC-1/BRD-1 complex is partially mediated by POLH-1.**

Next, we tested whether POLH-1-mediated TLS confers genomic stability in *smc-5* mutants in the absence of BRC-1/BRD-1 complex. As mentioned above, *polh-1(ok3317)* mutants were only mildly affected in germline development upon UV irradiation, but an additional *smc-5(ok2421)* mutation led to almost complete sterility of double mutant worms after treatment with 4mJ/cm<sup>2</sup> UV light (Figure III.13 A). In *brc-1* or *brd-1* mutant background UV-sensitivity of *smc-5;polh-1* mutants was mildly alleviated indicating that POLH-1 is partially required for the rescue. Nevertheless, the mild rescue observed, suggests that additional mechanisms might confer UV-resistance in *smc-5(ok2421)* mutants in the absence of BRC-1/BRD-1 complex. Because *brc-1(tm1145)* and *brd-1(gk297)* improved germline development in *smc-5* as well as *smc-5;polh-1* mutant background, we wondered whether worms are more resistant to UV irradiation when

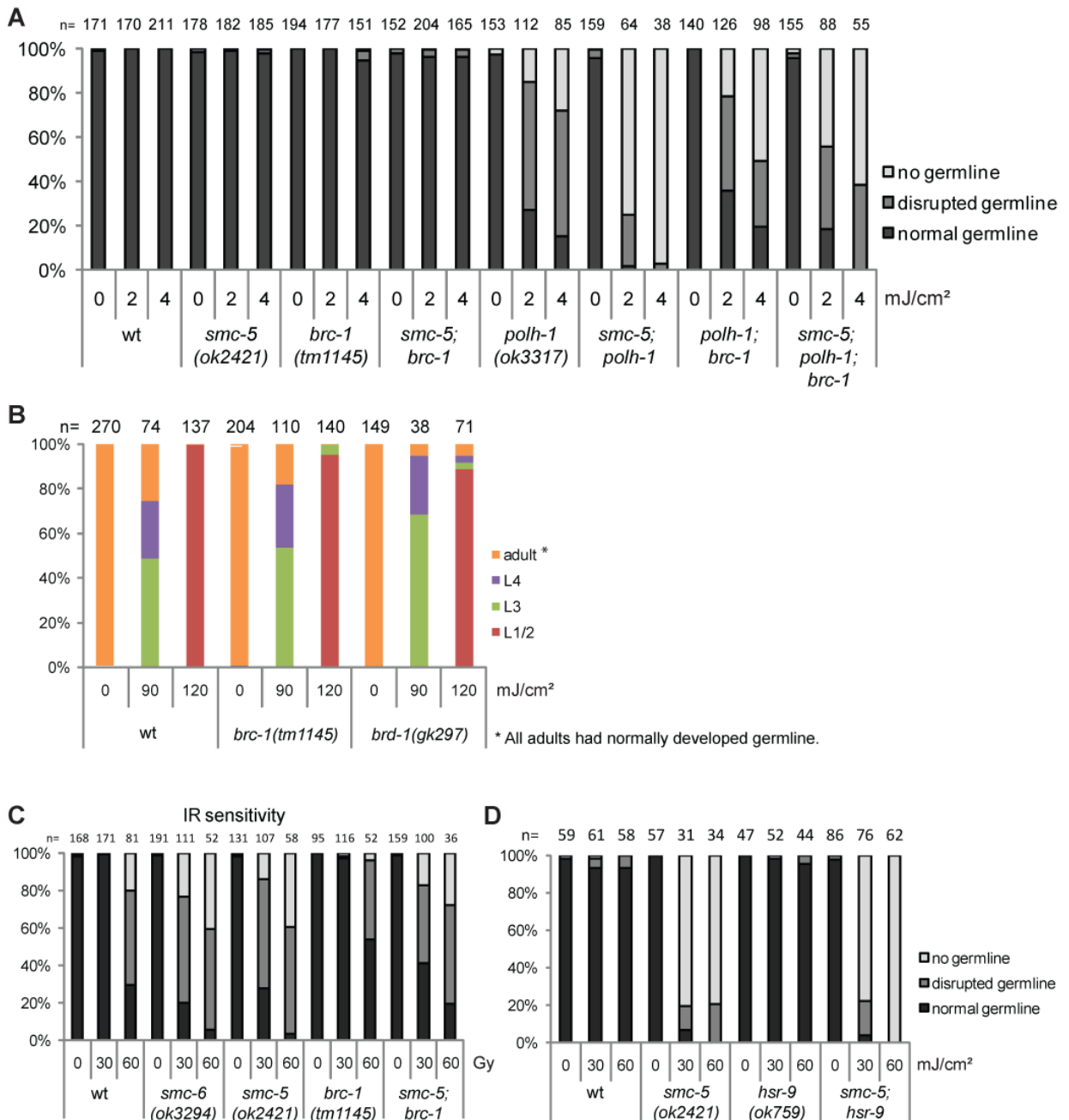


**Figure III.13 Rescue of *smc-5* defects by *brc-1* and *brd-1* mutation partially relies on POLH-1 and cannot overcome IR-sensitivity.**

**A** Germline development quantification of worms three days after irradiation with UVB at L1 stage or untreated control worms. The alleles denoted for the single mutants were combined in the respective double mutants. Worms were categorized into groups of 'normal', 'disrupted' and 'no germline' using a dissection microscope. Shown is one representative experiment.

**B** Percentage of larval stages 72h after UVB irradiation at L1 larval stage of the indicated genotypes.

**C and D** Germline development quantification of worms three days after irradiation with IR (**C**) or UVB (**D**) at L1 stage or untreated control worms. Worms were categorized into groups of 'normal', 'disrupted' and 'no germline' using a dissection microscope. Shown is one representative experiment.

BRC-1/BRD-1 complex is defective. Therefore, we irradiated worms mutant for *brc-1* or *brd-1* with 90 and 120mJ/cm<sup>2</sup> and documented developmental stages and fertility three days later.

Similar to wildtype, about 50-60% of BRC-1/BRD-1 deficient animals reached adulthood and displayed normally developed germlines (Figure III.13 B). Hence, BRC-1/BRD-1 complex disruption does not lead to improved germline development upon treatment with UV radiation. Instead, the data suggest that the function of BRC-1/BRD-1 complex is specifically corruptive for animals with impaired SMC-5/6 complex.

UV light typically leads to bulky lesions in the DNA whereas IR is thought to mainly induce DSBs. Replication fork collapse at a UV-lesion could lead to breakage of the DNA. Therefore, we tested if *smc-5* and *smc-6* mutants show the same defects in response to IR as to UV radiation. In line with previous reports (Bickel et al. 2010), worms with dysfunctional SMC-5/6 complex were sensitive to IR (Figure III.13 C). Irradiation with 30Gy impaired germline development in the absence of SMC-5/6 complex, whereas wildtype worms were not affected. *brc-1(tm1145)* allele did not compromise germline formation after IR. Interestingly, IR-induced sterility of *smc-5(ok2421)* mutant worms was not rescued by *brc-1(tm1145)* mutation (Figure III.13 C) in contrast to HU- and UV-induced germline defects (Figure III.12 A and B). These data suggest that DSB repair in L1 stage *smc-5* mutants does not involve corruptive actions of the BRC-1/BRD-1 complex, unlike processing of lesions introduced by UV irradiation or replication stress elicited by HU treatment. It should be noted that we cannot rule out that some lesions other than DSBs are induced by IR-treatment and, as indicated by previous studies (McIlwraith et al. 2005; Alan R Lehmann et al. 2007), results must be analyzed carefully.

Knowing that *smc-5* and *-6* mutants are IR sensitive (Figure III.13 C) and that the SMC-5/6 complex acts in concert with HR factors to ensure genomic stability (De Piccoli, Torres-Rosell, and Aragón 2009; Bickel et al. 2010; Chavez, Agrawal, and Johnson 2011; X. Li et al. 2013), we were interested in the genetic relationship to NHEJ. Utilizing the *ok759* deletion allele of *hsr-9*, the homologue of human 53BP1, we analyzed the UV-resistance of *hsr-9* single and *smc-5;hsr-9* double mutants. However, we did not observe any germline defect in worms lacking HSR-9 after irradiation with UV. Also sensitivity of *smc-5(ok2421)* mutant worms was not altered in an *hsr-9(ok759)* mutant background. This suggests that *hsr-9* is dispensable for resistance to UV light in wildtype and *smc-5* mutant *C. elegans*.

In the absence of the SMC-5/6 complex we found aberrant RAD-51 foci in the germ cells of the mitotic region that are dependent on BRC-1/BRD-1 (Figure III.12 C). To further characterize the role of the BRC-1/BRD-1 complex in worms lacking functional SMC-5/6 complex, we stained the germlines of *smc-5* and *smc-6* mutant strains with a BRD-1-specific antibody (Boulton et al. 2004) and observed an increase of BRD-1 on the DNA of mitotic germ cells compared to wildtype worms (Figure III.14).

Taken together, our results indicate that in the absence of a functional SMC-5/6 complex during replication, the BRC-1/BRD-1 complex accumulates on chromatin and triggers RAD-51 foci formation. Consequently, BRC-1/BRD-1 activity in *smc-5* and *smc-6* mutant cells becomes deleterious as it leads to the formation of HR-intermediates that cannot be resolved in the absence of SMC-5/6 complex, thus leading to genomic instability in proliferating cells. At the same time, POLH-1 counteracts fork stalling induced by SMC-5/6 depletion to support replication stress resistance (Figure III.15). In the absence of functional BRC-1/BRD-1 complex genomic instability of *smc-5* mutants is partially dependent on *polh-1*-mediated TLS (Figure III.13 A).

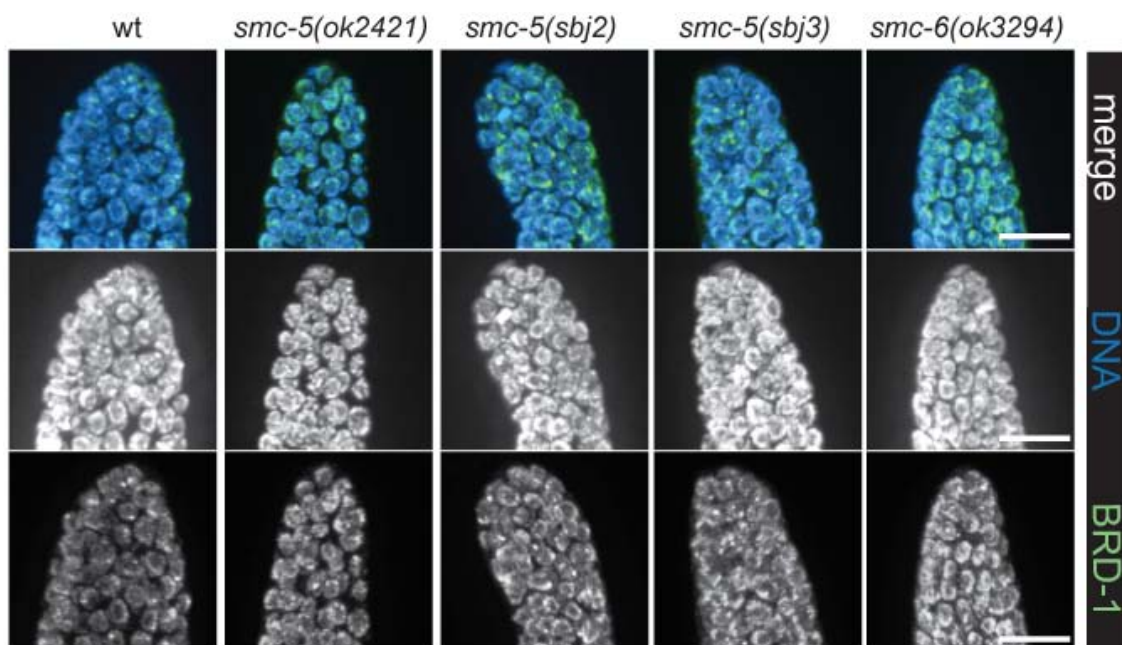


**Figure III.14 In the absence of SMC-5/6 complex BRD-1 accumulates on the DNA of germ cells.**

BRD-1-specific and DAPI staining of mitotic germ cells. Germlines were dissected from young adult worms. Representative images in extended view of stack spanning the whole germline are shown.

Scale bar = 10  $\mu$ m.

### 3.3 Discussion

#### 3.3.1 Landscape of EMS-induced mutations

Aiming at identifying null-alleles of genes required for UV resistance in *C. elegans* we utilized an EMS-based mutagenesis screen for UV-sensitive strains. After whole genome sequencing we observed a number of mutations that were common in all five strains sequenced. This phenomenon has been observed earlier (Flibotte et al. 2010) and attributed to errors in the wormbase reference and genetic drift between wildtype strains maintained separated from each other over an undetermined number of generations, though originating from the original N2 strain established by Brenner (1974).

For genetic analysis of single genes EMS-based mutagenesis is convenient to produce loss-of-function mutations. At the same time background mutations are induced that should be removed by outcrossing to the wildtype genome. However, we and others (Sarin et al. 2010) found a lack of correlation between fold outcrosses and the number of unique variations among several worm strains (Figure III.2 C). Interestingly, Sarin et al. reported a particular case where two EMS-induced mutations were retained in a strain during backcrossing to wildtype. It was not possible to remove these two mutations by phenotypical selection for the allele of interest because, while one of these mutations was lethal for *C. elegans*, the other rescued this effect and was therefore essential for this specific strain (Sarin et al. 2010). However, this mode of mutation retention may only account for a small fraction of variants, since it was shown that about 75% of the variants found in a strain, are exchanged after six rounds of backcrossing (Sarin et al. 2010). Surprisingly, the data indicate that outcrossing not only removes background mutations derived from EMS-treatment but also introduces new variants.

#### 3.3.2 The ATPase domain of SMC-5 is essential for UV-resistance.

Here, we identified two novel alleles of *smc-5* conferring UV-sensitivity. Strikingly, the *sbj2* allele, a missense mutation in a conserved site of the ATPase domain, maintained its ability to produce a stable mRNA transcript and recruit SMC-6 to the DNA (Figure III.5) while conferring genomic instability and DNA damage sensitivity. This suggests that SMC-5/6 heterodimer still forms but genomic instability arises when ATP hydrolysis is dysfunctional. These results are in line with previous studies in *Bacillus subtilis* showing that the ATPase domain is dispensable for

DNA binding of SMC complex, but in turn, DNA binding activates ATPase activity (T. Hirano 2002). ATP hydrolysis probably features dynamic conformational changes in the structure of the SMC complex dimer (compare Figure III.1). Closing of the arms of the V-shaped complex is likely mediated by ATP binding, thereby bringing together the two catalytic domains. Opening is assumed to be triggered by ATP hydrolysis (T. Hirano 2002; M. Hirano and Hirano 2006; Nasmyth and Haering 2009). In respect to SMC-5/6 function at replication forks in yeast it was hypothesized that ATP hydrolysis could keep a stalled fork in a conformation allowing RPA and Rad52 loading to ensure subsequent restart by HR (Irmisch et al. 2009).

### **3.3.3 The mutagenicity of DNA repair pathways**

The radiation of the sunlight displays a major obstacle to organisms as the containing UV light can directly react with the DNA and lead to formation of CPDs and 6,4-PPs. When not repaired, secondarily, these bulky lesions can generate DSB. Overload of the repair system by very high radiation doses or defects in the repair systems may lead to tissue degeneration and/or cancer. Furthermore, bulky lesions pose obstacles to the progression of the replication fork (Sale, Lehmann, and Woodgate 2012). Replication fork collapse can give rise to mutations and chromosomal aberrations (Petermann and Helleday 2010). In replicating cells, GG-NER is important for surveying the genome for helix-distorting lesions and removes them before they lead to replication fork stalling. Mutations that inactivate GG-NER lead to highly elevated skin cancer susceptibility in XP patients (Cleaver, Lam, and Revet 2009). Mutations affecting Pol $\eta$  cause the related XPV disease (Masutani et al. 1999; Alan R Lehmann 2011). In *C. elegans* GG-NER deficiency impairs primarily the proliferating cells of the germline and the embryo (Figure II.4 C, D and III.7 B). In contrast, TLS-mediated UV resistance is essential during the rapid cell divisions of the embryo but less important at later stages during development and for germline formation (Roerink et al. 2012 and Figure III.9 and III.10). TLS preserves ongoing DNA replication by incorporating nucleotides at lesions that cannot be accommodated by the replicative DNA polymerase complex and through its action prevents checkpoint activation, cell cycle delay and cell death (Sale, Lehmann, and Woodgate 2012; Roerink et al. 2012). As Pol $\eta$  preferably inserts non-templated deoxy-ATP opposite UV-induced thymidine dimers, its activity likely leads only to limited mutagenicity (Sale, Lehmann, and Woodgate 2012). However, TLS by Pol $\eta$  at non-cognate lesions or by other TLS polymerases may be more mutagenic when

replication is blocked by bulky lesions caused by genotoxins other than UV irradiation. Particularly relevant for the development of breast cancer are quinine derivatives, formed during endogenous metabolism of estradiol, that can induce bulky adducts (Yager and Davidson 2006). It is conceivable that BRCA1-mediated resolution of stalled replication forks at such adducts might to some extent counteract TLS-mediated mutagenicity. It will be very interesting to explore how the antagonizing functions of BRCA1/BARD1 in the maintenance of genome stability affect replication stress-induced genome instability during both, cancer development and therapeutic responses in *BRCA1*-mutated tumour cells. Intriguingly, the suppression of genome instability in the context of replication stalling amid dysfunctional SMC-5/6 suggests that the maintenance of familial *BRCA1* carrier mutations might confer selective advantages under certain conditions of genotoxic challenges.

However, when HR is recruited to stalled replication fork, resolution is facilitated by recombination-dependent repair and template switching (Petermann and Helleday 2010). Accumulation of RAD-51 and BRD-1 on the DNA (Figure III.8 A and III.14) support a model, where HR is activated in the absence of SMC-5/6 complex. Although HR is generally believed to be error-free, recent studies in *S. pombe* revealed that recombination-dependent restart of stalled replication forks can be mutagenic (Iraqi et al. 2012; Mizuno et al. 2013). In particular, induction of HR in the presence of homologous sequences in close proximity to the collapsed fork, like micro homology domains or inverted repeats lead to non-allelic homologous recombination and chromosomal rearrangements (Iraqi et al. 2012; Mizuno et al. 2013). Slippage of replication and mutation accumulation upon HR-mediated restart in the absence of SMC-5/6 may add to the transgenerational sterility of *smc-5* and *smc-6* mutants observed in our laboratory and by others (Bickel et al. 2010). *S. cerevisiae smc5-6* and *smc6-9* mutants display defects in the segregation of repetitive regions like ribosomal DNA and telomeres (Torres-Rosell et al. 2005), providing further evidence for slippage of replication when Smc5/6 complex is impaired. Sequencing experiments, to characterize alterations in subsequent generations of SMC-5/6 defective worms, started in Raymond Chan's laboratory, may shed some light on whether these mutants are especially prone to accumulate mutations at inverted repeats. In addition, mutations in *smc-5* and *-6* mutants may arise from error-prone NHEJ-mediated repair of DSB (as discussed later).

In contrast to GG-NER, the SMC-5/6 complex was dispensable for the removal of UV-induced lesions (Figure III.7 A). Instead, SMC-5/6 dysfunction sensitized cells to perturbed replication. In particular, the synergistic UV-sensitivity with *polh-1* mutant alleles suggests that SMC-5/6 confers UV resistance by stabilizing replication forks. In addition, the sensitivity of *smc-5* mutants to dysfunctional DIV-1 primase implies that transient fork stalling in the absence of exogenous DNA damage requires the SMC-5/6 complex for stability and to facilitate restart. The RAD-51 foci formation in *smc-5* mutants indicates that stalled replication forks lead to induction of HR, which is then not resolved. POLH-1 prevents the recruitment of HR and DSB formation via its TLS activity. Particularly in the absence of SMC-5/6, TLS becomes a major route for maintaining genome stability in the presence of UV-lesions. Consistently, mutations in *smc6* in *S. pombe* were shown to confer hypersensitivity to UV radiation and IR and genetically placed in the HR pathway (A R Lehmann et al. 1995). Indeed, in human cells the SMC5/6 complex localizes to sites of DSBs where it is required to recruit the related cohesin complex (Potts, Porteus, and Yu 2006). Despite finding SMC-6 localization to the DNA of germ cells (Figure III.5 B), we did not observe foci formation of SMC-6 upon DNA damage in *C. elegans*. However, a growing body of evidence suggests that SMC-5/6, together with cohesin, supports the stabilization of molecular intermediates and proximity during elaborate HR reactions. Hence, the SMC-5/6 complex not only promotes HR but also stabilizes replication forks and facilitates their restart (Irmisch et al. 2009).

There are different modes of HR upon replication fork stalling that differ in their substrate specificity and requirement for DSB formation. Analysis of RAD51 and MUS81 in mammalian cells revealed that there is an an early HR response to replication stress and a late one. While the early response does not seem to require MUS81 to induce DSB (Hanada et al. 2007), both rely on the action of RAD-51 (Petermann et al. 2010). Nevertheless, it remains unclear if MUS81 confers replication stress resistance by cleavage of replication forks or HR intermediates (Hanada et al. 2007). The notion of an early acting and a late HR response to replication stress could imply that the chronic treatment of *C. elegans*, as utilized here (Figure III.12 A), and short exposure to UV require different modes of HR for their repair. Furthermore, HR repair pathway choice depends on whether the replication block is located on the leading or the lagging strand as discussed by Zhang et al. (2013). It was suggested that lesions in the leading strand in human carcinoma cells lead to activation of MUS81-dependent resection and formation of one-ended

DSB. This structure can either be transformed into a two-ended DSB-like structure and be repaired by HR or is repaired by recombination directly (J. Zhang 2013). However, if the lagging strand carries a lesion, a stretch of DNA could be left out during replication by priming new Okazaki fragments behind the lesion and fill up the single-stranded stretch in the leading strand only later. Therefore, repair of lesions is supposed to require HR without DSB formation (J. Zhang 2013).

### **3.3.4 Restoring replication stress resistance in the absence of SMC-5/6 complex**

We found that *brc-1* and *brd-1* mutation could partially rescue the germline defects of worms lacking SMC-5/6 complex (Figure III.12). We demonstrate that inactivation of the BRC-1/BRD-1 complex suppresses RAD-51 foci formation and genome instability in *smc-5* mutants. In contrast, a *brc-1* mutation does not alleviate the recombination repair defects of meiotic or IR-induced DSBs in *smc-5* mutants (Bickel et al. 2010 and Figure III.13 C), which is consistent with an independent role for human BRCA1 post replication versus the functions required for DSB repair (Pathania et al. 2011). The BRC-1/BRD-1 complex plays an important role in HR and, when dysfunctional, evokes hypersensitivity to DSB-inducing IR (Boulton et al. 2004). BRCA1 has recently been implicated in promoting HR also at sites of stalled replication forks (Pathania et al. 2011) and was shown to promote the recruitment of RAD51 (Hanada et al. 2007; Feng and Zhang 2012). In line with our model, Pathania et al. (2011) place BRCA1 in a pathway parallel to NER to repair UV-induced lesions and suppress TLS. Our results suggest that the BRC-1/BRD-1-mediated initiation of HR at stalled replication forks requires the SMC-5/6 complex to resolve the recombination intermediates. SMC-5/6 in turn might regulate the chromatin dissociation of the BRC-1/BRD-1 complex (Figure III.14 and III.15). In the absence of SMC-5/6 the HR machinery assembles but fails to engage the intra-S phase checkpoint (Figure III.8 B). Consistent with this, *smc5/6* defective budding yeast fails to induce intra-S checkpoints but instead halts the cell cycle after the first mitotic cycle following *smc5/6* deprivation (Torres-Rosell et al. 2005). Indeed, in *C. elegans smc-5/6* mutants, RAD-51 foci persist and chromatin bridges are formed during ensuing mitosis. We conclude, the SMC-5/6 complex might play a dual role in maintaining fork stability and in resolving recombination intermediates when BRC-1/BRD-1 initiates HR (Figure III.15).

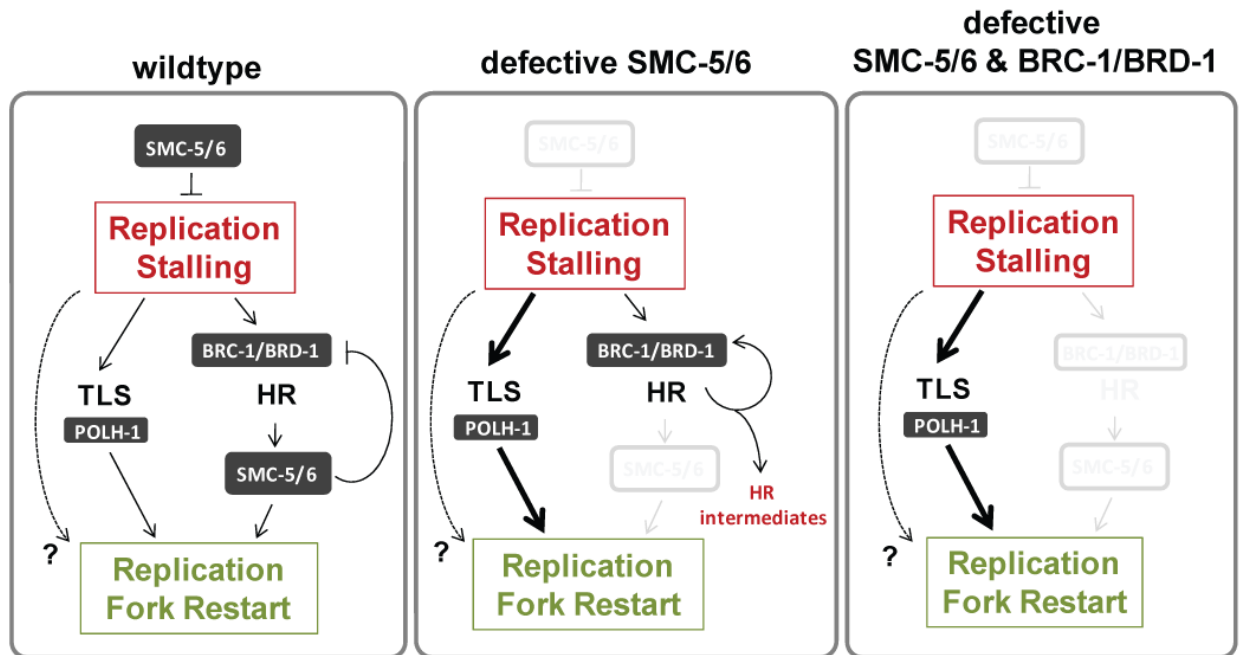


**Figure III.15 BRC-1/BRD-1 promotes genome instability when SMC-5/6 dysfunction leads to replication stalling and aberrant HR.**

Model for DNA repair mechanisms in the presence and absence of SMC-5/6. In proliferating wildtype cells SMC-5/6 prevents fork stalling. Upon stalling, TLS promotes read-through, while the BRC-1/BRD-1 complex initiates HR and SMC-5/6 promotes dissociation of BRC-1/BRD-1 from chromatin. Defective SMC-5/6 sensitizes to replication stalling and TLS becomes a major route for replication fork maintenance, while BRC-1/BRD-1 initiate HR that, however, in the absence of SMC-5/6 complex cannot be resolved and intermediates persist. In the absence of BRC-1/BRD-1 the formation of HR intermediates is prevented and the deleterious effects of replication fork barriers are mainly overcome by POLH-1-mediated TLS.

Rescue of *smc-5* and *-6* mutant defects through BRC-1/BRD-1 deficiency partially relies on the action of POLH-1 TLS polymerase (Figure III.13 A and III.15). However, finding improved germline development in *smc-5;polh-1;brc-1* compared to *smc-5;polh-1* double mutants suggests that DNA damage resistance in *smc-5* mutants does not solely rely on *polh-1*.

If in the absence of SMC-5/6 complex a replication fork stalls, the genome remains replicated incompletely. When cells are deficient for BRC-1/BRD-1 complex, recombination is not initiated, indicated by the RAD-51 foci that were absent in *smc-5;brc-1* and *smc-5;brd-1* double mutants in contrast to *smc-5* single mutants (Figure III.12 C). To compensate for the stalled replication fork that eventually may collapse, dormant origins could be activated (Woodward et al. 2006; Blow, Ge, and Jackson 2011). Before the onset of S-phase, origins are licensed in excess but the majority of these origins stay dormant and do not fire. However, upon replication inhibition, for instance upon HU treatment or DNA damage, additional replication forks are

initiated. ATR and CHK1 have been shown to stabilize blocked forks and delay the entry into mitosis to give time for DNA repair. In parallel, CHK1 restricts the number of awakening origins to replace the damaged forks only and avoid exaggerated replication resulting in mutations (Petermann et al. 2010; Blow, Ge, and Jackson 2011). Furthermore, Blow et al. (2011) state that firing of dormant origins could suppress inappropriate recombination or apoptosis by fast rescue of stalled forks. Therefore, it seems feasible that problems in DNA replication in mitotic cells of *smc-5* and *-6* mutants are alleviated by usage of additional origins. Further supporting this idea, it was shown that knockdown of MCM-7, a licensing factor, leads to impaired reproduction in HU-treated *C. elegans* (Woodward et al. 2006). If this theory of recruiting additional origins in absence of SMC-5/6 holds true, the prediction would be that, in the case of inactive HR, due to *brc-1* or *brd-1* mutation, additional forks are acquired and may support the action of TLS polymerase, POLH-1. Nevertheless, start of additional forks may also fuel the genomic instability when SMC-5/6 is dysfunctional, because, these new forks may be blocked by the persistent HR intermediates seen by RAD-51 accumulation.

Another possibility is that worms deficient for the SMC-5/6 and the BRC-1/BRD-1 complexes overcome DNA damage by employment of NHEJ. NHEJ acts in somatic tissues, whereas HR in *C. elegans* is most important for survival of germ cells (Ryu, Kang, and Koo 2013). It was reported that, although the 53BP1 homolog, HSR-9, is an inducer of NHEJ, it is dispensable for NHEJ in somatic cells in response to DNA damage. Surprisingly, the protein accumulated in the cell nucleus upon  $\gamma$ - and UV irradiation as well as HU treatment, but *hsr-9(ok759)* mutants were not delayed in development like *lig-4(ok716)* mutants (Ryu, Kang, and Koo 2013). In contrast, IR-induced killing of *rad-54* deficient embryos was alleviated by both, *lig-4* and *hsr-9* mutation, suggesting that both proteins are conferring genomic instability when HR is dysfunctional. Even though the SMC-5/6 complex has some role in HR, its defects were not rescued by *hsr-9(ok759)* (Figure III.13 D). The study by Ryu et al. (2013) implies that HSR-9 is only required under certain conditions to induce NHEJ and while *hsr-9* is dispensable for germline development in response to UV radiation (Figure III.13 D), NHEJ may be activated in *smc-5;brd-1* or *smc-5;brc-1* double mutants in parallel to TLS. This could be tested by knocking down NHEJ effectors, *cku-70*, *cku-80* and *lig-4*. However, there are two aspects that are in disfavour of the hypothesis that NHEJ alleviates replication stress sensitivity in SMC-5/6 defective worms. First, rescue of replication stress sensitivity would require formation of a DSB prior to ligation by

NHEJ, for instance by replication fork collapse and breakage; and second, previous studies in *C. elegans* suggest that NHEJ is dispensable for DNA repair in germ cells (Clejan, Boerckel, and Ahmed 2006).

## IV Role of microRNAs in the UV-response of young *C. elegans* larvae

### 4.1 Introduction

Gene regulation can be performed at different levels of gene expression. Transcription can be regulated by induction or repression of promoter activity. The stability and processing of the transcript may be differentially regulated. Also the rate of translation of the RNA into proteins and finally, protein stability, modification and binding of co-factors may influence activity and functionality. RNA interference (RNAi) presents a mechanism of posttranscriptional gene silencing (PTGS) that is mediated by small (~22nt) non-coding RNAs (reviewed in Lim et al. 2003; Bartel 2004). The phrase RNA interference (RNAi) was coined by Fire and Mello between 1980 and 1990 (Fire et al. 1991). They could show that feeding of *E. coli* expressing double stranded RNA (dsRNA) was efficient in inducing RNAi in *C. elegans* (L Timmons and Fire 1998). More recently it was reported that RNAi is systemic and can spread throughout the organism. The dsRNA is uptaken into cells in the intestine of the worm, then, the RNAi signal spreads into other tissues as well as to the offspring (Lisa Timmons et al. 2003). This makes RNAi in nematodes inheritable (Vastenhouw et al. 2006). There are different classes of small RNAs that are implicated in posttranscriptional gene regulation, e.g. microRNAs (miRNAs), small interfering RNAs (siRNAs) which can be produced from an exogenous trigger dsRNA or as endogenous siRNAs, piRNAs and 21U RNAs (Fischer 2010). The first miRNA to be discovered was *lin-4* in *C. elegans* (R. C. Lee, Feinbaum, and Ambros 1993). It was shown that *lin-4* RNA represses *lin-14* translation by binding to its 3'UTR, thereby regulating the developmental transition from L1 to L2 larval stage (Wightman, Ha, and Ruvkun 1993). After identification of *let-7* as another small non-coding RNA regulating larval transitions and cell fate, this new class of molecules was initially termed small temporally expressed RNAs (stRNAs) as they both control the timing of developmental programs (reviewed in Banerjee and Slack 2002). Only later it was found that members of this novel class of RNA molecules could have diverse functions and therefore were renamed to microRNAs (Lagos-Quintana et al. 2001; Lau et al. 2001; R. C. Lee and Ambros 2001). By now 223 precursor sequences containing 368 mature miRNAs are annotated for *C. elegans* on miRBase (version WBcel215) (Griffiths-Jones

2004). These numbers are several magnitudes higher for man where there are 1,872 hairpin structures encoding for 2,578 mature miRNAs.

#### **4.1.1 miRNA synthesis**

miRNAs are normally encoded distant from annotated genes but could also be found within introns. Then they are preferably oriented in the same direction as the mRNA expressed from that gene (Ruby, Jan, and Bartel 2007). This sub-class of miRNAs could skip certain steps in miRNA maturation and is referred to as mirtrons. Furthermore it was shown that certain miRNA genes form clusters and are contained in multi-cistronic primary transcripts (Lagos-Quintana et al. 2001; Lau et al. 2001). It is assumed that clustered miRNAs may be functionally related because they are co-expressed and under the control of the same promoters. miRNAs are transcribed by RNAP II. The primary transcript (pri-miRNA) is often very long (over 1kb), capped and poly-adenylated (reviewed in Ameres and Zamore 2013) (Figure IV.1).

#### **4.1.2 miRNA maturation**

Pri-miRNAs are targeted by a microprocessor complex containing the RNase III endonuclease Droscha (DRSH-1 in *C. elegans*) (Figure IV.1). A ~60-70nt stem loop precursor (pre-miRNA) is cleaved from the pri-miRNA that defines one end of the mature miRNA and produces an RNase III characteristic 5' phosphate and ~2nt 3' overhang. However, most mirtrons are independent of Droscha processing step because they are already transcribed as stem-loop precursor. Subsequently, the pre-miRNA is exported from the nucleus by Ran-GTP/Exportin5 (XPO-1 in *C. elegans*). In the cytoplasm Dicer RNase III endonuclease chops off the loop and leaves an imperfect duplex comprising the mature miRNA and the opposing strand termed miRNA\* (star strand) (Ketting et al. 2001). The dsRNA is loaded onto a protein complex called RNA induced silencing complex (RISC). It has been reported that different subtypes of RISC exist that vary in their protein composition. *let-7*, for instance, associates with multiple complexes distinct in size, which is dependent on the *let-7* sequence (Chan et al. 2008). These particular RISC complexes may bind miRNAs of similar sequence (e.g. *let-7* family members) but not unrelated miRNAs. Furthermore it has been put forward that ribonucleoprotein complexes associated with miRNAs (miRNP) are distinct from those utilized by siRNAs (Gu et al. 2007; Mourelatos et al. 2002). Argonaute (AGO) proteins are thought to be the core proteins of RISC mediated silencing of the

target mRNA. They could bind double-stranded and single-stranded RNA and some of them possess RNA slicer activity (reviewed in Bartel 2004). Usually, upon loading of the dsRNA onto the RISC, the miRNA\* is rapidly degraded as seen by low abundance of miRNA\* in sequencing

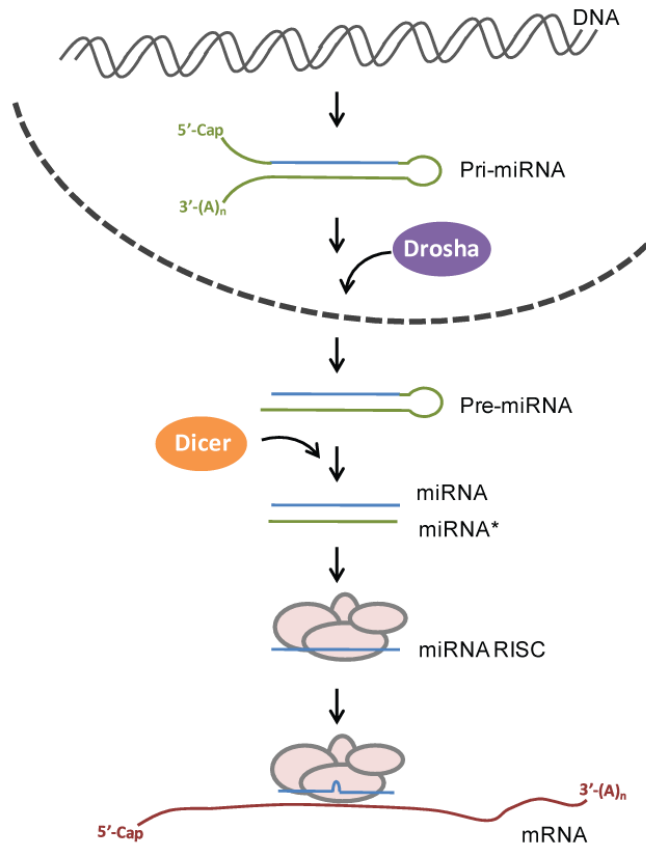


**Figure IV.1 miRNA maturation.**

After transcription of the miRNA gene, the polyadenylated and 5'-capped pri-miRNA is processed by endonuclease Drosha. In the cytoplasm the product of Drosha processing, the pre-miRNA, is digested by Dicer RNase. The double-stranded miRNA precursor is then loaded onto a miRNA RISC where the miRNA\* gets degraded. The ribonucleoprotein complex binds to target regions in the 3'-UTR of mRNAs partially complementary to the miRNA. This triggers posttranscriptional silencing of the mRNA by degradation or translation inhibition.

data of small RNAs as compared to the mature miRNA (Motameny et al. 2010; Warf, Johnson, and Bass 2011). Nonetheless, evidence has been accumulating that certain miRNA\* are used for target gene repression by the RISC and should be taken into account for characterization of miRNA functions (Guo and Lu 2010; Yang et al. 2011).

The characteristics of miRNA maturation are used by different softwares for identification of novel miRNAs such as miRScan (Lim, Lau, et al. 2003; Lim, Glasner, et al. 2003) or miRDeep (Friedländer et al. 2008; An et al. 2013). miRScan was executed on the *C. elegans* and human genome. Criteria for sequences to be denoted as potential miRNA are the prediction of a hairpin structure and conservation that is more stringent to the 5' end of the miRNA than to the 3' end. Furthermore the stem loop should be located outside predicted protein coding regions and be symmetrically shaped (Lim, Lau, et al. 2003). miRDeep has been especially developed for miRNA identification using sequencing data. Sequences are analyzed for their probability to be a

product of the RNAi machinery. Therefore, miRDeep searches in the sequencing data for the complementary strand and the loop region connecting these sequences with the mature miRNA being more abundant than the miRNA\* and the loop. Like miRScan, it calculates the likelihood of transcript folding into a hairpin miRNA precursor. Other requirements of the sequence to be a potential miRNA are the 3' overhang produced by Drosha and Dicer RNase III endonucleases and 5' conservation of the sequence. These features are summarized in a score denoted to every sequence, reflecting the likelihood of that sequence to be a miRNA (Friedländer et al. 2008).

### **4.1.3 Posttranscriptional gene silencing**

Translational repression and/or target mRNA degradation are mediated by base-pairing of the miRNA to complementary sequences in the 3'-UTR of mRNAs (Wightman, Ha, and Ruvkun 1993). Especially base 2-8 at the 5' end of the miRNA, referred to as seed region, have been shown to be of particular importance for target recognition (Brennecke et al. 2005). Biological relevance of the seed region is reflected by the high conservation of seed sequences in homologous metazoan miRNAs. Depending on the degree of complementarity the target is either translationally repressed if the binding is imperfect, or sliced and degraded when the binding is highly complementary. As siRNAs are usually perfect complementary to their target sequence, they lead to AGO-dependent target cleavage of the mRNA. In contrast, miRNA-mediated RNAi does not always induce target degradation. It was proposed that translational inhibition could be achieved either by blocking translation initiation (Ding and Grosshans 2009) or impeding polypeptide elongation (Olsen and Ambros 1999). After performing its action, the miRNP could carry out additional rounds of PTGS as shown by cell culture experiments with controlled concentration of target mRNA and let-7 (Hutvagner and Zamore 2002). Nevertheless, target binding reduces the stability of the miRNA itself and can lead to miRNA destruction (reviewed in Ameres and Zamore 2013).

The major challenge in miRNA characterization is the identification of target genes. Different softwares are available for prediction of target mRNAs, including pictar (Krek et al. 2005; Lall et al. 2006), TargetScan (Lewis, Burge, and Bartel 2005; Jan et al. 2011), ComiR (Coronnello et al. 2012), DIANA microT-CDS (Reczko et al. 2012) and microRNA.org (John et al. 2004; Betel et al. 2008). Despite some differences, all target predictions are based on complementarity of the miRNA seed to sequences in the 3'UTR (and coding sequence) of mRNAs and conservation

scores. Using pictar it was estimated that vertebrate miRNAs regulate ~200 transcripts each (Krek et al. 2005) and that about 10% of *C. elegans* transcripts are under control of miRNAs (Lall et al. 2006). Lewis et al. predict that actually one third of human genes are conserved miRNA targets based on TargetScan software application (Lewis, Burge, and Bartel 2005). Indeed, a larger fraction of human transcripts might be under control of miRNAs as compared to *C. elegans* because of differences in the 3'-UTR length. A recent report revealed an exponential correlation between mean 3'UTR length and the morphological complexity of organisms (C.-Y. Chen et al. 2012). Consistent with this finding, there is evidence for an enrichment of miRNA genes and targets in evolutionary higher developed organisms.

However, often there is only a modest effect of the miRNA on the mRNA target illustrated by a general independency of developmental progression and viability from individual miRNAs in *C. elegans* (Miska et al. 2007). Thus, regulation by miRNAs is rather a 'tuning' of mRNA expression than an on/off switch. Furthermore, the abundance of the miRNA in relation to the overall number of target sites in the transcriptome as well as the dissociation constant for seed match sites (Wee et al. 2012) plays into the degree of target regulation (reviewed in Ameres and Zamore 2013)

#### **4.1.4 miRNA classification**

miRNAs are divided into groups by three different means. As mentioned above, multiple miRNAs could be encoded on the same pri-miRNA molecule and are therefore thought to fulfill related functions (J. Wang et al. 2011). A well-known example is the polycistronic miR-17-92 cluster residing in an intron of the C13orf25 gene that is frequently amplified in lymphomas and overexpressed in lung cancer (Ota 2004; Hayashita et al. 2005; Olive, Jiang, and He 2010). Despite its role in lung cancer growth, miR-17-92 cluster is required for promoting neural stem cell expansion during normal neocortex development of mice (Bian et al. 2013). Because of its upregulation in tumor cell lines and primary tumors, the seven miRNAs comprised in miR-17-92 are referred to as oncogenic miRNAs (oncomiRs) (Hammond 2006).

Second, miRNAs are also grouped into miRNA families by the conservation of their seed sequence. Since the seed sequence is directing the target specificity, miRNAs with identical seed sequences might also share a pool of target mRNAs and are therefore acting redundantly. TargetScan offers the opportunity to search for targets of conserved miRNA families to account

for this redundancy. By way of example, miR-221 family (comprising miR-221 and miR-222) inhibits p27<sup>Kip1</sup> tumor suppressor (Galardi et al. 2007; le Sage et al. 2007), whereas let-7 family members are downregulated in a number of tumor types (C. D. Johnson et al. 2007; S. M. Johnson et al. 2005). Throughout the literature there are several examples for miRNA family members and their functional relationship.

Isoforms are a third group of miRNAs. Initially cleaved from the same pre-miRNA, the mature miRNAs could differ in 2-3 bases in length. These variations could arise from imprecise cleavage of precursors, terminal trimming or attachment of additional nucleotides during miRNA maturation. Moreover, paralogous hairpins and rare ADAR (adenosine deaminase acting on RNA)-editing events are possible sources of miRNA isoforms (reviewed in Ameres and Zamore 2013). Alterations at the 5'-end can produce different seed sequences leading to changed target specificity. Furthermore, differences in miRNA size could also change their affinity for different RISC complexes as suggested by studies in *Arabidopsis thaliana* (Ebhardt, Fedynak, and Fahlman 2010).

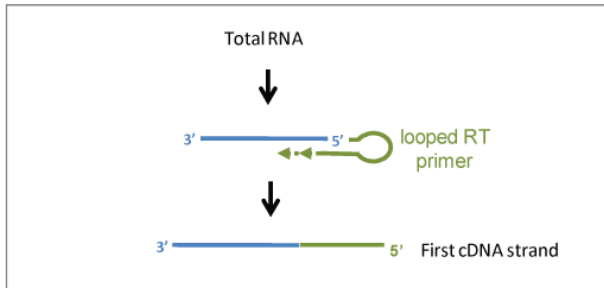
#### **4.1.5 Studying miRNAs**

Analysis of expression profiles can be addressed, for instance, by employment of locked nucleic acid (LNA) microarrays (Pothof et al. 2009). The limitation of this assay is that only known miRNAs can be analyzed and specificity could be a concern. With the advance of deep sequencing it became possible to analyze expression of known as well as to date unknown miRNAs (Friedländer et al. 2008; An et al. 2013). Classically, the results obtained by microarray experiments or sequencing are validated by northern blot analysis (Lau et al. 2001) or qPCR. Unlike real-time qPCR of mRNAs, specificity for miRNA quantification is rather limited. Because of the small size of miRNAs the highest specificity for miRNA amplification and detection can be reached by using a primer or a probe that is complementary to the miRNA itself. Generally, miRNAs need to be extended prior to qPCR amplification (Figure IV.2). In 2005, Chen et al. described an assay utilizing a miRNA stem-loop RT primer to elongate the small RNA during reverse transcription (C. Chen et al. 2005; Schmittgen et al. 2008). Subsequent qPCR is performed using TaqMan-based miRNA-specific primer sets (Figure IV.2A). Alternatively, small RNAs could be extended with a tailed primer during reverse transcription (Raymond et al. 2005). This could be done either with a miRNA-specific primer including the

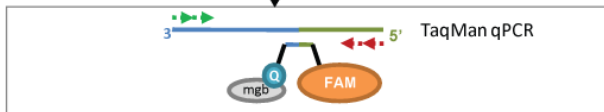
**A****small RNA qPCR assay using looped RT primer**

e.g. TaqMan@MicroRNA Assays (Applied Biosystems)

1. Reverse Transcription

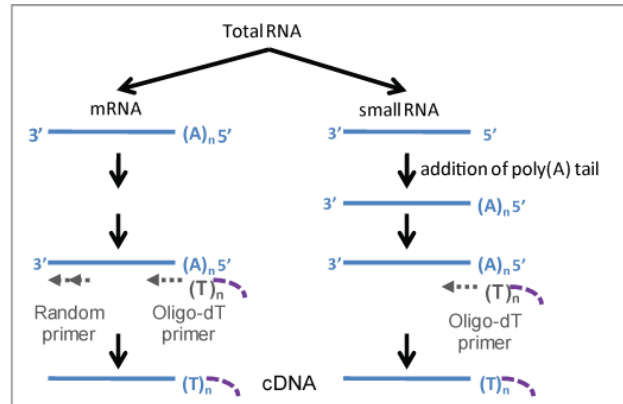


2. Real Time PCR

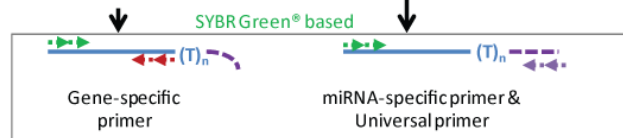
**B****small RNA qPCR assay using tailed RT primer**

e.g. miScript SYBR Green Kit (Qiagen)

1. Reverse Transcription



2. Real Time PCR

**Figure IV.2 Techniques for RT qPCR of small RNAs.**

**A** Small RNA qPCR assay using looped RT primer. During Reverse Transcription small RNAs are elongated using a looped primer that is specific for the miRNA to be analyzed. qPCR is performed using a miRNA-specific primer and primer directed against the loop region. Probes complementary to the miRNA-loop region containing a fluorescent dye (FAM), quencher (Q) and a minor groove binder (mgb) are used for detection of amplification. When the polymerase transcribes the strand, the bound probe will be cleaved and thereby release the fluorescent dye from the quencher resulting in a fluorescence signal.

**B** Small RNA qPCR assay using tailed RT primer. Prior to reverse transcription of the RNA sample into cDNA, RNA is polyadenylated. Next, reverse transcription is performed using an oligo-dT primer fused to universal tag sequence at its 5' end. Then, cDNA samples could be used for qPCR analysis utilizing miRNA-specific primer and primer directed against universal sequence. This protocol allows quantification of mRNA samples from the same cDNA reaction. Amplification during qPCR is monitored by binding of SYBR Green to double-stranded DNA.

tail sequence or by prior polyadenylation of the small RNAs and attachment of the tail to a poly-T primer (Figure IV.2B). Primer directed against the tail sequence is common to all assays whereas specificity is provided by a miRNA-specific forward primer. SYBR Green II fluorescence is used to monitor amplification (Figure IV.2B). The advantage of the SYBR Green-based technique over the TaqMan assay is the possibility to perform melting curve analysis on the amplicates to check for unspecific PCR byproducts. Furthermore, cDNA synthesized using miRNA-non-specific poly-T primer extended with universal tag may be used

for mRNA analysis at the same time whereas the method using a looped primer requires reverse transcription reaction for each miRNA to be analyzed and mRNAs separately. In particular, investigations comparing miRNA and mRNA levels to study target regulation benefit from the common preparation of the two molecule classes.

#### Biological functions of miRNAs

Unlike mammals, *C. elegans* lacks a non-specific interferon response to long dsRNA. To compensate for this, they could utilize RNAi, e.g. for defense against viruses (Wilkins et al. 2005; Schott et al. 2005) or transposons (Sijen and Plasterk 2003). Other than mammals, nematodes and plants have a RNA dependent RNA polymerase (RdRP) to amplify the dsRNA to ensure a robust RNAi response (Alder et al. 2003). Especially for siRNA driven gene silencing this plays an important role.

Irrespective of the role in defense against invading dsRNA elements, miRNAs have been implicated in a great variety of processes, including cell growth (C. D. Johnson et al. 2007; Olive, Jiang, and He 2010), apoptosis (Jovanovic and Hengartner 2006), differentiation (R. C. Lee, Feinbaum, and Ambros 1993; Banerjee and Slack 2002) and stress response (Leung and Sharp 2010). As mentioned afore, miRNAs could be both, oncogenes (oncomiRs) or tumor suppressors. For instance, *let-7* has a tumor suppressor role in suppressing RAS oncogene (S. M. Johnson et al. 2005; C. D. Johnson et al. 2007), miR-335 and -126 have been implicated in metastasis suppression in human breast cancer (Tavazoie et al. 2008) and miR-21 which is often overexpressed in breast tumors, promotes tumor growth (Si et al. 2007). Aberrant expression of miRNAs is observed in many different tumor types and could be connected to kind, progression status and prognosis of tumors (reviewed in Budhu, Ji, and Wang 2010). Thus, it has been suggested to apply clinical miRNA profiling for diagnosis and prognosis (Lu et al. 2005). In addition, targeting miRNAs is a potential treatment for cancer. In this context, there is ongoing debate about application of miRNA inhibitors, like anti-microRNA oligonucleotides (AMOs), miRNA sponges that could repress whole miRNA families by binding, miR-masking to prevent binding of miRNAs to certain targets, or utilization of small molecule inhibitors (Budhu, Ji, and Wang 2010).

Furthermore miRNAs have been also specifically implicated in the response to various stress conditions (Leung and Sharp 2010). Translation inhibition, oxidative stress (Leung, Calabrese, and Sharp 2006) and UV irradiation (Pothof et al. 2009) were efficient in relocalization of

Argonaute protein to stress granules. This relocalization from cytoplasm or P-granules to stress granules was dependent on components of the miRNA-processing machinery. DNA DSBs present a highly toxic insult to cells and need to be repaired. In the last decade evidence accumulated that the DNA damage response to DSBs is tightly regulated by miRNAs at all stages (H. Hu and Gatti 2011). In human miR-24 inhibits DSB-sensor H2AX, while the ATM and ATR kinases were shown to be regulated by miR-421. Even effectors of the DNA damage response, important for DNA repair, checkpoint activation and apoptosis induction, are regulated by a number of miRNAs. Interestingly, p53 tumor suppressor that coordinates the response to different stresses is directly regulated by a miRNA. miR-125b suppresses p53 under normal conditions in zebrafish and human (Le et al. 2009; B. Wang et al. 2002). Upon IR treatment, miR-125b is downregulated, thus, p53 inhibition is released and apoptosis executed. Downstream to DNA damage activation of p53, several miRNAs contribute to the cellular DNA damage response (reviewed in Hu and Gatti 2011). Among those, miR-34 family members are induced to halt cell-cycle progression.

Besides a rather well defined role of miRNAs in response to DSBs, their contribution to UV-induced DNA damage response, remains poorly understood. Importantly, the cellular DNA damage responses are specific to the kind of DNA damage because of differences in the required repair pathway and toxicity of the lesion itself.

However, a study from 2012 revealed miR-125b upregulation upon UV irradiation in cell culture (Tan et al. 2012). They provide evidence for miR-125b-dependent p38 $\alpha$  suppression to protect cells from UV-induced apoptosis. This illustrates that certain responses to different DNA damage types are shared.

#### **4.1.6 Aim of the study**

Here, we investigated the miRNAs differentially regulated upon UV irradiation in *C. elegans*. We aimed to define the role of miRNAs and their targets after irradiation to provide a better understanding of miRNA regulation of the DNA damage response. *C. elegans* as model organism is especially suitable for this purpose because of its rather short 3'-UTRs as compared to higher organisms (C.-Y. Chen et al. 2012). This might facilitate miRNA and target identification. Furthermore its genome is completely sequenced and many genetic tools are available.

## 4.2 Results

### 4.2.1 Establishment of a deep sequencing approach to analyze the miRNA profile upon UV irradiation

In order to characterize the miRNAs responding to UV irradiation we compared differentially regulated small RNAs in synchronized populations of *C. elegans*. L1 larvae at earliest developmental stage were irradiated with 60mJ/cm<sup>2</sup> or mock-treated. To give time for gene regulation, worms were incubated 4h in the presence of food (Figure IV.3). Importantly, after isolation of total RNA the integrity of the sample was determined using a Bioanalyzer (Agilent) to avoid a high load of degraded RNA in the small RNA fraction (Figure IV.4). RNA integrity number (RIN) was calculated using the Agilent software. Here, the entire electrophoretic trace of the RNA sample is taken into account and categorized by assigning numbers from 1 to 10 with 10 being the most intact. The curve of an RNA sample detected by gel electrophoresis typically shows a peak at the height of 18S and 28S fragment of rRNA. RIN calculation also reflects signal intensity at 5S rRNA region, inter-region between 18S and 28S as well as precursor region

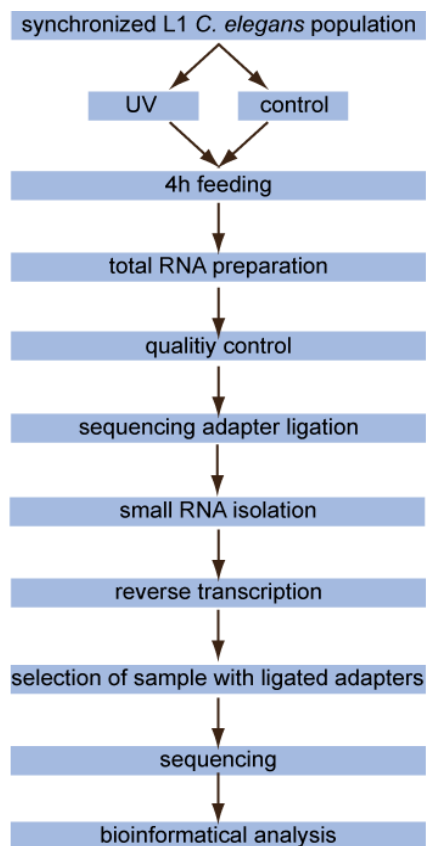


**Figure IV.3 Workflow for sequencing of differentially regulated small RNAs comparing untreated with UV-irradiated *C.elegans*.**

and post-region running at higher molecular weight than 28S fragment. All samples had a RIN  $\geq$  8.20, except for control sample 3. Since *C. elegans* is grown on *E. coli* OP50, all samples contained bacterial rRNA. The procaryotic rRNA 16S and 23S subunits as opposed to eukaryotic 18S and 28S subunits have a lower sedimentation rate and lower molecular weight. The contribution of bacterial RNA to the samples can be seen as a double peak in the curve of RNA signal intensity in Figure IV.4. The contamination with bacterial RNA in the *C. elegans* RNA samples leads also to a reduced RIN scoring. The contribution of bacterial RNA to the sample is most probably the reason for the software failing in RIN determination for control sample 3. Nevertheless, as judged from low abundance of small RNA fragments, RNA samples showed little degradation and good quality. Next, adapters for sequencing were ligated, small RNAs isolated and reverse transcription performed following sample preparation guide v.1.5 (Illumina) (Figure IV.3).

The obtained sequencing data were processed by several alignment and selection steps to find UV regulated miRNAs (Motameny et al. 2010) performed at the Cologne Center for Genomics (CCG). First, by alignment to the *C. elegans* genome not only the OP50-derived sequences were excluded from the pool of reads for further analysis but also reads of low quality or sequencing errors. Known miRNAs were identified by alignment to miRNA sequencing data from miRBase (Griffiths-Jones et al. 2008). Deep sequencing read length produced by Illumina Genome Analyzer typically is about 36 nucleotides long. Mature miRNAs are usually only 21-25 nucleotides long (reviewed in He and Hannon 2004). Hence, sequencing reads contain adapter

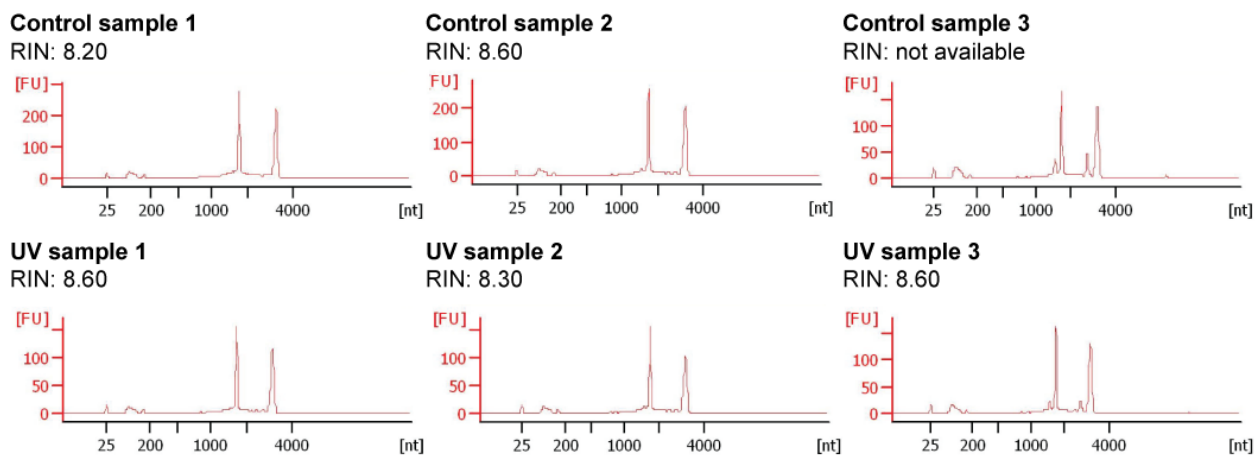


**Figure IV.4 RNA integrity of samples for small RNA sequencing.**

RNA integrity was determined using bioanalyzer and calculation of RIN as described in the text.

sequences that have to be removed prior to further analysis (Motameny et al. 2010). To narrow down the pool of reads even more, miRNA-unrelated non-coding short RNAs, like rRNAs, tRNAs, small nuclear, small nucleolar and small cytoplasmatic RNAs were filtered out using the University of Santa Cruz (UCSC) Genome Browser. During Illumina Sequencing single nucleotides could be introduced leading to sequencing errors that were excluded by removal of reads with low read number. Finally, expression analysis was performed to identify small regulatory RNAs specifically regulated upon UVB irradiation. Expression levels are represented as reads per million (rpm). This representation makes the normalization to a reference gene dispensable and is an advantage of sequencing technique over microarray or qPCR expression analysis.

#### 4.2.2 Sequencing reveals regulation of small RNAs after irradiation with UV light.

Deep sequencing produced between 19.5 million and 20.7 million reads for each sample of which between 50% and 67% aligned to the *C. elegans* genome (Table IV.1). These results are within the expected range and are similar to data obtained in previous studies (Warf, Johnson, and Bass 2011). About one quarter of all reads were known miRNAs. Expression analysis revealed 21 known miRNAs being significantly regulated after UV irradiation (Table IV.2). Of those, seven were downregulated and 14 upregulated. *lin-4* downregulation was strongest of all miRNAs identified after UV irradiation. Among the miRNAs that were downregulated, there were three members of the *let-7* family of miRNAs: *let-7*, *mir-48* and *mir-241* (Table IV.2). A list of all *let-7* family members and information about sequence conservation can be found in Figure IV.11 A. Although not significantly, also *mir-84*, *mir-795* and *mir-1821* were downregulated by trend. *mir-2211* has been initially identified in a screen for small non-coding RNAs regulated during *C. elegans* development (Kato et al. 2009). Until now not much is known about function and targets of this miRNA. Also *mir-1830* and *mir-1829c* are uncharacterized so

Sample	No. total reads	No. reads aligning to <i>C.elegans</i> genome	% of total reads aligning to <i>C. elegans</i> genome	No. of reads aligning to known miRNAs	% of reads aligning to known miRNAs
Control 1	19,505,375	12,987,240	67	5,569,023	29
Control 2	19,883,814	12,955,297	65	5,036,779	25
Control 3	20,709,499	10,382,101	50	5,036,779	23
UV 1	20,767,986	11,317,108	54	5,203,343	25
UV 2	20,584,702	12,661,736	62	4,939,950	24
UV 3	19,687,658	10,909,345	55	4,643,241	24

**Table IV.1 Sequencing output and alignment.**

far. However, here, they were found to be downregulated in UV-treated L1 larvae as well (Table IV.2). In 2010, De Lencastre et al. showed that *mir-71* and *mir-238* are upregulated with aging and mutants are short-lived (de Lencastre et al. 2010). In our sequencing approach we find both miRNAs being induced after treatment with UV light. *mir-80* is found in one cluster (within less than 3kb, according to wormbase.org) with *mir-238* and, consistently, is also upregulated in response to irradiation. Interestingly, it was documented that *mir-80* mutants show features of dietary restriction and are long-lived which is under control of the insulin/IGF-1 pathway (Vora 2011). Moreover, *mir-80* belongs to *mir-58* family of miRNAs (Alvarez-Saavedra and Horvitz 2010) of which also *mir-58* is induced upon UV irradiation. *mir-235* that is upregulated in L1 upon UV irradiation has been shown to be implicated in L1 diapause since its mutant fails to maintain diapause state in the absence of food (Kasuga et al. 2013). The human homologue, miR-92, is part of the oncogenic miR-17-92 cluster and is overexpressed in different types of cancer (Hayashita et al. 2005; Olive, Jiang, and He 2010). Three out of six *mir-51* family members (*mir51-56*) were also upregulated. In particular *mir-51*, *-52* and *-54* were 2.1-fold, 1.9-fold and 3.1-fold induced by UV irradiation, respectively (Table IV.2). Mutants for *mir-51* family members are characterized by embryonic lethality, failure in growth, male mating, and pharyngeal attachment, acting redundantly to each other (Shaw et al. 2010). *mir-64* was more abundant upon UV irradiation but no other miRNAs from the same cluster, including *mir-229*, *mir-65* and *mir-66*. Previously *mir-64* was found upregulated in a Parkinson's disease model of *C. elegans* (Martinez-Finley et al. 2011). To what extent this stands in connection to its UV responsiveness remains to be elucidated. In line with our finding that *mir-87* is upregulated upon UV irradiation, Kagias, K. and Pocock, R. (2011) describe defects in the DNA damage response, in body morphology under hypoxia and in reproduction. They attribute the phenotypes to the regulation of *rnr-1* (*RiboNucleotide Reductase-1*) that is important for dNTP biosynthesis. *mir-789*, *mir-228* and *mir-230* are significantly upregulated after irradiation but are uncharacterized, yet. Finally, *mir-2214\** was highly upregulated upon irradiation. So far it remains elusive how it is decided which strand of the pre-miRNA duplex is used for RISC-mediated gene silencing. While the miRNA\* strand was initially thought to function as a carrier strand for the miRNA, later studies showed conservation and biological functions for certain miRNA\*s (Okamura et al. 2008; Guo and Lu 2010; Yang et al. 2011; Tong et al. 2013).

miRNA	read sequence	fold change	p value	validation by qPCR
<i>lin-4</i>	TCCCTGAGACCTCAAGTGTGA	-13.28	0.012	yes
<i>mir-241</i>	TGAGGTAGGTGCCGAGAAATGA	-9.71	0.002	no
<i>mir-48</i>	TGAGGTAGGCTCAGTAGATGCCGA	-4.20	0.005	yes
<i>mir-2211</i>	TCAGGTAGAATTTAGAGGAGAAA	-2.46	0.030	yes
<i>let-7</i>	TGAGGTAGTAGTTGTATAGTT	-1.95	0.025	yes
<i>mir-1830</i>	AATGGCACTGCATGAATTCACGTTTTCTTTGCCTT	-1.74	0.015	yes
<i>mir-1829c</i>	AAGCGAAATTCAGATGTTGTA	-1.23	0.024	no
<i>mir-238</i>	TTTGTACTCCGATGCCATTCAGAATTCGTATGCCG	1.67	0.002	yes
<i>mir-789</i>	CCCTGCCTGGGTCACCA	1.70	0.002	no
<i>mir-71</i>	TGAAAGACATGGGTAGTGAGAATTCGTATCCGTC	1.83	0.009	yes
<i>mir-235</i>	TATTGCACTCTCCCCGGCCTGA	1.91	0.026	yes
<i>mir-52</i>	CACCCGTACATATGTTTTCGCGCT	1.92	0.008	no
<i>mir-58</i>	TGAGATCGTTTACGTACGGCAATTTTTGGATGGCGTT	1.98	0.006	no
<i>mir-51</i>	TACCCGTAGCTCCTATCCCTGTT	2.13	0.003	no
<i>mir-64</i>	TATGACACTGAAGCGAGTTGGAAAC	2.31	0.007	no
<i>mir-228</i>	AATGGCACTGCATGAATTCACGGGTCTCGTATTTTCG	2.48	0.001	no
<i>mir-87</i>	GTGAGCAAAGTTTCAGGTGAGC	2.52	0.006	no
<i>mir-230</i>	GTATTAGTTGTGCGACCCGGAGA	2.79	0.004	no
<i>mir-54</i>	TACCCGTAATCTTCATAATCCGAGC	3.15	0.002	no
<i>mir-80</i>	TGAGATCATTAGTTGAAAGCAG	3.44	0.003	no
<i>mir-2214*</i>	AATTCGGTCCGGAGTCAATGGG	5.70	0.001	yes
<i>ncRNAa</i>	GACCACCGGTCCGGAGTTTGTGGGT	1.77	0.004	yes
<i>ncRNAb</i>	GCCCTACTCTTCGCATCTCATC	-1.69	0.003	no
<i>ncRNAc</i>	CGGCGTTAGCTCTGTGTCAAACC	-4.03	0.000	yes
<i>ncRNAd</i>	AGTGGAGTGGATGACGACGACGA	-3.70	0.001	yes
<i>ncRNAe</i>	GAATAGATACGCGGTATGA	2.10	0.003	no
<i>ncRNAf</i>	GGAAATGGATTAGAATCGTGGAAA	-2.16	0.002	yes
<i>ncRNAg</i>	AATTGATGACTCAGGCAGGGACT	1.65	0.014	no
<i>ncRNAh</i>	CCTAGGAAATGAGAAAACCTCGGC	-1.76	0.050	no
<i>ncRNAi</i>	CGCGGGACTAGTCAAGTGTCCGGC	-3.67	0.036	no
<i>ncRNAj</i>	GGTGGTTTTCTCTGCAGTGATA	-1.87	0.018	no
<i>ncRNAk</i>	TGACTATCTCATCAACTTACAG	1.48	0.006	no
<i>ncRNAl</i>	TGGGGTTGTAGATATAGAAGA	1.37	0.021	no

Color code marks up- (green) and down- (red) regulated genes as found by sequencing analysis.

**Table IV.2 List of significantly ( $p \leq 0.05$ ) regulated small RNAs after UV irradiation.**

In addition we were able to identify 12 potentially novel miRNAs responsive to UV irradiation (Table IV.2). We used miRDeep software for this purpose. These new miRNAs are referred to as *non-coding RNAa-l (ncRNAa-l)* (Table IV.2).

For validation of sequencing data, qPCR experiments were performed using the same whole RNA samples as used for sequencing. To perform expression analysis using qPCR a reference

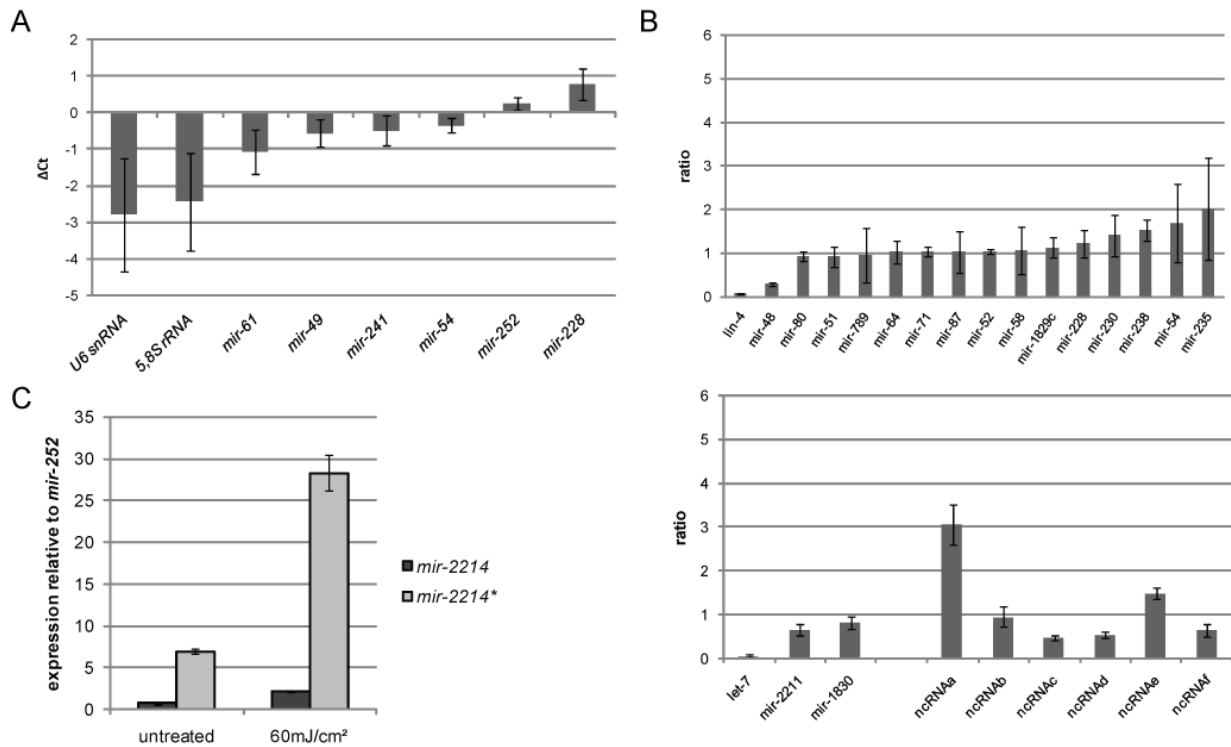


**Figure IV.5 Validation of sequencing results by qPCR.**

**A** Establishment of a small RNA reference for qPCR. qPCR analysis of miRNAs using miScript. Shown is the  $\Delta C_t$  as average difference between three control and three UV-treated samples. Error bars indicate standard deviation.

**B** miRNA expression analysis in UV-treated L1 larvae compared to untreated animals using miScript qPCR. Three biological replicates for each condition were examined. Analysis was performed in three independent experiments. Therefore results are shown in individual graphs. Error bars represent standard error of mean.

**C** Expression of *mir-2214\** and *mir-2214* relative to *mir-252* control in untreated and UV-treated L1 larvae determined using miScript qPCR. Three biological replicates were conducted for analysis. Error bars represent standard error of mean.

gene is needed for normalization. Commonly used references for small RNA assays are U6 snRNA and 5.8S rRNA. Furthermore six miRNAs that are not regulated after UV irradiation were chosen from the sequencing data (Figure IV.5A). miScript qPCR was performed on total RNA samples. Unexpectedly, U6 snRNA and 5.8S rRNA were downregulated by more than two Ct. *mir-252* showed the least difference between control and UV-treated samples and was therefore chosen as reference for further analysis (Figure IV.5A). RNA samples were transcribed into cDNA according to miScript (Qiagen) manual and qPCR performed. Of 33 candidate

miRNAs we could validate the UV-dependent regulation of 14 of them (Figure IV.5B and Table IV.2). Criteria for validation were that the miRNA was changed at least 1.5-fold and regulated in the same direction as determined by sequencing. For the other 19 no regulation could be found by qPCR (Figure IV.5B). There are several possible reasons for differences of expression regulation measured by sequencing and qPCR. Low abundance of the miRNA or minor expression changes may cause poor reproducibility. Furthermore, the two approaches differ in their detection technique of the miRNA, normalization method and also procession of data by software and threshold settings (Motameny et al. 2010). As mentioned earlier, primer design for miRNA qPCR presents a challenge because of small size of the miRNA which might affect melting temperature and specificity of the assay. Also the discrimination of precursor and mature miRNAs displays a major limitation for qPCR based expression analysis of small RNA molecules. Although regulation of only 42% of the miRNAs could be confirmed, regulation in the opposite direction between the two assays was never observed proofing the principle reproducibility and correctness of the sequencing and qPCR approach.

Finding *mir-2214\** regulation after UV irradiation prompted us to test expression levels and regulation of its complementary strand *mir-2214*. Both strands were more abundant after UV irradiation suggesting transcriptional regulation of the miRNA precursor (Figure IV.5B and C). In contrast to the expectation that the miRNA\* is degraded once the miRNA is loaded into the RISC we found *mir-2214\** over ten times higher abundant than *mir-2214* (Figure IV.5C). This finding is in line with expression data from our sequencing approach. Our results indicate that *mir-2214\** but not *mir-2214* could have a role in posttranscriptional regulation of the UVB response in *C. elegans*.

#### **4.2.3 Investigation of UV-dose-dependency and timing of the miRNA regulation.**

To further characterize the miRNA regulation after UV irradiation, two experiments were performed: First, we wanted to see whether our candidate miRNAs are regulated in a UVB dose-dependent manner (Figure IV.6A). Second step was examination of the miRNA response timing to identify beginning and peak of miRNA regulation as well as the time needed for recovery to normal expression levels (Figure IV.6B). In 2009 it has been suggested by Pothof et al. that UV-induced posttranscriptional regulation by miRNAs is timed after the fast protein modifications

followed immediately after DNA damage detection and before the late transcriptional regulated checkpoint activation.

For analysis of dose-dependency, L1 larvae were treated with UVB doses ranging from 20 to 100mJ/cm<sup>2</sup> (Figure IV.6A). *lin-4* and *let-7* were downregulated in a dose-dependent manner reaching a minimum with a dose between 60 and 80mJ/cm<sup>2</sup>. Dose-dependent upregulation was observed for *mir-235*, even stronger for *ncRNAa* and strongest for *mir-2214\** (Figure IV.6A). Despite some variation in expression levels in the biological replicates we confirmed *ncRNAc* downregulation in UV-treated worms. For *mir-71* and *mir-238* we could not reproduce the regulation observed in previous experiments. *mir-48*, *mir-2211*, *ncRNA d* and *ncRNA f* expression

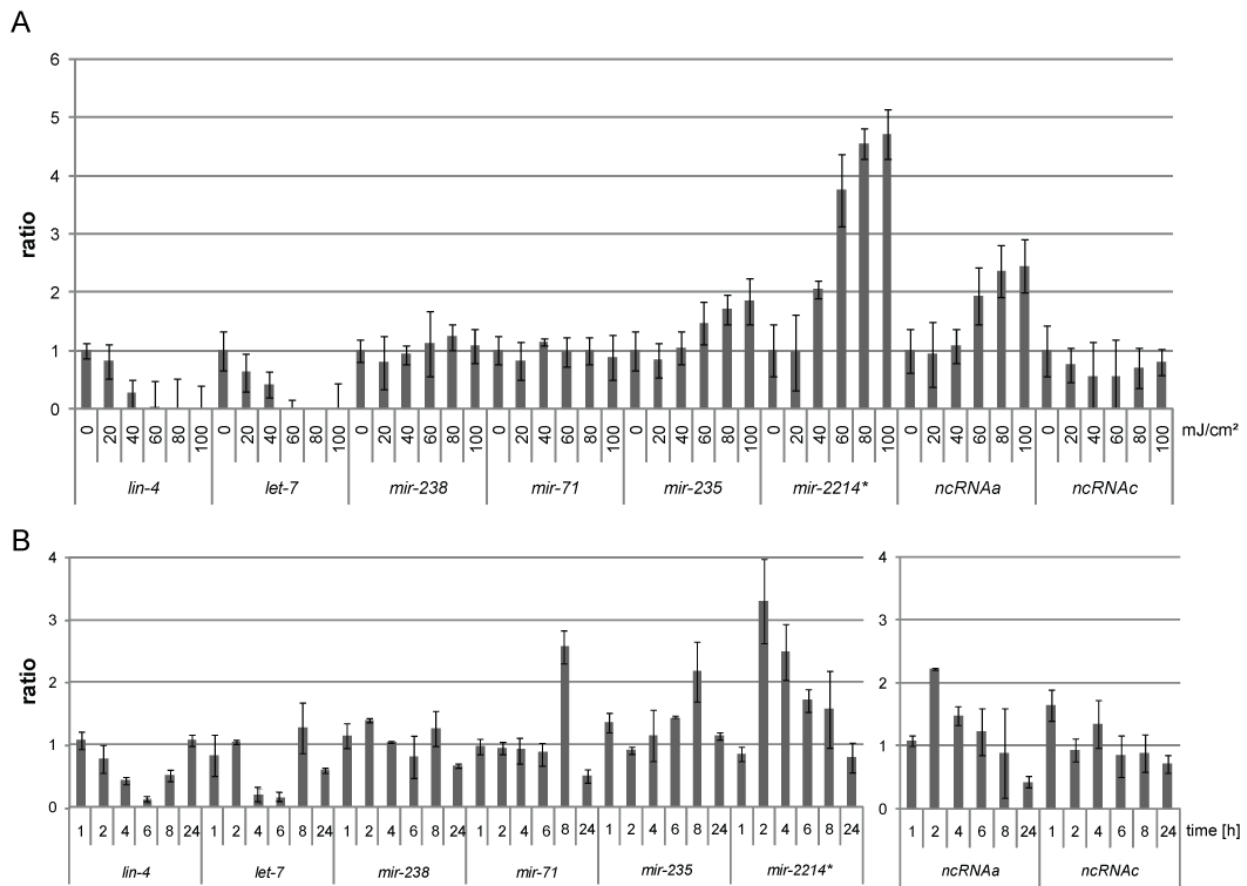


**Figure IV.6 miRNA candidate expression dose-dependency and timing.**

**A** Dose-dependency of candidate miRNAs measured by qPCR. Three independent biological replicates and for each three technical replicates were analyzed by miScript qPCR. Error bars represent standard error of mean.

**B** Timing of miRNA regulation after UV-treatment between 1h and 24h post irradiation. L1 larvae were irradiated with 60 mJ/cm<sup>2</sup> UV and RNA was isolated at the indicated timepoints after irradiation. qPCR for *ncRNAa* and *ncRNAc* was performed in a separate reaction and therefore data are shown in a different graph. Two biological duplicates and three technical replicates were used for miScript qPCR analysis. Error bars represent standard error of mean.

changes were not confirmed because of technical limitation of the assay as seen by double peaks in the amplicates' melting curves.

For characterization of miRNA response timing we irradiated synchronized L1 larvae with 60mJ/cm<sup>2</sup> UV and isolated RNA after 1h, 2h, 4h, 6h, 8h and 24h (Figure IV.6B). *lin-4* and *let-7* levels decreased in UV-treated samples compared to untreated controls starting at 4h post irradiation, reaching minimum at around 6h and returned to baseline levels 2h later. The next day miRNA expression levels were completely restored. These results are in line with a previous study on *let-7* expression in human lung cancer cells (Weidhaas et al. 2007). The authors showed that *let-7* is downregulated after 2h post IR treatment and recovered till the next day. *mir-238*, *mir-71*, *mir-235* and *ncRNAc* expression after UV irradiation over time was not clearly regulated. Induction of *mir-2214\** and *ncRNAa* peaked 2h after irradiation and recovered within the next 6 to 8h (Figure IV.6B). We also tested again *mir-2214* but found high variation probably ascribed to generally low abundance of *mir-2214* in the RNA samples. The general timing of the miRNA response further supports the hypothesis that the posttranscriptional regulation by miRNAs during the DNA damage response takes place after the fast re-localization and modification of repair and checkpoint proteins and before the late transcriptional response starting at around 9h after the DNA damaging insult (Pothof et al. 2009).

#### **4.2.4 *let-7* and *lin-4*, mediators of larval transitions, are differentially expressed after UV irradiation.**

In 2006 Baugh and Sternberg showed that YFP expression under the control of *lin-4* promoter is dependent on DAF-16/FOXO transcription factor (Baugh and Sternberg 2006). Hence, we hypothesized that also *lin-4* repression in response to UV irradiation is dependent on *daf-16*. We utilized two different *daf-16* mutant strains to test this (Figure IV.7B). However, we did not find any difference in *lin-4* regulation between wildtype and *daf-16(mn26)* point mutant. Opposite to our expectation we found even enhanced upregulation of *lin-4* at L2 larval stage with *daf-16(mu86)* deletion mutant.

*lin-4* and *let-7* are part of a regulatory network controlling developmental transitions in *C. elegans* (Figure IV.7A, reviewed in Flynt and Lai 2008). *lin-14* transcription factor suppression is crucial for L1 to L2 molting which is regulated by *lin-4* (Hristova et al. 2005). *let-7* is only induced at L4 larval stage (Figure IV.7A) where it is required to repress *lin-41* mRNA and

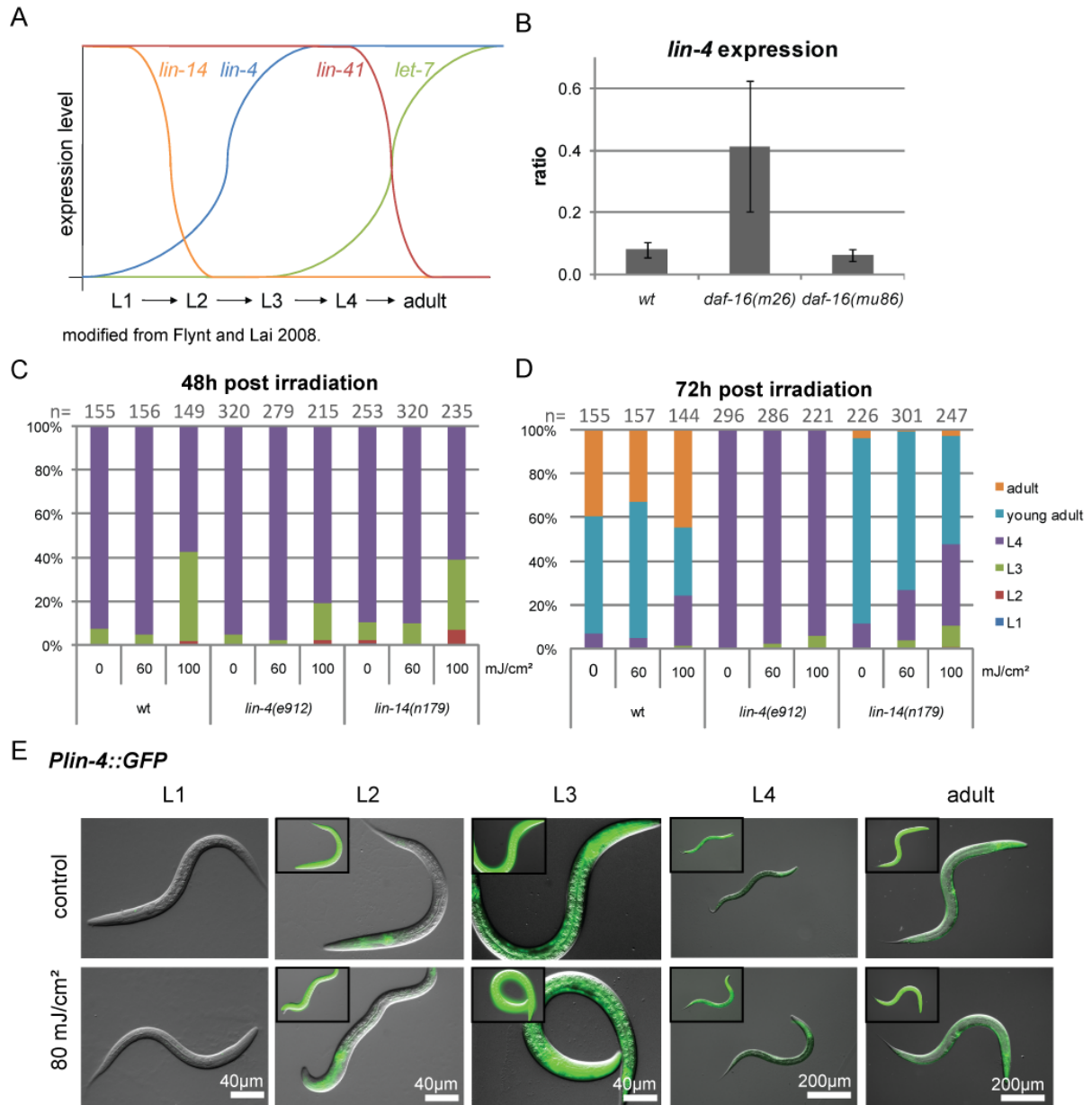


**Figure IV.7 *lin-4* and *lin-14* are dispensable for DNA damage response to UV irradiation.**

**A** Scheme showing regulation of *lin-14* by *lin-4* at L1/L2 transition and *lin-41* by *let-7* at L4/adult transition.

**B** Independency from *daf-16* of *lin-4* after UV-treatment. Worms of at L1 larval stage were irradiated with 100mJ/cm<sup>2</sup> UV and RNA was isolated 3.5h later. Three independent biological replicates and three technical replicates were used for TaqMan qPCR analysis. Error bars represent standard error of mean.

**C and D** Developmental progression of wildtype (wt), *lin-4* and *lin-14* mutants 48h and 72h after irradiation at L1 stage. The number of worms (n) is indicated on top of the columns.

**E** Irradiation does not change *Plin-4::GFP* expression throughout development. Synchronized worms at the indicated stage of development were irradiated with 80mJ/cm<sup>2</sup>. DIC and GFP pictures were taken 4h later. Micrographs of L1 larvae and inset pictures of L2 to adulthood display equal exposure time for GFP detection. Micrographs of L2 to adult worms were taken using a lower but equal exposure time to avoid overexposure in all images.

thereby, enable L4 to adult transition (Reinhart et al. 2000). Taking *lin-4* expression changes during development into account the changes observed upon UV irradiation could be caused by a delay in development of the UV-treated in comparison to untreated animals. In response to UV irradiation worms arrest transiently to give time for repair. Because of this untreated worms might have upregulated *lin-4* already at L1/L2 transition whereas irradiated worms did not due to developmental delay (Figure IV.7A).

To see what function *lin-4* repression has during the DNA damage response, L1 larvae were treated with UV radiation and developmental progression was documented. Wildtype worms were delayed in their development when treated with 100mJ/cm<sup>2</sup> UV 48h after irradiation (Figure IV.7C). The same was true for *lin-4* and *lin-14* mutants. 72h after L1 stage *lin-4* worms were still mainly at L4 stage while *lin-14* and wildtype worms progressed already to young adult and adult stage (Figure IV.7D). Slow development of *lin-4* was independent of UV irradiation. Despite strong repression of *lin-4* at L1 stage after UV-treatment (Figure IV.5B, Figure IV.6 and Figure IV.7B), we did not observe any changes in *Plin-4::GFP* reporter expression after irradiation with 80mJ/cm<sup>2</sup> UV (Figure IV.7E). Developmental delay in wildtype worms (Figure IV.7C and D) and no obvious changes in *Plin-4::GFP* expression at L1 stage (Figure IV.7E) further support the hypothesis that *lin-4* expression is suppressed in UV-treated larvae due to transient arrest in development providing time for repair.

Next, we assayed developmental progression of *let-7* mutant and a mutant for its target, *lin-41*, after irradiation (Figure IV.8). The experiment was performed in parallel at 15, 20 and 25 degrees because *let-7(n2853)* was reported to be a temperature sensitive allele showing the strongest phenotype at 25 degrees. *let-7* mutant and *lin-41* mutant worms were delayed compared to N2 worms at 20 (Figure IV.8B) and 25 degrees (Figure IV.8C). More strikingly, *let-7* mutant animals died at L3 larval stage at the semi-restrictive and restrictive temperature of 20 and 25 degrees leaving low number of worms for analysis of developmental progression. 48h after L1 stage almost all *let-7(n2853)* worms were dead but not in the UV-treated samples. However, *let-7* and *lin-41* mutants were not sensitive to UV-induced developmental arrest suggesting that they are dispensable UV-resistance.

As the target of *let-7*, *lin-41*, is repressed by *let-7* through binding to its 3'-UTR, *lin-41* expression changes are expected to be opposite to those of *let-7*. We investigated *lin-41* expression levels in response to different UV doses and followed its expression pattern through

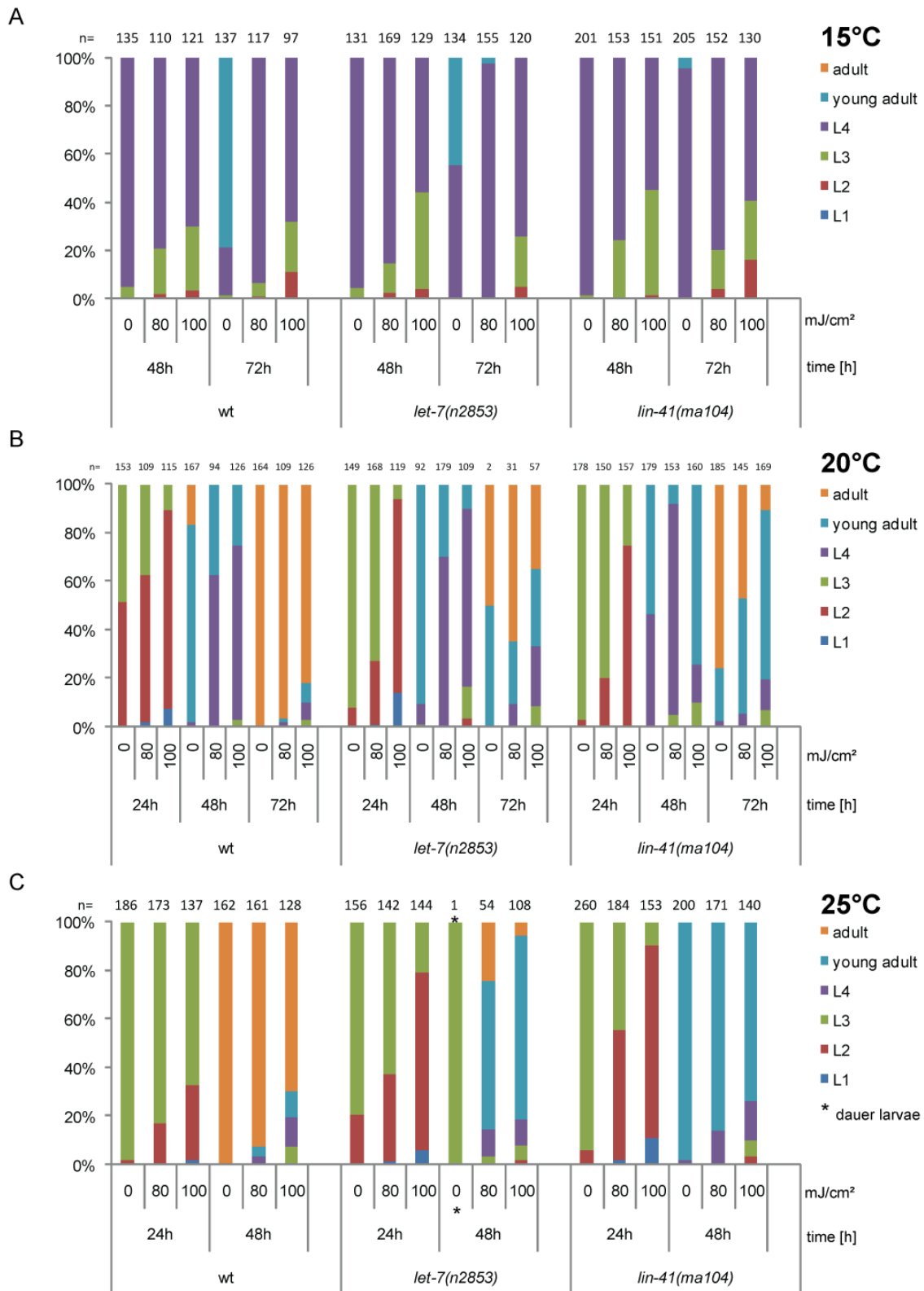


**Figure IV.8 Temperature-independent *let-7* and *lin-41* mutants are not sensitive to UV light.** Synchronized L1 larvae were irradiated with 0, 80 or 100mJ/cm<sup>2</sup> and incubated at 15°C (A), 20°C (B) or 25°C (C). Developmental progression was documented after 24, 48 and 72h. The number of worms analyzed is denoted on top of the columns (n) and illustrates dying of *let-7(n2853)* at the restrictive temperature of 20 and 25°C at L3 stage.

time. *lin-41* mRNA levels were downregulated using a dose of 60mJ/cm<sup>2</sup> but not with lower or higher UV dosages (Figure IV.9A). Paradoxically, this effect could be observed at 1h and 8h after irradiation (Figure IV.9B). In conclusion, the *lin-41* qPCR data indicate that *lin-41* expression is not opposite to *let-7* abundance. Therefore, we propose *let-7* regulates *lin-41* by translational repression rather than mRNA degradation. However, these findings stand in contrast to a study from 2005 where the authors show that *lin-41* mRNA levels are decreased in the presence of *let-7* but not in a *let-7* mutant (Bagga et al. 2005). Using a reporter strain expressing GFP under the control of *let-7* promoter we could confirm *let-7* upregulation during development (Figure IV.9C). While observing only low signal in the intestine and a head neuron at L1 stage, expression increased gradually in all tissues during development and was not changed if worms were UV-treated 4h prior to GFP documentation. In addition, we examined a *mir-48* promoter GFP reporter (Figure IV.9D). *mir-48* is a member of the *let-7* family of miRNAs and we found that it responds to UV irradiation by being suppressed four-fold at L1 stage (Table IV.2 and Figure IV.5B). Overall *Pmir-48::GFP* expression levels were much lower as compared to *let-7* reporter strain (Figure IV.9C and D). Starting from L3 larval stage expression in a head neuron was observed. Subsequently, with the beginning of L4 stage, expression was detectable in the whole body and strongest in the head neuron and the vulva. Like *let-7*, *mir-48* promoter activity was not changed upon UV-treatment (Figure IV.9D). Taken together, we conclude that *lin-41* is dispensable for a UV response in *C. elegans* and furthermore that *let-7* and *mir-48* promoter activity is robust in the presence of UV-induced DNA lesions, indicating that regulation might be executed rather on the posttranscriptional level. Alternatively, GFP reporters might not be sensitive enough to show expression level changes seen by sequencing and qPCR.

*let-7* is highly conserved and is represented in human by 10 family members (Figure IV.10A, Roush and Slack 2008). To see if the UV-induced suppression is conserved in human we utilized RNA samples from three different cell lines and performed qPCR for *let-7* family members a-i. U2OS osteosarcoma cells did not show regulation of any of the tested *let-7* miRNAs under the conditions used (Figure IV.10B). However, *let-7a* was slightly upregulated and *let-7b* downregulated in HEK293T cells (Figure IV.10C). Strikingly, we found suppression of *let-7a*, *let-7b*, *let-7c* and *let-7i* upon treatment with UV light in hTERT-immortalized normal human fibroblasts (*C5RO-hTERT*) (Figure IV.10D). On the one hand this shows that *let-7* miRNAs are

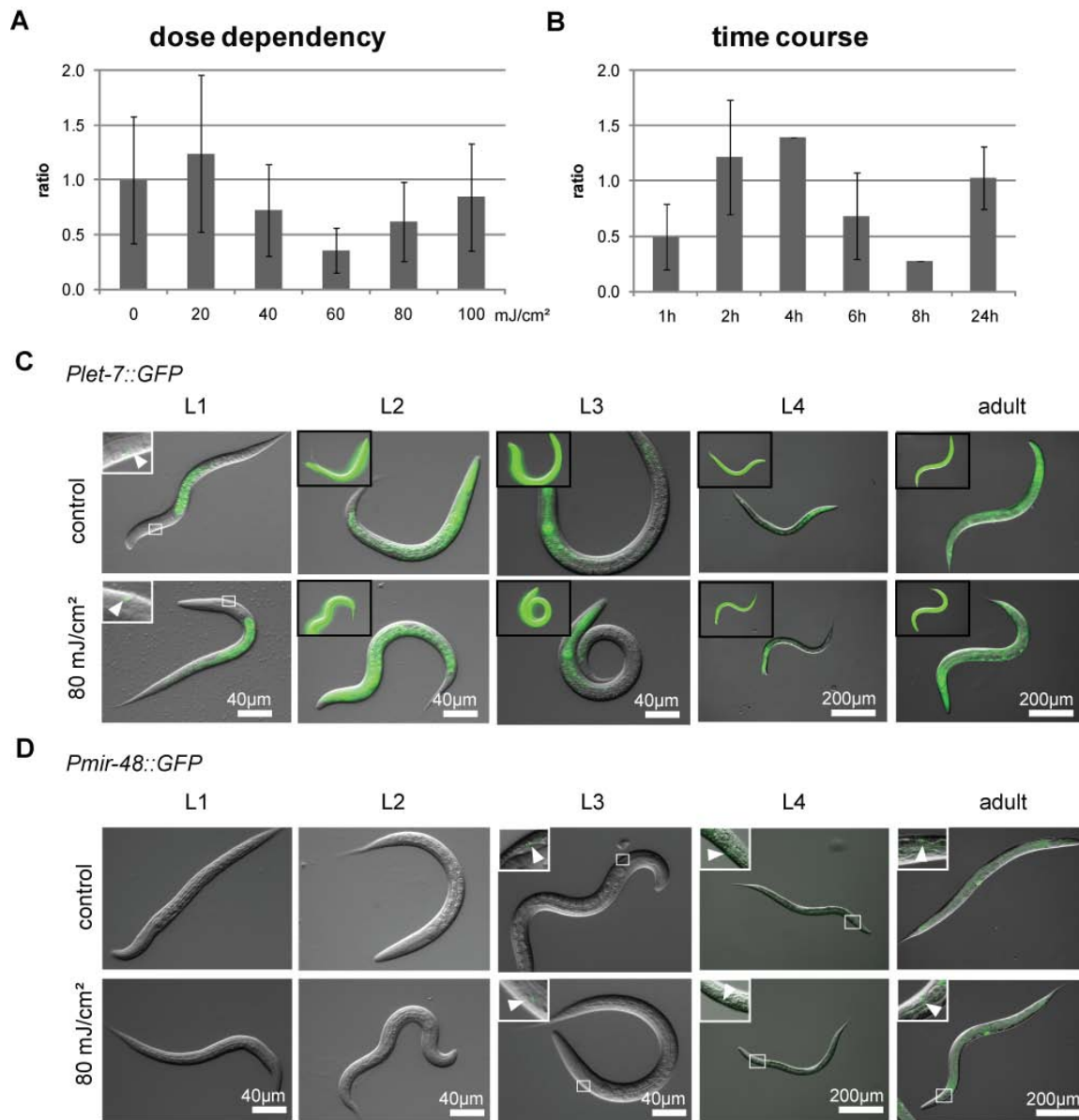


**Figure IV.9 *lin-41* mRNA levels and *let-7* and *mir-48* promoter activity are independent from UV irradiation.**

**A** Dose-dependency of *lin-41* mRNA expression was measured by qPCR. Three independent biological replicates and three technical replicates were used for miScript qPCR analysis. Error bars represent standard error of mean.

**B** Timing of *lin-41* expression after UV-treatment between 1h and 24h post irradiation. L1 larvae were irradiated with 60 mJ/cm<sup>2</sup> UV and RNA was isolated at the indicated time-points after irradiation. qPCR was normalized to actin, lamin and tubulin. Two biological duplicates and three technical replicates were used for miScript qPCR analysis. Error bars represent standard error of mean.

**C and D** Synchronized worms at the indicated stage of development were irradiated with 80mJ/cm<sup>2</sup> UV. DIC and GFP pictures were taken 4h later.

**C** *Plet-7::GFP* expression throughout development. Micrographs of L1 larvae and inset pictures of L2 to adulthood display equal exposure times for GFP detection. Micrographs of L2 to adulthood were taken using a lower but equal exposure time to avoid overexposure. Inset picture of L1 worms shows magnified view on GFP-expressing head neuron (arrow).

**D** *Pmir-48::GFP* expression throughout development. All pictures were taken using the same exposure time. Inset pictures show magnified view on GFP-expressing head neuron (arrow).

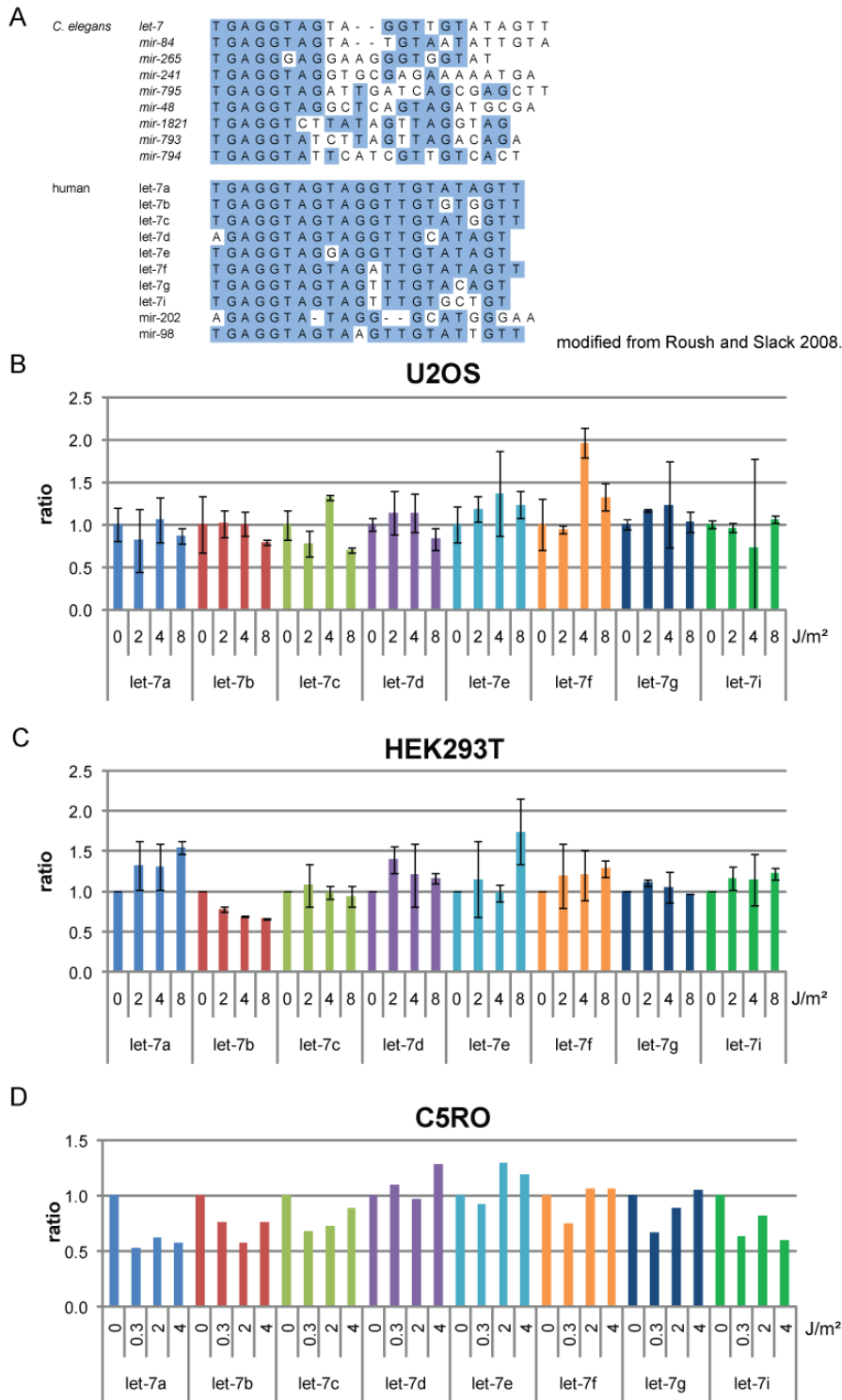


**Figure IV.10 UV-regulation of human let-7 family members is dependent on the cell type.**

**A** Conservation of let-7 family members in *C. elegans* and human; modified from Roush and Slack 2008. **B-D** let-7a-i are differentially expressed in different cell types and upon UV irradiation. Cells were irradiated with the indicated dose of UVC and RNA isolated [kindly provided by Dr. Björn Schumacher]. TaqMan-based qPCR was performed and values normalized to RNU24 and Z30 small non coding RNAs. Duplicate samples were analyzed of osteosarcoma (U2OS) (**B**) and human embryonic kidney 293 (HEK293T) (**C**) cells. Single samples of immortalized human fibroblast (C5RO-hTERT) (**D**) were used.

differentially regulated dependent on the cellular context and on the other hand it indicates that *C5RO-hTERT* cells are more similar to *C. elegans* larvae in their response to UV-induced DNA. Furthermore regulation of specific let-7 family members in response to UV points at different functions for certain family members to fine-tune posttranslational regulation of their targets. Despite this, it is most likely that they share many targets due to the strong conservation, especially, of the seed sequence.

These data suggest that *let-7* regulation observed in *C. elegans* (Table IV.2, Figure IV.5 and Figure IV.6) is not solely a result of developmental delay of UV-treated in comparison to untreated animals because *let-7* suppression is also found in C5RO cells that are not undergoing developmental transcriptional changes in contrast to *C. elegans* larvae. In conclusion, we propose that some *let-7* family members are downregulated in response to UV to release suppression of defined target mRNAs that become important for the reaction to UV-induced damage. The magnitude (and direction) is dependent on the cellular context, UV dose and the time after irradiation.

#### **4.2.5 mRNA target prediction of miRNAs with altered expression after UV irradiation.**

Finally, we were interested in the targets that are regulated by the UV-responsive miRNAs. We utilized three different prediction softwares to determine targets of the miRNAs that were found to respond to UV (Table IV.2 and Figure IV.11). First, we used microRNA.org (Enright et al. 2003; Betel et al. 2008; Betel et al. 2010) which is based on miRanda algorithm that calculates the complementarity and the thermodynamic features of possible miRNA 3'-UTR interactions. Second, we conducted ComiR (Coronnello et al. 2012) that integrates not only scores obtained from miRanda but combines it with the three target prediction algorithms PITA, TargetScan and mirSVR. Moreover, expression data are taken into account to calculate the likelihood of a site in the 3'-UTR of a mRNA to be bound by a certain miRNA. The third program that was used is DIANA microT-CDS v.5 (Reczko et al. 2012; Paraskevopoulou et al. 2013). The major difference to the other two algorithms is the integration of miRNA binding sites in coding sequences instead of only accounting for the 3'-UTR of mRNAs. Using default settings of the prediction programs we identified 8,083, 5,537 and 1,271 different targets employing microRNA.org, ComiR and microT-CDS, respectively (Figure IV.11 B). 265 determined targets were common for all three algorithms. Interestingly, the proportion of targets determined for

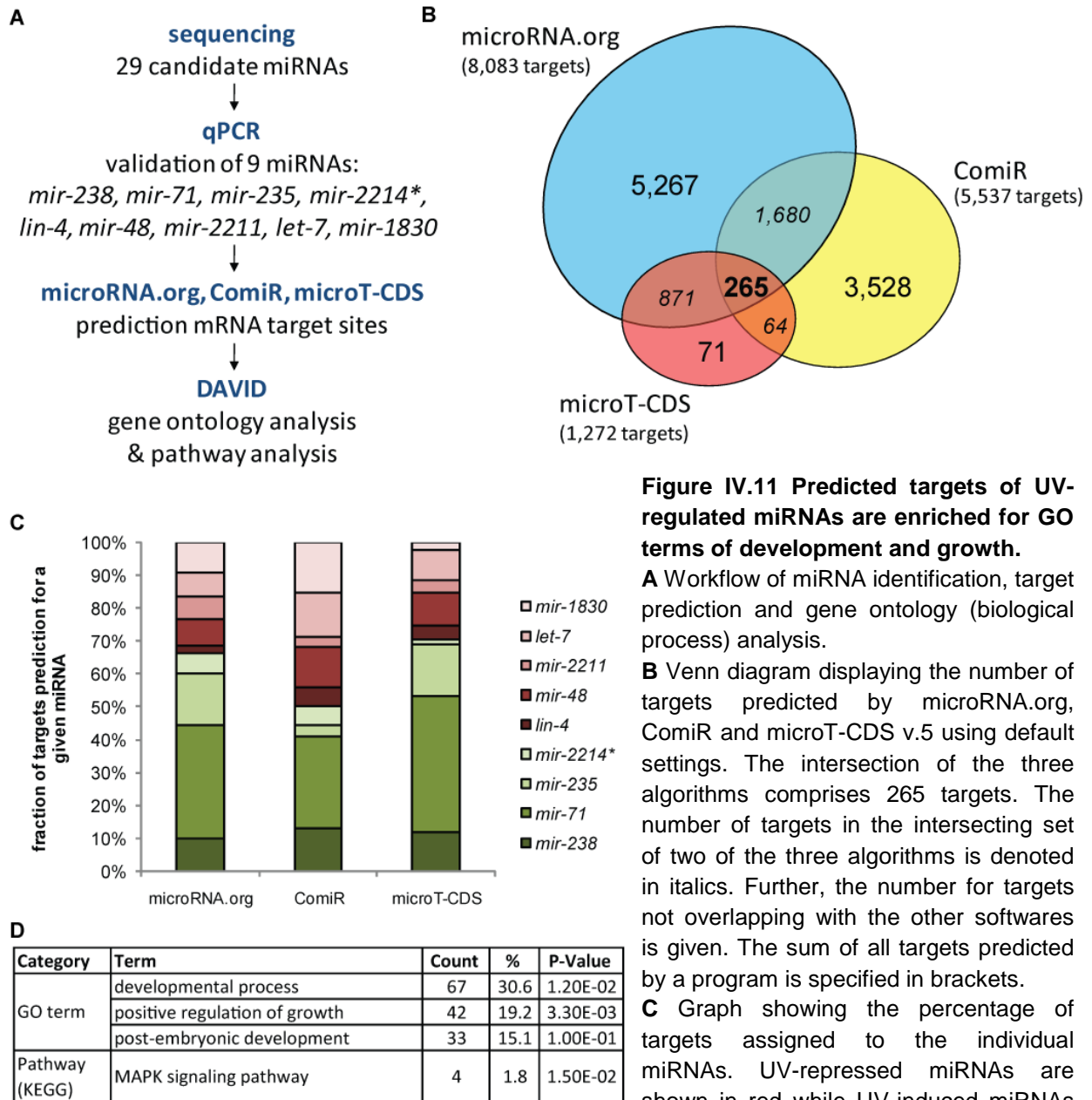


**Figure IV.11 Predicted targets of UV-regulated miRNAs are enriched for GO terms of development and growth.**

**A** Workflow of miRNA identification, target prediction and gene ontology (biological process) analysis.

**B** Venn diagram displaying the number of targets predicted by microRNA.org, ComiR and microT-CDS v.5 using default settings. The intersection of the three algorithms comprises 265 targets. The number of targets in the intersecting set of two of the three algorithms is denoted in italics. Further, the number for targets not overlapping with the other softwares is given. The sum of all targets predicted by a program is specified in brackets.

**C** Graph showing the percentage of targets assigned to the individual miRNAs. UV-repressed miRNAs are shown in red while UV-induced miRNAs

**D** Table showing enriched gene ontology terms for biological processes and pathways of predicted miRNA targets commonly predicted by microRNA.org, ComiR and microT-CDS v.5. Gene ontology analysis was performed using DAVID Functional Annotation 6.7 (Huang, Sherman, & Lempicki, 2009a, 2009b). Pathway analysis was performed executing Kyoto Encyclopedia of Genes and Genomes (KEGG) via DAVID webpage. Modified Fisher Exact P-Value is denoted.

each miRNA differed strongly between the single miRNAs but only slightly between the three softwares (Figure IV.11 C). For instance, we found a strong overrepresentation of targets bound by *mir-71* while all other miRNAs used for the analysis were associated with considerably fewer targets. This indicates that the *mir-71* binding site is conserved across a big variety of transcripts

and that a large group of mRNAs are potentially regulated by *mir-71*. Comparison of predicted targets of *mir-48* and *let-7* family members shows that 85% of all *let-7* targets are also predicted for *mir-48* and, the other way around, 76% of *mir-48* targets are also found among the *let-7*-regulated transcripts according to microRNA.org. A similar proportion of mRNA targets overlapping between *mir-48* and *let-7* was obtained conducting microT-CDS, whereas only about one half of the targets determined for *mir-48* were found in the set of *let-7* targets and vice versa when using ComiR.

In order to characterize the pool of all predicted target mRNAs, we performed gene ontology (GO) analysis using DAVID software (Huang, Sherman, and Lempicki 2009a; Huang, Sherman, and Lempicki 2009b). GO analysis on the 265 targets commonly predicted by all three algorithms revealed an enrichment of GO terms of development, positive regulation of growth and, in particular, post-embryonic development (Figure IV.11D). However, the same GO terms were found when the group of targets derived from the three algorithms were analyzed independently. Strikingly, also when only microRNA.org predicted targets of down- or upregulated miRNAs were considered, the same GO terms were found for both groups. Taken together, the miRNA target analysis shows that UV irradiation of *C. elegans* at L1 larval stage alters the miRNA expression profile, thereby, adjusting developmental progression and growth. Next, we were also interested in the pathways regulated by the group of regulated miRNAs (Figure IV.11D). Not only the shared pool of predicted targets of the three algorithms but also the independent sets of targets were enriched for proteins of the MAPK signaling pathway based on the Kyoto Encyclopedia of Genes and Genomes (KEGG). Analysis of the targets by PANTHER classification system revealed an enrichment of genes related to inflammation-mediated chemokine and cytokine signaling as well as Wnt signaling pathway. Furthermore, ComiR as well as microRNA.org predicted an enrichment of targets associated with the proteasome. In particular, miRNAs induced upon UV-treatment were predicted by microRNA.org to bind transcripts related to the proteasome. Importantly, we found that seven factors of the NER pathway are predicted to be targeted by the group of repressed miRNAs when conducting microRNA.org or ComiR. This is in line with the requirement of cells to repair UV damage after irradiation. Release of posttranslational repression by miRNAs presents a fast mechanism to make repair proteins available because it circumvents need for prior transcription.

## 4.3 Discussion

### 4.3.1 Establishment of sequencing-based screening for UV-regulated miRNAs

Here, we established a deep sequencing approach for analysis of small regulatory RNAs after treatment with UV light (Figure IV.3). This technique not only enabled us to define the pool of miRNAs responsive to UV irradiation but also finding novel miRNAs regulated upon DNA damage (Table IV.2). We obtained good integrity of RNA, shown using Bioanalyzer, and achieved high coverage of sequencing data utilizing Illumina Deep Sequencing method (Table IV.1). Data processing pipeline, which is described in detail in Motameny et al. 2010, was defined in order to analyze the dataset. To validate the set of candidate miRNAs we performed small RNA qPCR.

### 4.3.2 *lin-4* expression is repressed upon UV irradiation independently from DAF-16.

Using sequencing of small RNAs and qPCR expression analysis, we found *lin-4* miRNA downregulated upon UV irradiation in a dose-dependent manner in L1 larvae (Table IV.2, Figure IV.5B, Figure IV.6, and Figure IV.7B). In recent studies *lin-4* expression profiling is used as an marker for L1 development and progression into L2 larval stage (Baugh and Sternberg 2006; Kasuga et al. 2013). In line with this, *lin-4::YFP* reporter gene was found to be expressed within 12h of hatching in the presence of food but not under starvation conditions during L1 arrest (Baugh and Sternberg 2006). It is known that UV radiation induces a transient developmental arrest in a dose-dependent manner and we could measure this delay when we documented development of UV-treated L1 larvae (Figure IV.7 C and D, and Figure IV.8). Utilizing *lin-4* promoter fusion to GFP we provide evidence that expression changes in L1 larvae are not due to transcription repression but rather a result of posttranscriptional regulation of *lin-4* maturation. However, developmental delay using 100mJ/cm<sup>2</sup> is very mild (Figure IV.7C and D); hence, higher UV doses should be tested to provide more certainty. Taken together, we propose that *lin-4* is repressed independent of DAF-16/FOXO transcription factor (Figure IV.7B), when L1 larvae are irradiated with UV light to give time for repair of lesions. Time course experiment of *lin-4* regulation indicates that worms arrest until six hours after irradiation but then resume development and catch up to developmental state of untreated worms 24h after irradiation when using 60mJ/cm<sup>2</sup> UV (Figure IV.6B). However, *lin-4* as well as *lin-14* expression suppression

seem to be dispensable for UV-induced developmental delay (Figure IV.7). Therefore, we speculate that *lin-4* repression in response to UV is a consequence of developmental delay but no requirement.

### **4.3.3 miRNAs associated with L1 diapause state are induced upon UV-treatment.**

In previous studies, *mir-235* has been proven to be required for L1 arrest (Kasuga et al. 2013). Northernblot analysis showed that *mir-235* abundance declines upon feeding of L1 arrested larvae, which was partially repressed in *daf-16(mu86)* mutant. Furthermore, certain characteristics of L1 larvae are not maintained in *mir-235* mutant (Kasuga et al. 2013) indicating its requirement for maintenance of L1 status. Consistent with its role in sustaining arrest, we found *mir-235* upregulated in L1 larvae in response to UV irradiation (Table IV.2, Figure IV.5B and Figure IV.6). Kasuga et al. show that L1 larval arrest upon starvation is partially dependent on the suppression of *nhr-91* by direct binding of *miR-235* to the 3'-UTR of *nhr-91* mRNA. Thus, it would be interesting to investigate UV-sensitivity of *mir-235* mutant and *nhr-91* mutant and the requirement for UV-induced developmental delay.

Like *mir-235*, *mir-71* has been reported to play a role in L1 diapause induced by starvation (X. Zhang et al. 2011). It has been shown that starved *mir-71* mutant L1 larvae survive shorter than wildtype worms, which is partially dependent on repression of insulin receptor/PI3K pathway genes by binding of *mir-71* to the *age-1* and *unc-31* 3'-UTR. In contrast to *mir-235*, *mir-71* is dispensable for arrest of M-cell division during L1 diapause (Kasuga et al. 2013; X. Zhang et al. 2011). In addition to long-term survival, *miR-71* is also important for recovery from arrest state, for instance, by regulating timing of vulval cell divisions (X. Zhang et al. 2011). Upregulation of *mir-71* upon UV irradiation of L1 larvae could function as mediator of stress-induced transient L1 arrest (Table IV.2, Figure IV.5B). Despite its role in L1 diapause, *mir-71* was also shown to have effects on *C. elegans* lifespan. While loss of function mutations of *mir-71* decrease lifespan, *miR-71* overexpressing worms are long lived (de Lencastre et al. 2010; Lucanic et al. 2013). GFP reporter strain investigations revealed increasing *mir-71* expression in intestine during aging. Moreover intestinal *mir-71* was reported to enhance DAF-16 activity in the intestine (Boulias and Horvitz 2012). DAF-16/FOXO is a master regulator of stress resistance and longevity, downstream to insulin/insulin-like growth factor signaling (IIS) pathway in *C. elegans* (Kenyon 2010). Previous studies demonstrate that DAF-16 translocation to the nucleus and binding to its

targets induces defense mechanisms against a variety of different stressors. *daf-16* knockdown by RNAi does not further reduce lifespan of *mir-71* mutants providing further evidence that *mir-71* and *daf-16* act in the same pathway (de Lencastre et al. 2010; Lucanic et al. 2013). Remarkably, De Lencastre et al. reported that *mir-71* mutants are sensitive to heat and oxidative stress (de Lencastre et al. 2010). It would be very interesting to see if *mir-71* expression is induced in response to heat and oxidative stress and, test whether UV-irradiation decreases the lifespan of *mir-71* mutants. In the same study, the authors give preliminary evidence for a possible role of *mir-71* in DNA damage response. They show that longevity caused by knockdown of DNA damage checkpoint proteins CHK-1 and CDC-25.1 is suppressed in *mir-71* mutant background. Repression of *chk-1* and *cdc-25.1* could be a direct effect of *miR-71* binding to predicted target sites in the 3'-UTR of their mRNAs as hypothesized by De Lencastre and coworkers. However, *mir-71* expression is very dynamic throughout *C. elegans* development (Kato et al. 2009; Lucanic et al. 2013). Weak expression in embryos is followed by sudden peak of expression at L1 stage. After massive decline of *mir-71* abundance at L2 stage, expression gradually increases again in L3, L4 and throughout adult aging. The function of the strong expression changes of *mir-71* during *C. elegans* lifespan is not known yet, but could hint at a role for *mir-71* in developmental programs (Kato et al. 2009). Due to the rapid expression changes in young larvae, it remains challenging to dissect expression changes caused by transient developmental delay in L1 larvae upon UV irradiation from specific induction of *mir-71* as player in the DNA damage response.

Taken together, there are three possible explanations for *mir-71* upregulation in UV-treated L1 larvae that might add to the total expression changes seen in this study (Table IV.2, Figure IV.5B). First, after UV irradiation *mir-71* could be upregulated to induce arrest similar to starvation-induced L1 diapause. Alternatively, differences in *mir-71* abundance in UV-treated compared to untreated worms could be the result of heterochronic expression of *miR-71* during early larval stages. Finally, *mir-71* might be induced as a key player in stress response given that *mir-71* is important for stress resistance to starvation, heat stress, oxidative stress and possibly UV irradiation. Previous studies suggest that *mir-71* could confer stress resistance partially by activating DAF-16 (de Lencastre et al. 2010; X. Zhang et al. 2011; Boulias and Horvitz 2012; Lucanic et al. 2013).

Like *mir-71* and *mir-235*, also *mir-238* is upregulated in starvation-induced L1 diapause as reported earlier (Karp et al. 2011). All three miRNAs are also upregulated upon UV irradiation in L1 larvae (Table IV.2). Furthermore, *mir-71* and *mir-238* share some more characteristics. Both were shown to confer resistance to oxidative stress, upregulated during adult aging and mutants are short-lived whereas overexpression prolongs lifespan (de Lencastre et al. 2010). Thus, *mir-71*, *mir-235* and *mir-238* seem to act in concert to regulate L1 arrest and resistance to certain stresses like UV light.

#### 4.3.4 Small RNA sequencing indicates UV-dependent regulation of a set of miRNAs

Strikingly, we found strong induction of *mir-2214\** upon UVB-irradiation. Star sequence was much higher abundant than *mir-2214* (Figure IV.5C) and also regulated to a bigger extent (Figure IV.5B and C) suggesting that *mir-2214\**-driven PTGS after UV-treatment is more relevant than regulation mediated by *mir-2214*.

In our sequencing approach we found that *mir-80* as well as *mir-58* are increased in UV-treated compared to untreated worms (Table IV.2). Both are members of the *mir-58* family of miRNAs, comprising *mir-58*, *mir-80*, *mir-81*, *mir-82* and *mir-1843*. The family is conserved in other nematodes and *Drosophila* but not in mammals (Alvarez-Saavedra and Horvitz 2010). In 2010, it was documented that phenotypes are absent in the single mutants of *mir-58* family members but, in contrast, deletion of all family members was accompanied with slow movement, decrease in body size, failure in dauer stage formation and an egg-laying defect, all of which could be rescued introducing a *mir-80* expressing transgene. Another study claims that *mir-80* deletion mutants are long lived which is dependent on certain stress response proteins including DAF-16 (Vora 2011). However, neither *mir-80* nor *mir-58* induction upon UV irradiation could be reproduced (Figure IV.5) which might rely on the restrictions of miRNA qPCR method or *mir-80* being a false positive hit in the sequencing approach.

Also UV-dependent regulation of *mir-2211*, *mir-1829c*, *mir-789*, *mir-64*, *mir-228*, *mir-87* and *mir-230* is left uncertain. Alternative methods to sequencing and miScript PCR should be utilized to test miRNA regulation, for example northern blot, microarray assays or TaqMan-based qPCR. Furthermore, sequencing revealed upregulation of three *mir-51* family members (Table IV.2). Previously it was documented that deletion of *mir-51* family (*mir-52/53/54/55/56*) are embryonic lethal whereas mutation of single family members alone had no obvious effect (Alvarez-

Saavedra and Horvitz 2010). Lethality could be rescued by expression of a *mir-51* transgene alone, implying strong redundancy between the family members. However, it was suggested that the contribution to the phenotype is correlated to the expression level and timing of the respective miRNA. Interestingly, Brenner et al. showed that upregulation of *mir-51* family members could suppress the developmental timing defects of *let-7* family mutants. Moreover, they found a slight, yet not significant, increase in *let-7* expression in *mir-52/53/54/55/56* deletion mutant (J. L. Brenner, Kemp, and Abbott 2012). In line with reciprocal expression patterns of *mir-51* and *let-7* families, we find that members of the *let-7* family are downregulated upon irradiation with UV whereas *mir-51*, *mir-52* and *mir-54* are induced (Figure IV.5B). Taken together, these findings suggest that there is some dependency of *let-7* family on *mir-51* regulation.

#### **4.3.5 *let-7* is downregulated in response to UV irradiation**

Further analysis of *let-7* expression profile by qPCR revealed specific repression of *let-7* after irradiation with 20 to 60mJ/cm<sup>2</sup> UV but not higher dosages (Figure IV.6A). Time course experiment indicated that *let-7* expression decreased gradually after irradiation, reaching a minimum at four to six hours after irradiation and returned to baseline levels eight hours after treatment (Figure IV.6B). Nevertheless, using *let-7* and *mir-48* promoter fusions to GFP we did not find any induction of promoter activity upon irradiation (Figure IV.9C and D). Early studies on *let-7* uncovered a role in L4 to adult transition by repressing *lin-41* mRNA (Figure IV.7A) (Reinhart et al. 2000). Therefore, we argued that UV-regulation of *let-7* expression might also affect *lin-41* mRNA abundance. Strikingly, we found that *lin-41* mRNA is downregulated upon irradiation with dosages between 40 and 80mJ/cm<sup>2</sup> (Figure IV.9A). This stands in contrast to our expectation that *let-7* and *lin-41* would show expression changes in opposite directions. Time course expression profiling also did not show *lin-41* expression complementary to *let-7* regulation (Figure IV.9B). Despite the expression changes elicited by irradiation of the worms, we did not observe UV-sensitivity of *let-7* or *lin-41* mutant animals (Figure IV.8). However, compared to wildtype worms, *let-7(n2853)* and *lin-41(ma104)* mutants were impaired in development independently of irradiation (Figure IV.8B and C). Absence of altered UV-sensitivity of *let-7* mutant could indicate redundancy with the other *let-7* family members in regulation of UV-responsive target genes. Although it is likely that *let-7* family members share a

pool of targets, it has been shown that they are expressed in different tissues and control different molting events during *C. elegans* development. While *let-7* is most important for L4 to adult transition (Figure IV.7A and Figure IV.8B and C), it was reported that *mir-48*, *mir-84* and *mir-241* are induced at L2 larval stage to regulate transition to L3 stage (Abbott et al. 2005). *mir-48* and *mir-241* are most probably expressed from one cluster, further supporting their functional relationship. Spatiotemporal separation of *mir-48* and *let-7* expression patterns can be easily followed by analyzing GFP reporter strains (Figure IV.9C and D). Expression of the *let-7* miRNA family members in different tissues is accompanied by different transcriptomes that are available for the respective miRNA. Hence, regulation of individual *let-7* family members might cause different responses dependent on the tissue that they are expressed in. Common downregulation of *let-7* family members suggests that there is at least a shared group of mRNAs that is regulated upon UV irradiation. Information about spatiotemporal expression of miRNAs and transcripts is not taken into account by commonly used target prediction softwares displaying a clear disadvantage of these programs. Expression analysis of the *let-7* homologues in human cells reveals an elaborate mechanism regulating *let-7* isoforms dependent on the cell type, and irradiation (Figure IV.10). While there is no clear regulation detectable in U2OS cells, *let-7a* is induced and *let-7b* repressed in HEK293T cells in response to UV irradiation (Figure IV.10B and C). Consistent with *let-7b* suppression upon irradiation in HEK293T cells, we find similar decrease in C5RO immortalized cells. Along with *let-7b*, also *let-7a*, *let-7c*, *let-7g* and *let-7i* are downregulated in a UV-dependent manner in immortalized fibroblasts (Figure IV.10C). When analyzing these data it has to be taken into account that *let-7* presents a tumor suppressor gene that might be deregulated in cancer cells. Therefore, resistance of *let-7* expression to repression by UV irradiation could be also caused by low baseline expression in the oncogenic cells (S. M. Johnson et al. 2005; C. D. Johnson et al. 2007; Weidhaas et al. 2007). On the other hand it was described previously that different cell types and tissues also differ in their regulation of *let-7* (Saleh et al. 2011). In 2011, Saleh et al. screened for miRNAs responsive to stress. They find that *let-7a* and *let-7b* are decreased after IR or UV irradiation, etoposide (a topoisomerase II inhibitor and anti-cancer drug) and H<sub>2</sub>O<sub>2</sub> treatment. Using chromatin immunoprecipitation, they show that downregulation after IR is dependent on p53 that binds directly to sites in the *let-7* promoter. However, utilizing mouse model they do not find *let-7* suppression in all tissues and propose regulation is only found in IR-sensitive tissues (Saleh et al. 2011). Comparison of IR-

regulated miRNAs in different cell types supports the hypothesis that expression changes are strictly cell-type specific and that each cell type might respond with a different set of miRNAs (Chaudhry 2009; Cha et al. 2009; H. Hu and Gatti 2011).

Two of the top-score targets of *let-7*, *mir-48* and *mir-241*, all of them being downregulated in response to UV irradiation (Table IV.2), are *daf-16* and *daf-12* as predicted by microRNA.org. Moreover, experimentally it has been demonstrated that *let-7* family members and *daf-12* are negatively regulating each other (Grosshans et al. 2005; Hammell, Karp, and Ambros 2009). To date it remains open to show direct regulation of *daf-16* mRNA by the *let-7* family. Assuming that *daf-16* is posttranscriptionally suppressed by *let-7* family, *daf-16* expression would be increased after UV irradiation, when *let-7* miRNAs are downregulated. The same is true for *daf-12*. DAF-16 and DAF-12, both, are acting downstream to DAF-2 insulin receptor and confer longevity and stress resistance upon activation (Lapierre and Hansen 2012). Therefore, inhibition of *let-7* family members could be beneficial to cells challenged by UV-induced lesions.

#### **4.3.6 UV-responsive miRNAs are predicted to fine-tune growth, development and MAPK signaling**

Target prediction of UV-regulated miRNAs provided deeper insights into the mechanisms involved in the response to irradiation. Throughout the study we found repeatedly molecules regulating development of *C. elegans* and we could show that development is arrested transiently, most likely to give time for repair of UV-induced lesions. Targets predicted for the UV-regulated miRNAs were enriched for terms of development and growth and are therefore proof of principle that the predicted targets are reflecting the expected biological processes.

Interestingly, we notice that UV-responsive miRNAs are potentially regulating MAPK signaling pathway (Figure IV.11D). It was documented previously that MAPK signaling is induced upon IR or cisplatin treatment of mammalian cells which is a prerequisite for ERCC1 NER protein induction (Yacoub et al. 2001; W. Li and Melton 2012). Furthermore, it was shown that *C. elegans* strains carrying mutations in RAS/MAPK pathway are IR-sensitive, supporting the importance of MAPK signaling for the DNA damage response (Weidhaas et al. 2006). Here, we uncover additional layers of this signaling cascade controlled by miRNAs. For example, MAP kinase kinase, *mek-1*, is predicted to be targeted by *mir-71*, *mir-2214\** as well as *mir-1830* to fine-tune its expression when using microRNA.org. In total 27 players of MAPK signaling are

predicted targets of UV-regulated miRNAs. It is feasible that UV-regulated miRNAs not only modify translational rate of mRNAs encoding MAPK proteins but also DNA repair genes directly. Among the targets of miRNAs suppressed by UV irradiation are several players of the NER pathway, which specifically repairs UV-induced lesions. Damage sensors of transcription-coupled NER, *csb-1*, as well as global genome NER damage sensor, *xpc-1*, have predicted binding sites for *mir-2211* according to microRNA.org. In addition, *xpc-1* has also a predicted binding site for *mir-235*. Finally, PCNA homologue, *pcn-1*, and DNA ligase *lig-1*, that function in the last steps of NER, are potentially inhibited by the *let-7* family members *let-7* and *mir-48*.

It is known since long time that *rad-23* is not only essential for global genome NER but also interacts with the proteasome through an ubiquitin-like domain (Schauber et al. 1998). It was shown that yeast Rad23p and its mammalian homologues suppress target degradation, for instance XPC NER protein to enhance DNA repair capacity (reviewed in Van Laar, Van der Eb, and Terleth 2002; Dantuma, Heinen, and Hoogstraten 2009). On the other hand, it was reported that human RAD23 might function as an ubiquitin receptor to shuttle targets to the proteasome for degradation. miRNAs might be an additional link between the proteasome and the DNA damage response since all parts of the proteasome are micorRNA.org-predicted targets of UV-induced miRNAs. Lid-subunits Rpn3, Rpn5, Rpn6, Rpn8, Rpn9 and Rpn12, transcripts of proteasome base proteins Rpn2, Rpt1, Rpt2, Rpt6 and Rpt5 as well as the core particles  $\alpha 1$ ,  $\alpha 2$ ,  $\alpha 3$ ,  $\alpha 4$ ,  $\alpha 5$ ,  $\alpha 7$ ,  $\beta 2$  and  $\beta 6$  might be targets of upregulated miRNAs and thus, could be downregulated upon UV irradiation. Many of those are potential *mir-71* targets putting *mir-71* in the center of proteasomal subunit posttranscriptional suppression in response to UV irradiation.

## V Material & Methods

### 5.1 *C. elegans* culture maintenance

Worms were maintained at 20°C on nematode growth medium (NGM) agar plates with *Escherichia coli* strain OP50 as food source according to standard protocols (S. Brenner 1974) unless otherwise indicated. Given that loss of the SMC-5/6 complex leads to transgenerational sterility in *C. elegans* (Bickel et al. 2010), all strains used in this study were stabilized by maintaining them in a heterozygous state using a GFP marked variant of the genetic balancer *mIn1* (II) (Edgley and Riddle 2001). For all experiments homozygous worms were employed. The following alleles and strains were used:

Strain	Genotype
BJS101	<i>smc-5(ok2421)/mIn1[mIs14 dpy-10(e128)] II; xpc-1(tm3886) IV.</i>
BJS121	<i>smc-5(ok2421)/mIn1[mIs14 dpy-10(e128)] II;brd-1(gk297) III.</i>
BJS123	<i>smc-5(ok2421)/mIn1[mIs14 dpy-10(e128)] II; brc-1(tm1145) III.</i>
BJS125	<i>smc-5(ok2421)/mIn1[mIs14 dpy-10(e128)] II; hsr-9(ok759) I.</i>
BJS127	<i>smc-5(ok2421)/mIn1[mIs14 dpy-10(e128)] II; div-1(or148) III.</i>
BJS144	<i>smc-5(ok2421)/mIn1[mIs14 dpy-10(e128)] II; polh-1(ok3317)</i>
BJS146	<i>smc-5(ok2421)/mIn1[mIs14 dpy-10(e128)] II; polh-1/rad-2(mn156) III.</i>
BJS179	<i>smc-5(ok2421)/mIn1[mIs14 dpy-10(e128)] II; brc-1(tm1145) III; polh-1(ok3317) III.</i>
BJS19	?( <i>sbj19</i> ) III.
BJS2	<i>smc-5(sbj2) II.</i>
BJS21	<i>csb-1(ok2335) X; xpc-1(tm3886) IV.</i>
BJS3	<i>smc-5(sbj3) II.</i>
BJS4	<i>xpg-1(sbj4) I.</i>
BJS78	<i>smc-5(sbj3)/mIn1[mIs14 dpy-10(e128)] II.</i>
BJS79	<i>smc-5(sbj2)/mIn1[mIs14 dpy-10(e128)] II.</i>
BJS99	<i>smc-5(ok2421)/mIn1[mIs14 dpy-10(e128)] II; csb-1(ok2335) X.</i>
CF1038	<i>daf-16(mu86) I.</i>
CT8	<i>lin-41(ma104) I.</i>
DR26	<i>daf-16(m26) I.</i>
DR441	<i>lin-14(n179) X.</i>
DR721	<i>lin-4(e912) II.</i>
DW102	<i>brc-1(tm1145) III.</i>
EU548	<i>div-1(or148) III.</i>
FX03886	<i>xpc-1(tm3886) IV.</i>
MT7626	<i>let-7(n2853) X.</i>
N2	wildtype.
RB1801	<i>csb-1(ok2335) X.</i>
RB1872	<i>smc-5(ok2421) II.</i>
SP488	<i>rad-2(mn156) III.</i>
	<i>xpg-1(tm1682) I.</i>

TG1565	<i>xpg-1(tm1670) I.</i>
VC573	<i>hsr-9(ok759) I.</i>
VC655	<i>brd-1(gk297) III.</i>
VT1072	<i>unc-119(ed3) III; mals134. [Plin-4::GFP]</i>
VT1153	<i>unc-119(ed3) III; mals137. [Plet-7::GFP]</i>
VT1259	<i>unc-119(ed3) III; mals150. [Pmir-48::GFP]</i>
XF656	<i>polh-1(ok3317) III.</i>
YE57	<i>smc-5(ok2421)/mln1[mls14 dpy-10(e128)] II.</i>
YE58	<i>smc-6(ok3294)/mln1[mls14 dpy-10(e128)] II.</i>

## 5.2 Synchronizing worms

In order to obtain a synchronized population of worms they were either filtered with 11µm Nylon net filters (Millipore) to obtain L1 larvae only or bleached. For bleaching, gravid adult worms were washed three times with M9 buffer and then incubated with 1:5 Sodium hypochloride solution (Sigma-Aldrich) dissolved in 0.25M KOH until worms were lysed. Eggs were centrifuged at 2,000xg and washed three times with M9 buffer. After addition of M9 supplemented with tetracycline and ampicillin (100µg/ml each), worms were allowed to hatch at 20 °C over night.

## 5.3 Genotyping of worm strains

Worms were lysed for 1h at 65°C followed by incubation at 95°C for 10min to inactivate protease K. 1µl lysate was added to a PCR reaction using Mango Taq DNA polymerase (Bioline), colored Mango Taq 5x buffer (Bioline), MgCl<sub>2</sub> solution (Bioline) in a final concentration of 2.5mM, 250µM each dNTP (Roche) diluted in distilled water. PCR reactions were performed with C1000 Thermal Cycler (BioRad) under the following conditions:

95 °C 4 min  
 95 °C 30 sec }  
 60 °C 30 sec } 35x  
 72 °C 2 min }  
 72 °C 7 min

The PCR product was loaded on a 1% TAE based agarose gel supplemented with ethidium bromide (Carl-Roth) and run at 110V using a BioRad Power Supply in TAE buffer. Detection and documentation of the bands were performed using Wealtec UV transilluminator and DeVisionG Software. The following primers were used for genotyping:

<b>Allele specificity</b>	<b>Sequence (5'-3')</b>	
<i>e912</i>	CGAGTCTCCCTTACTGCAA	
<i>e912</i>	GAACTAGCTCCAGTGTGA	
<i>gk297</i>	ACGATTCCCCTCATGCTTCTTCTAC	
<i>gk297</i>	TGTGAGAGGAATCGCTTTTCGAGAAA	
<i>gk297</i>	CTGACAGTTGAAGGGCGTTTTGTC	
<i>m26</i>	AACTCGAACCACCACTCAAC	
<i>m26</i>	TGGAGATGCTGGTAGATCAG	
<i>m26</i>	AACCAACTGGTACAGGAATAAG	
<i>ma104</i>	ATTTTCAGAGCGATTTCGTGAGCG	
<i>ma104</i>	CATACGTCATTGTGACCTCTACAG	
<i>mn156</i>	ACCCGTTTTCTGGCTTTCTAGC	followed by
<i>mn156</i>	CGTGTGAGCTCCGGCTCTTTTC	XhoI restriction
<i>mu86</i>	TGTCTACCTCTCCTCCTGTG	
<i>mu86</i>	TCCTGCTTAATCTGAACTCCA	
<i>mu86</i>	CAGTGAGTTCTCTGGAATTGG	
<i>n2853</i>	CAACAATGGAGCATACGGAG	
<i>n2853</i>	GCTCCATGGATACATTACTCAA	
<i>ok2335</i>	GGCTGGGGGATTCAAATTATC	
<i>ok2335</i>	GAAGACTGATCATCGGAGCG	
<i>ok2335</i>	CAAAGGGCTCGAAGGATCTG	
<i>ok2421</i>	GCCCATTATGGATGTAAGGAAGAG	
<i>ok2421</i>	GTGGATACGTGCACGGTTT	
<i>ok2421</i>	TCTGGAGTTTTGAGAACCATCTG	
<i>ok3294</i>	ATCGAGGAAACACGGTGAAG	
<i>ok3294</i>	TGTGTGAGCCGAATCTGAAA	
<i>ok3317</i>	CCGAAGCGAAGTTAAAATGCCCTC	
<i>ok3317</i>	ATTTTTGGGCGAATTTTTCC	
<i>ok3317</i>	CGATTGCAGTGCACCTTAGG	
<i>ok3317</i>	CCGAAGCGAAGTTAAAATGCCCTC	
<i>ok759</i>	TCACCAATTGAAGAAGGAGAGGGAGA	
<i>ok759</i>	GACCAGAATCCAATCGAACATCGGA	
<i>ok759</i>	GTCTTCTGTTGCAACAGAGCGTCT	
<i>or148</i>	AACCAACCCGACAAGCGTCTC	followed by
<i>or148</i>	AACTTTCCAGCCTGGCCGAG	Avall restriction
<i>sbj2</i>	GATGTTTCGAGGAAGCTGATGTTCCG	followed by
<i>sbj2</i>	GTGGTTCCATTCCACATTCCAACC	Bnpl restriction
<i>tm1145</i>	TTCAAGTCACTGCCGCCAGAG	
<i>tm1145</i>	GAAATTGTCGCATCGTCGGCATT	
<i>tm1145</i>	TGACCAACCTCGGAGGGTATTTATGT	
<i>tm1145</i>	GCATTCCGCCGAGGAGCCT	
<i>tm1145</i>	GCCAGTGGTATGCTTTTTGGCAC	
<i>tm1670</i>	TTCAAGATATGGGAATCACTGG	
<i>tm1670</i>	GCCGTAATCTGCTATTTCTC	
<i>tm1670</i>	AGAGACGATTTACAAGGAGAC	
<i>tm1682</i>	TTCTGTAGAATTTGCACCT	
<i>tm1682</i>	AAATATGTGCTTGTGAGGG	
<i>tm1682</i>	TTCCATAATCCAGTGATTCCC	
<i>tm3886</i>	CAGTATTACAGCCGGAGAAAAG	
<i>tm3886</i>	GTTTCTGTTTCTGAGCCATTC	

Allele specificity	Sequence (5'-3')
<i>tm3886</i>	CAGTGAAGGTCTTTTGTGGTG

## 5.4 qPCR expression analysis

### 5.4.1 RNA preparation

*C. elegans* were washed with M9 buffer, prior to RNA preparation with 1ml TRIzol reagent (Invitrogen). Homogenization of worms was performed using Peqlab homogenizer and zirconia beads (Carl-Roth). After homogenization at 6,800xg for two times 20sec, the samples were either frozen at -80°C or RNA isolation was continued. To remove debris supernatant was transferred into a fresh 1.5ml tube after centrifugation for five minutes at 4°C and 13,000xg. 200µl Chloroform, or alternatively 100µl 1-Bromo-3-chloropropane (Sigma-Aldrich), were added and samples were mixed. Samples were incubated at room temperature for two minutes prior to phase separation by centrifugation 10min at 4°C and 13,000xg. The upper clear phase was transferred into a fresh tube and mixed with 500µl Isopropanol. To ensure complete precipitation of RNA, samples were incubated for 10min at room temperature. Next, RNA was washed with 700µl of 75 % Ethanol and spun at 7500xg to remove supernatant from RNA precipitate. Nucleic acids were dried by incubation at room temperature for two minutes and then resolved in 30 to 50µl water for 10 to 20min at 68°C. RNA concentration and purity was determined using Nanodrop 8000 (Thermo Scientific).

### 5.4.2 Quantitative real-time PCR

miRNA expression was analyzed using miScript SYBR Green qPCR assays (Qiagen) or TaqMan MicroRNA Assays (Applied Biosystems) and mRNA expression was performed according to chapter V.5.4.3.

#### 5.4.2.1 mRNA expression analysis

Reverse transcription of RNA samples was performed using 1µg RNA in 11.5µl nuclease free water. To dissolve secondary structures diluted RNA samples were preheated at 70°C for 2min and then 8.5µl Reverse Transcription (RT) master mix was added which consisted of the following reagents (Invitrogen):

<b>component</b>	<b>RT master mix for one reaction (µl)</b>
5x RT buffer	4
DTT	2
dNTP mix (10mM)	1
random hexamers (50µM)	1
Nuclease free water	4.16
SuperScript® III Reverse Transcriptase	0.5
<i>total volume</i>	8.5

RT was done utilizing C1000 Thermal Cycler (BioRad) under the following conditions:

42°C 90min

92°C 5min

4°C until freezing at -20°C or proceeding with qPCR.

For qPCR, first forward and reverse primers were mixed in a total volume of 5µl (1.25 µl of each primer and 2.5µl nuclease free water). Then, the following components (Invitrogen) were mixed:

<b>component</b>	<b>qPCR master mix for one reaction (µl)</b>
10x buffer qPCR	2.50
MgCl <sub>2</sub> (50mM)	1.25
dNTP (10mM)	0.50
SYBR Green (1:400)	0.075
cDNA sample (1:5)	2.50
Primer mix	5.00
Nuclease free water	13.07
Platinum® Taq DNA Polymerase	0.10
<i>total volume</i>	25.00

qPCR was performed in CFX96™ Real-Time PCR Detection System (Bio-Rad) according to the following settings:

95°C 3min

94°C 10sec	} 40x
58°C 20sec	
72°C 20sec	

Execution of melting curve analysis.

#### 5.4.2.2 TaqMan MicroRNA Kit

All agents were thawed on ice to avoid degradation. The master mix for reverse transcription reaction consisted of the following ingredients:

<b>component</b>	<b>RT master mix for one reaction (μl)</b>
dNTP mix (100nM total)	0.15
MultiScribe RT enzyme (50U/μl)	1.00
10x RT Buffer	1.50
RNase Inhibitor (20U/μl)	0.19
Nuclease free water	4.16
Template RNA (1-10ng)	5.00
<i>total volume</i>	<i>12.00</i>

The components were mixed gently and centrifuged briefly to spin down all reagents from the wall of the reaction tube. Next, 3μl RT primer were added to 12μl reverse transcription master mix while keeping the samples on ice. After mixing gently and a short centrifugation, the reaction was incubated for 5min on ice. Subsequently, RT reaction was executed using the thermal cycler according to the following settings:

16°C 30min

42°C 30min

85°C 5min

4°C forever

Subsequently samples were either stored at -20°C or used directly for qPCR. Reaction components are listed in the following list:

<b>component</b>	<b>qPCR master mix for one reaction (μl)</b>
TaqMan MicroRNA Assay (20x)	1.00
Product from the RT reaction (200ng)	1.33
TaqMan 2x Universal PCR Master Mix	10.00
Nuclease free water	7.67
<i>total volume</i>	<i>20.00</i>

Reaction was pipetted on ice and real-time qPCR cycler was programmed to execute the following protocol:

95°C 10min

95°C 15sec

60°C 60sec

} 35x

Target amplification was detected by measurement of FAM fluorescence dye.

### 5.4.2.3 miScript qPCR

After thawing all components on ice, reverse transcription master mix was prepared according to the following list:

<b>component</b>	<b>RT master mix for one reaction (µl)</b>
miScript RT Buffer, 5x	4
Nuclease free water	variable
miScript Reverse Transcriptase Mix	1.5
Template RNA (1ul)	variable, (1µg)
<i>total volume</i>	<i>20</i>

Pipetting was performed on ice to avoid RNA degradation and reaction was executed using a thermal cycler according to the following protocol:

37°C 60min

95°C 5min

4°C forever

Subsequently samples were either stored at -20°C or used directly for qPCR. Reaction components are listed in the following list:

<b>component</b>	<b>qPCR master mix for one reaction (µl)</b>
2x QuantiTect SYBR Green PCR master mix	10
10x miScript Universal Primer	2
10x miRNA-specific primer	2
Nuclease free water	variable
Template cDNA	variable, (1-3ng/reaction)
<i>total volume</i>	<i>20</i>

Reaction was pipetted on ice and real-time qPCR cycler was programmed to execute the following protocol:

95°C 15min

94°C 15sec  
55°C 30sec  
70°C 30sec

} 35x

Execution of melting curve analysis.

Target amplification was detected by measurement of SYBR Green fluorescence dye.

qPCR was performed in CFX96™ Real-Time PCR Detection System (Bio-Rad) by detection of SYBR Green binding or FAM dye as indicated. The following primers were used for amplification:

<b>specificity</b>	<b>forward primer (5'- 3')</b>	<b>reverse primer (5'- 3')</b>
<i>unc-60</i>	CCACCATGTACCCAGGAATT	AGAGGGAAGCGAGGATAGAT
<i>lmn-1</i>	ACGATAAATTGGTGGTGGAGA	TCTTCTCCAGAGCCTTGATT
<i>tbg-1</i>	CAATGTGCCCATCAATTCGG	AACAAGAAGCGAGTGACGTC
<i>lin-41</i>	AGCAGCAGTGAAGGTGACTCA	ACAGCTTGCAAGCCCCTCG
<i>smc-5</i>	TACAACAATTATGCCAGTTCC	TGTCGTAATGCTTTCCATGAG
5.3S rRNA	CTCGATGCAACCGATCCATCGCT	miScript universal primer (Qiagen)
<i>let-7</i>	CGCGAGGTAGTAGGTTGTATAGTT	
<i>lin-4</i>	CTCCCTGAGACCTCAAGTGTGA	
<i>mir-1829c</i>	CGCGCGAAATTCAAGATGGTTGTA	
<i>mir-1830</i>	GCGAGGTTTTCACGTTTTCTAGGC	
<i>mir-2211</i>	CGCTCAGGTAGAATTTAGAGGAGA	
<i>mir-2214</i>	GTTGACAACAACCTTGACCGGCG	
<i>mir-2214*</i>	ATTCGGTCCGGAGTCAATGGG	
<i>mir-228</i>	CAATGGCACTGCATGAATTCACGG	
<i>mir-228</i>	CAATGGCACTGCATGAATTCACGG	
<i>mir-230</i>	CGTATTAGTTGTGCGACCAGGAGA	
<i>mir-235</i>	TTGCACTCTCCCCGGCCTGA	
<i>mir-238</i>	CTTTGTACTCCGATGCCATTCAGA	
<i>mir-241</i>	CGTGAGGTAGGTGCGAGAAATGA	
<i>mir-252</i>	CGATAAGTAGTAGTGCCGCAGGTA	
<i>mir-48</i>	TGAGGTAGGCTCAGTAGATGCGA	
<i>mir-49</i>	CAAGCACCACGAGAAGCTGCAGA	
<i>mir-51</i>	ATACCCGTAGCTCCTATCCATGTT	
<i>mir-52</i>	CACCCGTACATATGTTTCCGTGCT	
<i>mir-54</i>	CACCCGTAATCTTCATAATCCGAG	
<i>mir-54</i>	GGCCCGTAATCTTCATAATCCGAG	
<i>mir-58</i>	CGTGAGATCGTTCAGTACGGCAAT	
<i>mir-61</i>	CGCTGACTAGAACCGTTACTCATC	
<i>mir-64</i>	CTATGACACTGAAGCGTTACCGAA	
<i>mir-71</i>	GCGATGAAAGACATGGGTAGTGA	
<i>mir-789</i>	CCTGCCTGGGTCACCAATTGT	
<i>mir-80</i>	CGAGCTTTCGACATGATTCTGAAC	
<i>mir-87</i>	CGTGAGCAAAGTTTCAGGTGTGC	
<i>ncRNAa</i>	GACCACCGGTCCGGAGTTTGTGGGT	
<i>ncRNAb</i>	CGCCCTACTCTTCGCATCTCATC	
<i>ncRNAc</i>	CGGCGTTAGCTCTGTGTCAAACC	
<i>ncRNAd</i>	AGTGGAGTGGATGACGACGACGA	
<i>ncRNAe</i>	GCGAATAGATACGCGGTATGACG	
<i>ncRNAf</i>	GCGGAAATGGATTAGAATCGTGG	
<i>ncRNAg</i>	CGTTGATGACTCAGGCAGGGACT	
<i>ncRNAh</i>	GCGAGGAAATGAGAAAACCTCGGC	
<i>ncRNAi</i>	CGCGGGACTAGTCAAGTGTCGG	
<i>ncRNAj</i>	GGTGGTTTTTCTCTGCAGTGCCG	
<i>ncRNAk</i>	GCGCCCTCTCATCAACTTACAG	

<i>ncRNAI</i>	CGGGGTTGTAGATATAGCCGC
<i>U6 snRNA</i>	TGCGCAGGGGCCATGCTAATC

To check for byproducts and specificity of the reaction, melting curve analysis was performed in the case of SYBR green detection of amplicates. Ratio of expression mRNA levels between sample and control were calculated according to Pfaffl et al. (Pfaffl 2001) using the following formula:

$$\text{ratio} = 2^{(Ct \text{ sample untreated} - Ct \text{ sample treated})} / 2^{(Ct \text{ reference untreated} - Ct \text{ reference treated})}$$

To show relative expression levels the following formula was utilized:

$$\text{relative expression} = 2^{-(Ct \text{ sample} - Ct \text{ reference})}$$

## 5.5 Isolation of genomic DNA

Worms were grown on four 92mm NGM plates to obtain a large amount of worms. Animals were washed from the plate into tubes and washes twice with M9 buffer. In order to remove as many *E. coli* as possible tubes were incubated for 1h in 10ml M9 at 20°C rolling and washed again twice with M9 buffer. After transferring worms into 1.5ml tube and centrifugation for 5min at 18,000xg and 4°C as much liquid as possible was removed. Then samples were stored at -80°C and before further processing the next day. After thawing samples at room temperature DNA was isolated according to Genra Purgene Kit (Qiagen). First, 3ml Cell Lysis Solution and 15µl Proteinase K (20mg/ml) were added. Then, samples were incubated for 3h at 55°C in a thermo block distributed on two 2ml tubes. Next 7.5µl RNaseA solution was pipetted into each of the two tubes of a sample and incubated in a shaking thermo block for 30min at 37°C. Subsequently, tubes were cooled down on ice. The solution was transferred into a 15ml tube and mixed with 1ml Protein Precipitation Solution. To get rid of the protein precipitate tubes were centrifuged for 10min at 2,000xg and supernatant transferred into a new tube. Finally, DNA was precipitated by addition of 3ml Isopropanol and inverting the tube 50 times. Supernatant was removed after 3min centrifugation at 2,000xg and pellet dried at room temperature for 30min. DNA was resolved in 100µl Hydration Solution, incubated at 65°C for another 30min and concentration measured utilizing Nanodrop 8000. Integrity of the DNA samples was determined on 0.7% agarose gel using 50ng DNA.

## **5.6 GFP reporter strain analysis**

Bleached and starvation synchronized worms were transferred on five NGM plates seeded with OP50. After 4h (to analyze L1 larvae), 10h (to analyze L2 larvae), 24h (to analyze L3 larvae), 50h (to analyze L4 larvae) or 72h of feeding, worms were irradiated with 80mJ/cm<sup>2</sup> UVB. Worms were kept at 20°C for another 4h and then prepared for microscopy. For that purpose 2% agarose pads were made and worms were picked into a small drop of 30mM Sodium Azide (NaN<sub>3</sub>) on top of the agarose pads, in order to paralyze the animals. After covering the slides carefully with a cover slip, worms were analyzed using Axio Imager A1 (Carl Zeiss).

## **5.7 Immunostaining and microscopy**

Worms were paralyzed prior to dissection with 20mM sodium azide in egg buffer (Edgar 1995) containing 0.2% Tween20. The samples were fixed on poly-lysine coated slides using 3.7% paraformaldehyde in egg buffer and 0.2% Tween20. After 5 min incubation at room temperature the worms were freeze cracked by submersion in liquid nitrogen and afterwards incubated in a 1:1 mixture of methanol and acetone at -20 °C for 10min. The samples were permeabilized by washing three times 10min in PBS 1% TritonX100, followed by washing 5min with PBS 0.1% Tween20 (washing buffer). To saturate unspecific binding sites, the slides were incubated with washing buffer containing 10% donkey serum (blocking buffer) for 30min at room temperature. Primary antibodies were diluted in blocking buffer and incubated on slides in a humid chamber at room temperature over night. After three times washing, secondary antibodies were diluted in blocking buffer and allowed to bind at room temperature for 2h in the dark. Excess antibody was removed by washing three times and slides were mounted using Dapi Fluoromount G (SouthernBiotech). Pictures were taken at UltraView VoX (Perkin Elmer) Spinning Disc microscope using EMCCD C9100-50 CamLink camera and processed with Volocity 6.1.1 Demo (PerkinElmer). Blocking was not applied for SMC-6 stainings.

## **5.8 Developmental staging assay**

Bleached and starvation synchronized worms were grown on NGM plates seeded with OP50. After four hours of feeding, worms were irradiated with UVB of the indicated dose and incubated for 24h and 48h before documentation of the developmental stage by inspection at the Leica M165C stereomicroscope.

## **5.9 Screening for novel UV-sensitive *C. elegans* strains**

### **5.9.1 EMS mutagenesis**

Synchronized L1 wildtype worms were plated on NGM plates seeded with *E. coli* OP50, grown until L4, then washed with M9 buffer for 2min at 2,000xg to remove bacteria, and treated with 30mM EMS in M9 buffer for 4h at RT. Residual EMS was neutralized with 1M NaOH and removed by two washes with 4ml M9 buffer. The worms were then plated on OP50-seeded NGM plates. When worms reached adulthood, they were bleached and the next day starvation synchronized L1 larvae were frozen at -80°C.

### **5.9.2 Screening and selection of worms**

To identify novel DNA repair factors in *C. elegans* we took advantage of the very specific phenotypes observed for NER mutant worms. We treated wildtype worms with EMS (as described above) and thereby induced random mutations in the genomes of their progeny. While the F1 generation carries these mutations heterozygously, one quarter of the F2 generation carries the mutations homozygously according to Mendelian laws. By screening the F2 generation for DNA-damage sensitivity, we were able to identify recessive alleles of DNA repair genes. For each round of screening EMS-treated worms from the -80°C stock were thawed and F2 generation synchronized by bleaching the F1. The adult F2 worms were picked on single NGM-plates plated with OP50 and allowed to lay eggs. After 4-6 h egg laying we recovered the adults by maintaining them in M9 supplemented with OP50 in 96-well-plate at 20°C shaking. The F3 generation was treated with 60mJ/cm<sup>2</sup> UVB at L1 stage in order to induce helix-distorting lesions. After five days the worms reached adulthood and control wildtype worms started to lay eggs. Therefore, we have chosen this time point to screen for plates containing sterile or arrested animals. Worms carrying mutations in *csb-1*, *xpc-1* or *xpa-1* served as control for UV-sensitivity in TCR, GG-NER or the downstream processing pathway of NER, respectively.

### **5.9.3 SNP mapping of novel UV-sensitive alleles (Davis et al. 2005)**

This method is based upon SNPs occurring between the Bristol-derived reference wildtype strain and the Hawaiian CB4856 strain. After crossing the novel mutant with CB4856, the F2 generation was screened for worms with wildtype phenotype and UV-sensitivity phenotype. To

do so, about 200 F2 hermaphrodites were picked on single 33mm OP50-seeded NGM plates on which they laid eggs for 3-4h before they were backed up on new plates. The next morning F3 L1 larvae were treated with 60mJ/cm<sup>2</sup> UVB and three days later worm strains were assigned to UV-sensitive (according to the respective mutant analyzed) or UV-resistant phenotype. This was done until we obtained 40-50 F2 strains with UV-sensitive mutant phenotype. Subsequently, these strains were pooled for lysis and PCR was performed to obtain amplicons, which span eight SNPs per chromosome. Master mix was prepared according to the following table.

<b>component</b>	<b>master mix for one reaction (µl)</b>
10x buffer with MgCl <sub>2</sub> (Roche)	52
Nuclease free water	424
dNTPs (Roche)	10,4
lysat	20

9,8µl were distributed into every second row of a 96-well plate and 1µl primer mix containing forward and reverse primer were added. PCR cycler was programmed to execute the following settings:

94°C	4min	
94°C	15sec	} 35x
60°C	45sec	
72°C	1min	
72°C	5min	
4°C	forever	

The 48 amplicons were digested by the restriction enzyme DraI, thereby specifically cutting the SNPs in either the Bristol or the Hawaiian strain. This was done adding directly 6µl digestion master mix to the PCR samples.

<b>component</b>	<b>master mix for one reaction (µl)</b>
DraI (20,000units/ml); (NEB)	12.5
10x buffer 4 (NEB)	160
Nuclease free water	430

The 96-well plate was covered again with foil and incubated over night at 37°C before loading on 2.5% agarose gel supplemented with ethidium bromide. Analysis after agarose gel electrophoreses revealed a strain-specific pattern. When the pooled samples were analyzed, all chromosomes displayed bands of Bristol and Hawaiian strain except for the chromosome to which the mutation of interest is linked to. For the chromosome where the mutation is located

just Bristol bands were visible, at least in the region where the mutation is located. Information about particular fragment sizes can be found in Davis et al., 2005.

#### **5.9.4 Whole genome sequencing**

Whole-genome sequencing (based on Illumina system) and MAQ gene analysis (Bigelow et al. 2009) was performed at Cologne Center for Genomics (CCG) to identify mutations in the candidate strains derived from EMS-based screening. *C. elegans* genomic sequence version WS201 from [www.wormbase.org](http://www.wormbase.org) served as reference.

#### **5.10 Egg-laying and hatching rate**

Number of eggs laid per worm per hour was determined by picking three worms, 24h post L4, on three independent plates. After four hours at 20°C, adults were removed, number of eggs determined and two days later hatching rate was documented utilizing Leica M165C stereomicroscope.

#### **5.11 Germline development assay**

Day one adults were bleached and eggs hatched over night at 20°C shaking. In case of *smc-5* mutants, homozygous F1 from heterozygous mothers were used for synchronization by bleaching. L1 larvae were transferred to OP50-seeded NGM plates and treated with the indicated dose of radiation. Three days after treatment the number of worms with normal germline, malformed germline or no germline was documented using the Leica M165C stereomicroscope. Micrographs of germline development were taken using Axio Imager A1 (Carl Zeiss).

#### **5.12 HU treatment**

Worms were synchronized at early L1 development by hatching eggs in the absence of a bacterial food source. The starved L1 larvae were transferred to NGM plates seeded with OP50 bacteria to resume development. For HU treatment, L1 larvae were transferred to NGM plates containing indicated concentration of HU. After growth for 72h, the adult worms were harvested for analyses.

### 5.13 RNAi-mediated gene knockdown

Knockdown by RNAi was performed by feeding of *E. coli* to *C. elegans* (L Timmons and Fire 1998; Kamath et al. 2003). Here, we used the *C. elegans* ORF-RNAi library compromising *E. coli* HT115(DE3) transformed with Isopropyl- $\beta$ -D-thiogalactopyranosid (IPTG) inducible vector pPD129.36 (Rual et al. 2004). This vector has been cloned to express double-stranded RNA to drive degradation of target mRNAs of *C. elegans*. As control, bacteria containing the empty vector, were fed to worms. RNAi bacterial clones were maintained at -80°C stock and, upon thawing, grown in LB supplemented with ampicillin at 37°C over night. In order to obtain single colonies liquid culture was streaked out on LB-agar plates containing ampicillin and tetracyclin. In parallel plasmids were isolated (using NucleoSpin® Plasmid Miniprep Kit – Macherey-Nagel) and identity of the clone was confirmed by sequencing at GATC Biotech. RNAi plates to feed *C. elegans* were prepared (compare chapter 5.18.4 RNAi plates) and over-night culture grown in LB supplemented with ampicillin at 37°C, was streaked out and dried over night at 37°C. Plates were stored at 4°C and no longer than one week. 25 L4 stage worms were picked on 92mm RNAi plates and maintained at 20°C until F1 generation reached L4 stage. In the case of *smc-5* or *smc-6* balanced strains, heterozygous worms were picked. Next, F1 homozygous L4 larvae were transferred on fresh 33mm RNAi plates and incubated over night to reach adulthood. The next day worms were bleached and F2 homozygous worms hatched in the absence of food to synchronize populations. Finally, F1 larvae were plated on fresh 33mm RNAi plates and treated as outlined in the text.

### 5.14 Generation of males for crossing

Six L4 stage hermaphrodites were picked on six individual OP50-seeded NGM plates and incubated at 30°C. After 5 ½h, 6h and 6 ½h two plates were transferred to a 20°C incubator. The high temperature leads to an enhancement of non-disjunction events in the germline of the L4 larvae and plates can be screened for males three days later.

## **5.15 small RNA sequencing and bioinformatical analysis**

### **5.15.1 small RNA sequencing**

Quality-checked RNA samples were processed and sequencing executed at the Cologne Center for Genomics (CCG) following Illumina deep sequencing protocols.

### **5.15.2 Data analysis**

Data procession and expression analysis was performed by Susanne Motameny at CCG according to Motameny et al. 2010 and as described in the text.

## **5.16 CPD repair assay using slotblot**

To obtain a large number of worms *COPAS BIOSORT* (Complex Object Parametric Analyzer and Sorter) was used to collect about 1,500 homozygous F1 L4 larvae and young adults. Setup for selection of homozygous YE57 worms was established with the help of Dr. Daniel Magner (Max Planck Institute for Biology of Aging, Cologne). Worms were bleached 24h later and grown on 92mm OP50-seeded NGM plates at 20°C. Day one adult worms were treated with 60mJ/cm<sup>2</sup> UVB and either processed directly or maintained at 20°C for 24h to allow time for repair. After washing with ice-cold M9 buffer samples were quick-frozen in liquid nitrogen. Genomic DNA was prepped using Genra Puregene Tissue Kit (Qiagen). 3ml of cell lysis solution and 15µl Proteinase K (20mg/ml) were added and the mix was incubated for 3h at 55°C. Samples were allowed to cool down to room temperature before adding 15µl of RNase A solution and 30min incubation at 37°C. Samples were cooled for 3min on ice and 1ml of protein precipitation solution was added. After vortexing for 20sec and 10min centrifugation at 2,000xg, supernatant was transferred to a new tube. For DNA precipitation 3ml of isopropanol were added and tubes gently inverted 50 times. Then samples were centrifuged for 3min at 2,000xg and the pellet was allowed to air dry for 10min at RT. Genomic DNA was solved in DNA rehydration buffer and concentration measured using a Nanodrop 8000. A 1:2 dilution series starting with 1µg was prepared and dilutions were denatured for 5min at 95°C, put directly on ice, and blotted onto an Hybond nylon membrane (Amersham) using a Whatman 96-well slot blotting device at 300mbar vacuum. Cross-linking of the DNA was carried out for 2h at 80°C. The membrane was blocked for 30min in 3% milk/PBS. Anti-Cyclobutane Pyrimidine Dimers antibody was diluted

1:15,000 in PBS containing 0.1% Tween20 (PBST). The membrane was incubated in antibody solution over night at 4°C, washed three times in PBST and incubated 1h with 1:10,000 secondary antibody solution Peroxidase-conjugated AffiniPure Goat Anti-Mouse IgG + IgM [H+L] (JacksonImmuno Research) in PBST at room temperature and washed three times in PBST. DNA lesions were visualized by ECL plus Western blotting reagent (Amersham) and exposing CL-Xposure Film (Thermo Scientific).

## 5.17 Antibodies used

Reactivity	Host	Dilution	Source	Application	Specifications
RAD-51	rabbit	1:300	Acris/SDIX	IF	
SMC-6	rabbit	1:200	Raymond Chan , University of Michigan	IF	
Phospho-Chk1 (Ser345)	rabbit	1:50	Cell Signaling Technology	IF	
BRD-1	rabbit	1:100	Simon Boulton, London Research Institute	IF	
mouse	donkey	1:400	Invitrogen - Life Technologies Corporation	IF	Alexa Fluor488-labeled
rabbit	donkey	1:400	Jackson Immuno Research	IF	DyLight 594-conjugated
rabbit	donkey	1:400	Jackson Immuno Research	IF	DyLight 549-conjugated
CPDs	mouse	1:15,000	Cosmobio Co.,Ltd	SB	
mouse	goat	1:10,000	Jackson Immuno Research	SB	HRP-conjugated

IF: Immunofluorescence; SB: DNA Slotblot

## 5.18 Growth media & solutions

### 5.18.1 Single worm lysis buffer

Tris pH 8.0	30mM
EDTA pH 8.0	0.5M
NaCl	100mM
NP40	0.7%
Tween20	0.7%
Protease K (20mg/ml)	1:40

### 5.18.2 M9 buffer

KH <sub>2</sub> PO <sub>4</sub>	3g
NaHPO <sub>4</sub>	6g
NaCl	5g

Distilled water up to 1 l

After autoclaving, MgSO<sub>4</sub> was added to a final concentration of 1mM.

### 5.18.3 NGM plates

Bacto Peptone	2.5g
NaCl	3g
Serva Agar	17g
Distilled water	952ml

Solution was autoclaved at 121 °C for 20 min and then cooled down to 56 °C before addition of:

0.1 M CaCl <sub>2</sub>	10ml
0.1 M MgSO <sub>4</sub>	10ml
5 mg/ml Cholesterol	1ml

Now the solution was mixed for 5 min and the last components were added:

1M KPO <sub>4</sub>	25ml
10,000 units/ml Nystatin	2.5ml

### 5.18.4 RNAi plates

RNAi plates were prepared like NGM plates but supplemented with 3mM IPTG and 100ng/ml ampicillin. IPTG should be sterile filtered and Ampicillin solved in Ethanol.

### 5.18.5 2x Freezing buffer

NaCl	5.8g
KH <sub>2</sub> PO <sub>4</sub>	6.8g
Glycerol	300g
5M NaOH	1.12ml

Distilled water up to 1l

Solution was autoclaved before usage.

### 5.18.6 2x Bleaching solution

1M KOH	12,5ml
NaClO	10ml

Distilled water up to 50ml final volume.

#### **5.18.7 LB**

NaCl 10g

Tryptone 10g

Yeast Extract 5g

Distilled water up to 1l

Solution was autoclaved before usage.

#### **5.18.8 LB-agar plates**

LB medium was supplemented with 18g Agar before autoclaving.

#### **5.18.9 PBS**

Na<sub>2</sub>HPO<sub>4</sub> 1.44g

KH<sub>2</sub>PO<sub>4</sub> 0.24g

NaCl 8g

KCl 0.2g

Distilled water up to 1l

Solution was adjusted to pH 7.4 using 0.1M NaOH and autoclaved before usage.

#### **5.18.10 50x TAE**

Tris 242g

Acetic acid 57ml

0.5M EDTA 100ml

Distilled water up to 1l

Solution was adjusted to pH 8.5 using NaOH.

#### **5.18.11 TE buffer**

All primer stocks were diluted in TE.

1M Tris-HCl pH 8.0 2ml

0.5M EDTA pH 8.0 0.4ml

Distilled water up to 200ml

### 5.18.12 0.5M EDTA

EDTA 186.1g

NaOH 20g

Distilled water up to 1l

Solution was adjusted to pH 8.0 so that EDTA is soluble and autoclaved before usage.

## VI List of abbreviations

µm	Micrometre
4-NQO	4-nitroquinoline-N-oxide
6,4-PP	6,4-photoproduct
ABC transporter	ATP-binding cassette transporter
ADAR	Adenosine deaminase acting on RNA
AMO	Anti-microRNA antisense oligodeoxyribonucleotide
ATP	Adenosine triphosphate
ATPase	ATP hydrolase
BER	Base excision repair
bp	Base pair
BRCT domain	BRCA1 C-terminal domain
CCG	Cologne Center for Genomics
cm	Centimetre
CPD	Cyclobutane pyrimidine dimer
CS	Cockayne syndrome
Ct	Cycle threshold
C-terminus	Carboxy-terminus
ctrl	Control
DAPI	4',6-diamidino-2-phenylindole
DDR	DNA damage repair
DIC	Differential interference contrast
DNA	Deoxyribonucleic acid
dNTP	Deoxyribonucleotide
dsRNA	Double-stranded RNA
DTC	Distal tip cell
EMS	Ethylmethane sulfonate
F1 generation	First filial generation
F2 generation	Second filial generation

FA	Fanconi anemia
FAM	6-carboxyfluorescein
G1 phase	Gap 1 phase of cell cycle
G2 phase	Gap 2 phase of cell cycle
GFP	Green fluorescent protein
GG-NER	Global-genome nucleotide excision repair
GO	Gene ontology
h	Hours
HR	Homologous recombination
HU	Hydroxyurea
ICL	Interstrand crosslink
IPTG	Isopropyl- $\beta$ -D-thiogalactopyranosid
IR	Ionizing radiation
M phase	Mitosis phase of cell cycle
MAPK	Mitogen-activated protein kinases
MAQ Gene	Mapping and Assembly with Qualities Gene
Mb	Mega base
min	Minutes
miRNA	MicroRNA
miRNP	MicroRNA ribonucleoprotein complex
mJ	Milli-Joule
mm	Millimetre
MMS	Methyl methanesulfonate
MRN	Mre11-Rad50-Nbs1 in yeast/ MRE11-RAD50-NBS1 in human
mRNA	Messenger RNA
NER	Nucleotide excision repair
NGM	Nematode growth medium
NHEJ	Non-homologous end joining
nm	Nanometre
Nse	Non-Smc element
N-terminus	Amino-terminus
oncomiR	Oncogenic microRNA
P0 generation	Parental generation
PAR-CLIP	Photoactivatable-Ribonucleoside-Enhanced Crosslinking and Immunoprecipitation
PCR	Polymerase chain reaction
piRNA	PIWI-interacting RNA
pre-miRNA	Precursor miRNA

pri-miRNA	Primary miRNA
PTGS	Posttranscriptional gene silencing
qPCR	Quantitative polymerase chain reaction
rad	Radiation sensitive
RAS	Rat sarcoma
RdRP	RNA dependent RNA polymerase
RIN	RNA integrity number
RING domain	Really Interesting New Gene domain
RISC	RNA-induced silencing complex
RNA	Ribonucleic acid
RNAi	RNA interference
RNAP	RNA polymerase
ROS	Reactive oxygen species
rpm	Reads per million
rRNA	Ribosomal RNA
RT	Reverse transcription
S phase	DNA synthesis phase of cell cycle
siRNA	Small interfering RNA
SMC	Structural Maintenance of Chromosomes
SNP	Single nucleotide polymorphism
SSB	Single-strand break
stRNA	Small temporally expressed RNAs
SUMO	Small ubiquitin-like modifier
TC-NER	Transcription-coupled nucleotide excision repair
TFIIH	Transcription factor IIH
TLS	Translesion synthesis
UTR	Untranslated region
UV	Ultraviolet
V(D)J	Variable, Diverse, and Joining gene segments
wt	wildtype
XP	Xeroderma pigmentosum
XPV	Xeroderma pigmentosum variant
YFP	Yellow fluorescent protein

## VII Acknowledgements

Funding came from the Dieter Platt and the IGSDHD graduate fellowships. In particular, IGSDHD gave me the opportunity to attend two meetings in the USA.

I would like to thank the members of the Schumacher group, for instance Maria for identification of BJS2, support and keeping the boys under control. Michi was a great help in understanding and handling worms. Sebastian helped with the immunostainings and gave some good company. Furthermore, I am grateful for Giorgi, Alexander, Najmeh, Markus, Diletta, Alessandro, Ashley, Kim and Hui-Ling for being not only colleagues but friends. Rebecca helped with making some important findings and people from the Hoppe laboratory were always helpful in providing a refuge whenever needed, good advices and useful discussions. Further, I want to thank Raymond for this fruitful cooperation. Also, ‘merci’ to my *smc-5*-buddy, Julien. In particular, I want to thank Vipin and Laia for being good friends and Jenny for all her support and brighten up the days in the laboratory. Last but not least I want to thank Björn for his support and guidance. Finally, I would like to thank my family and all the people helping and keeping me from getting crazy.

## VIII References

- Abbott, Allison L, Ezequiel Alvarez-Saavedra, Eric A Miska, Nelson C Lau, David P Bartel, H Robert Horvitz, and Victor Ambros. 2005. “The Let-7 MicroRNA Family Members Mir-48, Mir-84, and Mir-241 Function Together to Regulate Developmental Timing in *Caenorhabditis Elegans*.” *Developmental Cell* 9 (3) (September): 403–14. doi:10.1016/j.devcel.2005.07.009.
- Alder, Matthew N, Shale Dames, Jeffrey Gaudet, and Susan E Mango. 2003. “Gene Silencing in *Caenorhabditis Elegans* by Transitive RNA Interference.” *RNA (New York, N.Y.)* 9 (1) (January): 25–32.
- Altun, Z. F., and D. H. Hall. 2006. “CAENORHABDITIS *Elegans* AS A GENETIC ORGANISM.” In *WormAtlas*.
- Alvarez-Saavedra, Ezequiel, and H Robert Horvitz. 2010. “Many Families of *C. Elegans* microRNAs Are Not Essential for Development or Viability.” *Current Biology: CB* 20 (4) (February 23): 367–73. doi:10.1016/j.cub.2009.12.051.
- Ameres, Stefan L., and Phillip D. Zamore. 2013. “Diversifying microRNA Sequence and Function.” *Nature Reviews Molecular Cell Biology* advance on (June 26). doi:10.1038/nrm3611.
- Ampatzidou, Eleni, Anja Irmisch, Matthew J O’Connell, and Johanne M Murray. 2006. “*Smc5/6* Is Required for Repair at Collapsed Replication Forks.” *Molecular and Cellular Biology* 26 (24) (December): 9387–401. doi:10.1128/MCB.01335-06.

- An, Jiyuan, John Lai, Melanie L Lehman, and Colleen C Nelson. 2013. "miRDeep\*: An Integrated Application Tool for miRNA Identification from RNA Sequencing Data." *Nucleic Acids Research* 41 (2) (January): 727–37. doi:10.1093/nar/gks1187.
- Angelo, Giana, and Marc R Van Gilst. 2009. "Starvation Protects Germline Stem Cells and Extends Reproductive Longevity in *C. Elegans*." *Science (New York, N.Y.)* 326 (5955) (November 13): 954–8. doi:10.1126/science.1178343.
- Bagga, Shveta, John Bracht, Shaun Hunter, Katlin Massirer, Janette Holtz, Rachel Eachus, and Amy E Pasquinelli. 2005. "Regulation by Let-7 and Lin-4 miRNAs Results in Target mRNA Degradation." *Cell* 122 (4) (August 26): 553–63. doi:10.1016/j.cell.2005.07.031.
- Bailly, Aymeric P, Alasdair Freeman, Julie Hall, Anne-Cécile Déclais, Arno Alpi, David M J Lilley, Shawn Ahmed, and Anton Gartner. 2010. "The Caenorhabditis Elegans Homolog of Gen1/Yen1 Resolves Links DNA Damage Signaling to DNA Double-strand Break Repair." *PLoS Genetics* 6 (7) (July): e1001025. doi:10.1371/journal.pgen.1001025.
- Banerjee, Diya, and Frank Slack. 2002. "Control of Developmental Timing by Small Temporal RNAs: a Paradigm for RNA-mediated Regulation of Gene Expression." *BioEssays: News and Reviews in Molecular, Cellular and Developmental Biology* 24 (2) (February): 119–29. doi:10.1002/bies.10046.
- Barriere, A, and MA Felix. 2006. "Isolation of *C. Elegans* and Related Nematodes". WormBook.
- Bartek, Jiri, and Jiri Lukas. 2007. "DNA Damage Checkpoints: From Initiation to Recovery or Adaptation." *Current Opinion in Cell Biology* 19 (2) (April): 238–45. doi:10.1016/j.ceb.2007.02.009.
- Bartel, David P. 2004. "MicroRNAs: Genomics, Biogenesis, Mechanism, and Function." *Cell* 116 (2) (January 23): 281–97.
- Bartocci, Cristina, and Eros Lazzarini Denchi. 2013. "Put a RING on It: Regulation and Inhibition of RNF8 and RNF168 RING Finger E3 Ligases at DNA Damage Sites." *Frontiers in Genetics* 4 (January): 128. doi:10.3389/fgene.2013.00128.
- Baugh, L. Ryan, and Paul W. Sternberg. 2006. "DAF-16/FOXO Regulates Transcription of cki-1/Cip/Kip and Repression of Lin-4 During *C. Elegans* L1 Arrest." *Current Biology* 16 (8) (April): 780–785. doi:10.1016/j.cub.2006.03.021.
- Bednarski, Jeffrey J, and Barry P Sleckman. 2012. "Lymphocyte Development: Integration of DNA Damage Response Signaling." *Advances in Immunology* 116 (January): 175–204. doi:10.1016/B978-0-12-394300-2.00006-5.
- Betel, Doron, Anjali Koppal, Phaedra Agius, Chris Sander, and Christina Leslie. 2010. "Comprehensive Modeling of microRNA Targets Predicts Functional Non-conserved and Non-canonical Sites." *Genome Biology* 11 (8) (January): R90. doi:10.1186/gb-2010-11-8-r90.
- Betel, Doron, Manda Wilson, Aaron Gabow, Debora S Marks, and Chris Sander. 2008. "The microRNA.org Resource: Targets and Expression." *Nucleic Acids Research* 36 (Database issue) (January 11): D149–53. doi:10.1093/nar/gkm995.
- Bian, Shan, Janet Hong, Qingsong Li, Laura Schebelle, Andrew Pollock, Jennifer L Knauss, Vidur Garg, and Tao Sun. 2013. "MicroRNA Cluster miR-17-92 Regulates Neural Stem Cell Expansion and Transition to Intermediate Progenitors in the Developing Mouse Neocortex." *Cell Reports* 3 (5) (April 24): 1398–1406. doi:10.1016/j.celrep.2013.03.037.

- Bickel, Jeremy S, Liting Chen, Jin Hayward, Szu Ling Yeap, Ashley E Alkers, and Raymond C Chan. 2010. "Structural Maintenance of Chromosomes (SMC) Proteins Promote Homolog-independent Recombination Repair in Meiosis Crucial for Germ Cell Genomic Stability." Edited by R. Scott Hawley. *PLoS Genetics* 6 (7) (July): e1001028. doi:10.1371/journal.pgen.1001028.
- Bigelow, Henry, Maria Doitsidou, Sumeet Sarin, and Oliver Hobert. 2009. "MAQGene: Software to Facilitate C. Elegans Mutant Genome Sequence Analysis." *Nature Methods* 6 (8) (August): 549. doi:10.1038/nmeth.f.260.
- Blow, J Julian, Xin Quan Ge, and Dean A Jackson. 2011. "How Dormant Origins Promote Complete Genome Replication." *Trends in Biochemical Sciences* 36 (8) (August): 405–14. doi:10.1016/j.tibs.2011.05.002.
- Boulias, Konstantinos, and H Robert Horvitz. 2012. "The C. Elegans microRNA Mir-71 Acts in Neurons to Promote Germline-mediated Longevity through Regulation of DAF-16/FOXO." *Cell Metabolism* 15 (4) (April 4): 439–50. doi:10.1016/j.cmet.2012.02.014.
- Boulton, Simon J, Anton Gartner, Jérôme Reboul, Philippe Vaglio, Nick Dyson, David E Hill, and Marc Vidal. 2002. "Combined Functional Genomic Maps of the C. Elegans DNA Damage Response." *Science (New York, N.Y.)* 295 (5552) (January 4): 127–31. doi:10.1126/science.1065986.
- Boulton, Simon J, Julie S Martin, Jolanta Polanowska, David E Hill, Anton Gartner, and Marc Vidal. 2004. "BRCA1/BARD1 Orthologs Required for DNA Repair in Caenorhabditis Elegans." *Current Biology: CB* 14 (1) (January 6): 33–9.
- Branzei, Dana, Julie Sollier, Giordano Liberi, Xiaolan Zhao, Daisuke Maeda, Masayuki Seki, Takemi Enomoto, Kunihiro Ohta, and Marco Foiani. 2006. "Ubc9- and Mms21-mediated Sumoylation Counteracts Recombinogenic Events at Damaged Replication Forks." *Cell* 127 (3) (November 3): 509–22. doi:10.1016/j.cell.2006.08.050.
- Brennecke, Julius, Alexander Stark, Robert B Russell, and Stephen M Cohen. 2005. "Principles of microRNA-target Recognition." *PLoS Biology* 3 (3) (March): e85. doi:10.1371/journal.pbio.0030085.
- Brenner, John L, Benedict J Kemp, and Allison L Abbott. 2012. "The Mir-51 Family of microRNAs Functions in Diverse Regulatory Pathways in Caenorhabditis Elegans." *PloS One* 7 (5) (January): e37185. doi:10.1371/journal.pone.0037185.
- Brenner, S. 1974. "The Genetics of Caenorhabditis Elegans." *Genetics* 77 (1) (May): 71–94.
- Budhu, Anuradha, Junfang Ji, and Xin W Wang. 2010. "The Clinical Potential of microRNAs." *Journal of Hematology & Oncology* 3 (January): 37. doi:10.1186/1756-8722-3-37.
- Callen, Elsa, Robert B Faryabi, Megan Luckey, Bingtao Hao, Jeremy A Daniel, Wenjing Yang, Hong-Wei Sun, et al. 2012. "The DNA Damage- and Transcription-associated Protein Paxip1 Controls Thymocyte Development and Emigration." *Immunity* 37 (6) (December 14): 971–85. doi:10.1016/j.immuni.2012.10.007.
- Cha, Hwa Jun, Sangsu Shin, Hoesook Yoo, Eun-Mee Lee, Seunghee Bae, Kwang-Hee Yang, Su-Jae Lee, In-Chul Park, Young-Woo Jin, and Sungkwan An. 2009. "Identification of Ionizing Radiation-responsive microRNAs in the IM9 Human B Lymphoblastic Cell Line." *International Journal of Oncology* 34 (6) (June 1): 1661–1668.
- Chan, Shih-Peng, Gopalakrishna Ramaswamy, Eun-Young Choi, and Frank J Slack. 2008. "Identification of Specific Let-7 microRNA Binding Complexes in Caenorhabditis Elegans." *RNA (New York, N.Y.)* 14 (10) (October): 2104–14. doi:10.1261/rna.551208.

- Chapman, J Ross, Martin R G Taylor, and Simon J Boulton. 2012. "Playing the End Game: DNA Double-strand Break Repair Pathway Choice." *Molecular Cell* 47 (4) (August 24): 497–510. doi:10.1016/j.molcel.2012.07.029.
- Chaudhry, M Ahmad. 2009. "Real-time PCR Analysis of micro-RNA Expression in Ionizing Radiation-treated Cells." *Cancer Biotherapy & Radiopharmaceuticals* 24 (1) (February 25): 49–56. doi:10.1089/cbr.2008.0513.
- Chavez, Alejandro, Vishesh Agrawal, and F Brad Johnson. 2011. "Homologous Recombination-dependent Rescue of Deficiency in the Structural Maintenance of Chromosomes (Smc) 5/6 Complex." *The Journal of Biological Chemistry* 286 (7) (February 18): 5119–25. doi:10.1074/jbc.M110.201608.
- Chen, Caifu, Dana A Ridzon, Adam J Broomer, Zhaohui Zhou, Danny H Lee, Julie T Nguyen, Maura Barbisin, et al. 2005. "Real-time Quantification of microRNAs by Stem-loop RT-PCR." *Nucleic Acids Research* 33 (20) (January): e179. doi:10.1093/nar/gni178.
- Chen, Cho-Yi, Shui-Tein Chen, Hsueh-Fen Juan, and Hsuan-Cheng Huang. 2012. "Lengthening of 3'UTR Increases with Morphological Complexity in Animal Evolution." *Bioinformatics (Oxford, England)* 28 (24) (December 15): 3178–81. doi:10.1093/bioinformatics/bts623.
- Chen, J, D P Silver, D Walpita, S B Cantor, A F Gazdar, G Tomlinson, F J Couch, et al. 1998. "Stable Interaction Between the Products of the BRCA1 and BRCA2 Tumor Suppressor Genes in Mitotic and Meiotic Cells." *Molecular Cell* 2 (3) (September): 317–28.
- Chen, Yu-Hung, Koyi Choi, Barnabas Szakal, Jacqueline Arenz, Xinyuan Duan, Hong Ye, Dana Branzei, and Xiaolan Zhao. 2009. "Interplay Between the Smc5/6 Complex and the Mph1 Helicase in Recombinational Repair." *Proceedings of the National Academy of Sciences of the United States of America* 106 (50) (December 15): 21252–7. doi:10.1073/pnas.0908258106.
- Cho, Young-Wook, Teresa Hong, Sunhwa Hong, Hong Guo, Hong Yu, Doyeob Kim, Tad Guszczynski, et al. 2007. "PTIP Associates with MLL3- and MLL4-containing Histone H3 Lysine 4 Methyltransferase Complex." *The Journal of Biological Chemistry* 282 (28) (July 13): 20395–406. doi:10.1074/jbc.M701574200.
- Christensen, Devin E, Peter S Brzovic, and Rachel E Klevit. 2007. "E2-BRCA1 RING Interactions Dictate Synthesis of Mono- or Specific Polyubiquitin Chain Linkages." *Nature Structural & Molecular Biology* 14 (10) (October): 941–8. doi:10.1038/nsmb1295.
- Ciccia, Alberto, and Stephen J Elledge. 2010. "The DNA Damage Response: Making It Safe to Play with Knives." *Molecular Cell* 40 (2) (October 22): 179–204. doi:10.1016/j.molcel.2010.09.019.
- Cleaver, James E, Ernest T Lam, and Ingrid Revet. 2009. "Disorders of Nucleotide Excision Repair: The Genetic and Molecular Basis of Heterogeneity." *Nature Reviews. Genetics* 10 (11) (November): 756–68. doi:10.1038/nrg2663.
- Clejan, Iuval, Julie Boerckel, and Shawn Ahmed. 2006. "Developmental Modulation of Nonhomologous End Joining in *Caenorhabditis Elegans*." *Genetics* 173 (3) (July): 1301–17. doi:10.1534/genetics.106.058628.
- Coleman, Kara A, and Roger A Greenberg. 2011. "The BRCA1-RAP80 Complex Regulates DNA Repair Mechanism Utilization by Restricting End Resection." *The Journal of Biological Chemistry* 286 (15) (April 15): 13669–80. doi:10.1074/jbc.M110.213728.
- Coronnello, Claudia, Ryan Hartmaier, Arshi Arora, Luai Huleihel, Kusum V Pandit, Abha S Bais, Michael Butterworth, et al. 2012. "Novel Modeling of Combinatorial miRNA Targeting Identifies SNP with Potential

- Role in Bone Density.” Edited by Kevin Chen. *PLoS Computational Biology* 8 (12) (January): e1002830. doi:10.1371/journal.pcbi.1002830.
- Costes, S V, I Chiolo, J M Pluth, M H Barcellos-Hoff, and B Jakob. 2010. “Spatiotemporal Characterization of Ionizing Radiation Induced DNA Damage Foci and Their Relation to Chromatin Organization.” *Mutation Research* 704 (1-3) (January): 78–87. doi:10.1016/j.mrrev.2009.12.006.
- Dantuma, Nico P, Christian Heinen, and Deborah Hoogstraten. 2009. “The Ubiquitin Receptor Rad23: At the Crossroads of Nucleotide Excision Repair and Proteasomal Degradation.” *DNA Repair* 8 (4) (April 5): 449–60. doi:10.1016/j.dnarep.2009.01.005.
- Davis, M Wayne, Marc Hammarlund, Tracey Harrach, Patrick Hullett, Shawn Olsen, and Erik M Jorgensen. 2005. “Rapid Single Nucleotide Polymorphism Mapping in *C. Elegans*.” *BMC Genomics* 6 (January): 118. doi:10.1186/1471-2164-6-118.
- De Lencastre, Alexandre, Zachary Pincus, Katherine Zhou, Masaomi Kato, Siu Sylvia Lee, and Frank J Slack. 2010. “MicroRNAs Both Promote and Antagonize Longevity in *C. elegans*.” *Current Biology: CB* 20 (24) (December 21): 2159–68. doi:10.1016/j.cub.2010.11.015.
- De Piccoli, Giacomo, Jordi Torres-Rosell, and Luis Aragón. 2009. “The Unnamed Complex: What Do We Know About Smc5-Smc6?” *Chromosome Research: an International Journal on the Molecular, Supramolecular and Evolutionary Aspects of Chromosome Biology* 17 (2) (January): 251–63. doi:10.1007/s10577-008-9016-8.
- Deans, Andrew J, and Stephen C West. 2011. “DNA Interstrand Crosslink Repair and Cancer.” *Nature Reviews. Cancer* 11 (7) (July): 467–80. doi:10.1038/nrc3088.
- Ding, Xavier C, and Helge Grosshans. 2009. “Repression of *C. elegans* microRNA Targets at the Initiation Level of Translation Requires GW182 Proteins.” *The EMBO Journal* 28 (3) (February 4): 213–22. doi:10.1038/emboj.2008.275.
- Ebhardt, H Alexander, Amber Fedynak, and Richard P Fahlman. 2010. “Naturally Occurring Variations in Sequence Length Creates microRNA Isoforms That Differ in Argonaute Effector Complex Specificity.” *Silence* 1 (1) (January): 12. doi:10.1186/1758-907X-1-12.
- Edgar, L G. 1995. “Blastomere Culture and Analysis.” *Methods in Cell Biology* 48 (January): 303–21.
- Edgley, M L, and D L Riddle. 2001. “LG II Balancer Chromosomes in *Caenorhabditis elegans*: mT1(II;III) and the mIn1 Set of Dominantly and Recessively Marked Inversions.” *Molecular Genetics and Genomics: MGG* 266 (3) (November): 385–95. doi:10.1007/s004380100523.
- Encalada, S E, P R Martin, J B Phillips, R Lyczak, D R Hamill, K A Swan, and B Bowerman. 2000. “DNA Replication Defects Delay Cell Division and Disrupt Cell Polarity in Early *Caenorhabditis Elegans* Embryos.” *Developmental Biology* 228 (2) (December 15): 225–38. doi:10.1006/dbio.2000.9965.
- Enright, Anton J, Bino John, Ulrike Gaul, Thomas Tuschl, Chris Sander, and Debora S Marks. 2003. “MicroRNA Targets in *Drosophila*.” *Genome Biology* 5 (1) (January): R1. doi:10.1186/gb-2003-5-1-r1.
- Félix, Marie-Anne, and Fabien Duveau. 2012. “Population Dynamics and Habitat Sharing of Natural Populations of *Caenorhabditis Elegans* and *C. Briggsae*.” *BMC Biology* 10 (January): 59. doi:10.1186/1741-7007-10-59.
- Feng, Zhihui, and Junran Zhang. 2012. “A Dual Role of BRCA1 in Two Distinct Homologous Recombination Mediated Repair in Response to Replication Arrest.” *Nucleic Acids Research* 40 (2) (January): 726–38. doi:10.1093/nar/gkr748.

- Fire, A, D Albertson, S W Harrison, and D G Moerman. 1991. "Production of Antisense RNA Leads to Effective and Specific Inhibition of Gene Expression in *C. Elegans* Muscle." *Development (Cambridge, England)* 113 (2) (October): 503–14.
- Fischer, E J Sylvia. 2010. "Small RNA-mediated Gene Silencing Pathways in *C. Elegans*." <http://biochemistry.ucsf.edu/courses/genetics/wp-content/uploads/2011/10/RNAi-background.pdf>.
- Flibotte, Stephane, Mark L Edgley, Iasha Chaudhry, Jon Taylor, Sarah E Neil, Aleksandra Rogula, Rick Zapf, et al. 2010. "Whole-genome Profiling of Mutagenesis in *Caenorhabditis Elegans*." *Genetics* 185 (2) (June 1): 431–41. doi:10.1534/genetics.110.116616.
- Flynt, Alex S, and Eric C Lai. 2008. "Biological Principles of microRNA-mediated Regulation: Shared Themes Amid Diversity." *Nature Reviews. Genetics* 9 (11) (November): 831–42. doi:10.1038/nrg2455.
- Fournane, Sadek, Ksenia Krupina, Charlotte Kleiss, and Izabela Sumara. 2012. "Decoding Ubiquitin for Mitosis." *Genes & Cancer* 3 (11-12) (November): 697–711. doi:10.1177/1947601912473477.
- Fousteri, M I, and A R Lehmann. 2000. "A Novel SMC Protein Complex in *Schizosaccharomyces Pombe* Contains the Rad18 DNA Repair Protein." *The EMBO Journal* 19 (7) (April 3): 1691–702. doi:10.1093/emboj/19.7.1691.
- Friedländer, Marc R, Wei Chen, Catherine Adamidi, Jonas Maaskola, Ralf Einspanier, Signe Knospel, and Nikolaus Rajewsky. 2008. "Discovering microRNAs from Deep Sequencing Data Using miRDeep." *Nature Biotechnology* 26 (4) (April): 407–15. doi:10.1038/nbt1394.
- Galardi, Silvia, Neri Mercatelli, Ezio Giorda, Simone Massalini, Giovanni Vanni Frajese, Silvia Anna Ciafrè, and Maria Giulia Farace. 2007. "miR-221 and miR-222 Expression Affects the Proliferation Potential of Human Prostate Carcinoma Cell Lines by Targeting p27Kip1." *The Journal of Biological Chemistry* 282 (32) (August 10): 23716–24. doi:10.1074/jbc.M701805200.
- Gartner, Anton, Amy J MacQueen, and Anne M Villeneuve. 2004. "Methods for Analyzing Checkpoint Responses in *Caenorhabditis Elegans*." *Methods in Molecular Biology (Clifton, N.J.)* 280 (January): 257–74. doi:10.1385/1-59259-788-2:257.
- Goenzyz, Pierre, and S. Lesilee Rose. 2005. "Asymmetric Cell Division and Axis Formation in the Embryo." *WormBook*. [http://www.wormbook.org/chapters/www\\_asymcelldiv/asymcelldiv.html](http://www.wormbook.org/chapters/www_asymcelldiv/asymcelldiv.html).
- Greenstein, David. 2005. "Control of Oocyte Meiotic Maturation and Fertilization." *WormBook: the Online Review of C. Elegans Biology* (January): 1–12. doi:10.1895/wormbook.1.53.1.
- Griffiths-Jones, Sam. 2004. "The microRNA Registry." *Nucleic Acids Research* 32 (Database issue) (January 1): D109–11. doi:10.1093/nar/gkh023.
- Griffiths-Jones, Sam, Harpreet Kaur Saini, Stijn van Dongen, and Anton J Enright. 2008. "miRBase: Tools for microRNA Genomics." *Nucleic Acids Research* 36 (Database issue) (January 11): D154–8. doi:10.1093/nar/gkm952.
- Grosshans, Helge, Ted Johnson, Kristy L Reinert, Mark Gerstein, and Frank J Slack. 2005. "The Temporal Patterning microRNA Let-7 Regulates Several Transcription Factors at the Larval to Adult Transition in *C. Elegans*." *Developmental Cell* 8 (3) (March): 321–30. doi:10.1016/j.devcel.2004.12.019.

- Gu, Sam G, Julia Pak, Sergio Barberan-Soler, Mustapha Ali, Andrew Fire, and Alan M Zahler. 2007. "Distinct Ribonucleoprotein Reservoirs for microRNA and siRNA Populations in *C. Elegans*." *RNA (New York, N.Y.)* 13 (9) (September): 1492–504. doi:10.1261/rna.581907.
- Gumienny, T L, E Lambie, E Hartwig, H R Horvitz, and M O Hengartner. 1999. "Genetic Control of Programmed Cell Death in the *Caenorhabditis Elegans* Hermaphrodite Germline." *Development (Cambridge, England)* 126 (5) (February): 1011–22.
- Guo, Li, and Zuhong Lu. 2010. "The Fate of miRNA\* Strand through Evolutionary Analysis: Implication for Degradation as Merely Carrier Strand or Potential Regulatory Molecule?" *PloS One* 5 (6) (January): e11387. doi:10.1371/journal.pone.0011387.
- Hammell, Christopher M, Xantha Karp, and Victor Ambros. 2009. "A Feedback Circuit Involving Let-7-family miRNAs and DAF-12 Integrates Environmental Signals and Developmental Timing in *Caenorhabditis Elegans*." *Proceedings of the National Academy of Sciences of the United States of America* 106 (44) (November 3): 18668–73. doi:10.1073/pnas.0908131106.
- Hammond, Scott M. 2006. "RNAi, microRNAs, and Human Disease." *Cancer Chemotherapy and Pharmacology* 58 Suppl 1 (November): s63–8. doi:10.1007/s00280-006-0318-2.
- Hanada, Katsuhiko, Magda Budzowska, Sally L Davies, Ellen van Drunen, Hideo Onizawa, H Berna Beverloo, Alex Maas, Jeroen Essers, Ian D Hickson, and Roland Kanaar. 2007. "The Structure-specific Endonuclease Mus81 Contributes to Replication Restart by Generating Double-strand DNA Breaks." *Nature Structural & Molecular Biology* 14 (11) (November): 1096–104. doi:10.1038/nsmb1313.
- Harper, J Wade, and Stephen J Elledge. 2007. "The DNA Damage Response: Ten Years After." *Molecular Cell* 28 (5) (December 14): 739–45. doi:10.1016/j.molcel.2007.11.015.
- Hartman, P S, and R K Herman. 1982. "Radiation-sensitive Mutants of *Caenorhabditis Elegans*." *Genetics* 102 (2) (October): 159–78.
- Hayashita, Yoji, Hiroataka Osada, Yoshio Tatematsu, Hideki Yamada, Kiyoshi Yanagisawa, Shuta Tomida, Yasushi Yatabe, Katsunobu Kawahara, Yoshitaka Sekido, and Takashi Takahashi. 2005. "A Polycistronic microRNA Cluster, miR-17-92, Is Overexpressed in Human Lung Cancers and Enhances Cell Proliferation." *Cancer Research* 65 (21) (November 1): 9628–32. doi:10.1158/0008-5472.CAN-05-2352.
- He, Lin, and Gregory J Hannon. 2004. "MicroRNAs: Small RNAs with a Big Role in Gene Regulation." *Nature Reviews. Genetics* 5 (7) (July): 522–31. doi:10.1038/nrg1379.
- Herman, Michael A. 2006. "Hermaphrodite Cell-fate Specification." In *WormBook*.
- Hirano, Michiko, and Tatsuya Hirano. 2006. "Opening Closed Arms: Long-distance Activation of SMC ATPase by hinge-DNA Interactions." *Molecular Cell* 21 (2) (January 20): 175–86. doi:10.1016/j.molcel.2005.11.026.
- Hirano, Tatsuya. 2002. "The ABCs of SMC Proteins: Two-armed ATPases for Chromosome Condensation, Cohesion, and Repair." *Genes & Development* 16 (4) (February 15): 399–414. doi:10.1101/gad.955102.
- Hirano, Tatsuya. 2006. "At the Heart of the Chromosome: SMC Proteins in Action." *Nature Reviews. Molecular Cell Biology* 7 (5) (May): 311–22. doi:10.1038/nrm1909.
- Holway, Antonia H, Seung-Hwan Kim, Adriana La Volpe, and W Matthew Michael. 2006. "Checkpoint Silencing During the DNA Damage Response in *Caenorhabditis Elegans* Embryos." *The Journal of Cell Biology* 172 (7) (March 27): 999–1008. doi:10.1083/jcb.200512136.

- Hristova, Marta, Darcy Birse, Yang Hong, and Victor Ambros. 2005. "The Caenorhabditis Elegans Heterochronic Regulator LIN-14 Is a Novel Transcription Factor That Controls the Developmental Timing of Transcription from the Insulin/insulin-like Growth Factor Gene Ins-33 by Direct DNA Binding." *Molecular and Cellular Biology* 25 (24) (December): 11059–72. doi:10.1128/MCB.25.24.11059-11072.2005.
- Hu, Hailiang, and Richard A Gatti. 2011. "MicroRNAs: New Players in the DNA Damage Response." *Journal of Molecular Cell Biology* 3 (3) (June 23): 151–8. doi:10.1093/jmcb/mjq042.
- Hu, Patrick J. 2007. "Dauer." *WormBook: the Online Review of C. Elegans Biology* (January): 1–19. doi:10.1895/wormbook.1.144.1.
- Huang, Da Wei, Brad T Sherman, and Richard A Lempicki. 2009a. "Systematic and Integrative Analysis of Large Gene Lists Using DAVID Bioinformatics Resources." *Nature Protocols* 4 (1) (January): 44–57. doi:10.1038/nprot.2008.211.
- Huang, Da Wei, Brad T. Sherman and Richard A Lempicki. 2009b. "Bioinformatics Enrichment Tools: Paths Toward the Comprehensive Functional Analysis of Large Gene Lists." *Nucleic Acids Research* 37 (1) (January): 1–13. doi:10.1093/nar/gkn923.
- Hubbard, E Jane Albert, and David Greenstein. 2005. "Introduction to the Germ Line." *WormBook: the Online Review of C. Elegans Biology* (January): 1–4. doi:10.1895/wormbook.1.18.1.
- Huen, Michael S Y, Shirley M H Sy, and Junjie Chen. 2010. "BRCA1 and Its Toolbox for the Maintenance of Genome Integrity." *Nature Reviews. Molecular Cell Biology* 11 (2) (March): 138–48. doi:10.1038/nrm2831.
- Huertas, Pablo. 2010. "DNA Resection in Eukaryotes: Deciding How to Fix the Break." *Nature Structural & Molecular Biology* 17 (1) (January): 11–6. doi:10.1038/nsmb.1710.
- Hurley, Laurence H. 2002. "DNA and Its Associated Processes as Targets for Cancer Therapy." *Nature Reviews. Cancer* 2 (3) (March): 188–200. doi:10.1038/nrc749.
- Hutvagner, György, and Phillip D Zamore. 2002. "A microRNA in a Multiple-turnover RNAi Enzyme Complex." *Science (New York, N.Y.)* 297 (5589) (September 20): 2056–60. doi:10.1126/science.1073827.
- Iraqi, Ismail, Yasmina Chekkal, Nada Jmari, Violena Pietrobon, Karine Fréon, Audrey Costes, and Sarah A E Lambert. 2012. "Recovery of Arrested Replication Forks by Homologous Recombination Is Error-prone." Edited by Sue Jinks-Robertson. *PLoS Genetics* 8 (10) (January): e1002976. doi:10.1371/journal.pgen.1002976.
- Irmisch, Anja, Eleni Ampatzidou, Ken'ichi Mizuno, Matthew J O'Connell, and Johanne M Murray. 2009. "Smc5/6 Maintains Stalled Replication Forks in a Recombination-competent Conformation." *The EMBO Journal* 28 (2) (January 21): 144–55. doi:10.1038/emboj.2008.273.
- Jackson, Stephen P, and Jiri Bartek. 2009. "The DNA-damage Response in Human Biology and Disease." *Nature* 461 (7267) (October 22): 1071–8. doi:10.1038/nature08467.
- Jan, Calvin H, Robin C Friedman, J Graham Ruby, and David P Bartel. 2011. "Formation, Regulation and Evolution of Caenorhabditis Elegans 3'UTRs." *Nature* 469 (7328) (January 6): 97–101. doi:10.1038/nature09616.
- Jeppesen, Dennis Kjølhed, Vilhelm A Bohr, and Tinna Stevnsner. 2011. "DNA Repair Deficiency in Neurodegeneration." *Progress in Neurobiology* 94 (2) (July): 166–200. doi:10.1016/j.pneurobio.2011.04.013.

- John, Bino, Anton J Enright, Alexei Aravin, Thomas Tuschl, Chris Sander, and Debora S Marks. 2004. "Human MicroRNA Targets." *PLoS Biology* 2 (11) (November): e363. doi:10.1371/journal.pbio.0020363.
- Johnson, Charles D, Aurora Esquela-Kerscher, Giovanni Stefani, Mike Byrom, Kevin Kelnar, Dmitriy Ovcharenko, Mike Wilson, et al. 2007. "The Let-7 microRNA Represses Cell Proliferation Pathways in Human Cells." *Cancer Research* 67 (16) (August 15): 7713–22. doi:10.1158/0008-5472.CAN-07-1083.
- Johnson, Steven M, Helge Grosshans, Jaclyn Shingara, Mike Byrom, Rich Jarvis, Angie Cheng, Emmanuel Labourier, Kristy L Reinert, David Brown, and Frank J Slack. 2005. "RAS Is Regulated by the Let-7 microRNA Family." *Cell* 120 (5) (March 11): 635–47. doi:10.1016/j.cell.2005.01.014.
- Jovanovic, M, and M O Hengartner. 2006. "miRNAs and Apoptosis: RNAs to Die For." *Oncogene* 25 (46) (October 9): 6176–87. doi:10.1038/sj.onc.1209912.
- Kamath, Ravi S, Andrew G Fraser, Yan Dong, Gino Poulin, Richard Durbin, Monica Gotta, Alexander Kanapin, et al. 2003. "Systematic Functional Analysis of the *Caenorhabditis Elegans* Genome Using RNAi." *Nature* 421 (6920) (January 16): 231–7. doi:10.1038/nature01278.
- Kang, Young-Hoon, Min-Jung Kang, Jeong-Hoon Kim, Chul-Hwan Lee, Il-Taeg Cho, Jerard Hurwitz, and Yeon-Soo Seo. 2009. "The MPH1 Gene of *Saccharomyces Cerevisiae* Functions in Okazaki Fragment Processing." *The Journal of Biological Chemistry* 284 (16) (April 17): 10376–86. doi:10.1074/jbc.M808894200.
- Karp, Xantha, Molly Hammell, Maria C Ow, and Victor Ambros. 2011. "Effect of Life History on microRNA Expression During *C. Elegans* Development." *RNA (New York, N.Y.)* 17 (4) (April): 639–51. doi:10.1261/rna.2310111.
- Kasuga, Hidefumi, Masamitsu Fukuyama, Aya Kitazawa, Kenji Kontani, and Toshiaki Katada. 2013. "The microRNA miR-235 Couples Blast-cell Quiescence to the Nutritional State." *Nature* 497 (7450) (May 5): 503–506. doi:10.1038/nature12117.
- Kato, Masaomi, Alexandre de Lencastre, Zachary Pincus, and Frank J Slack. 2009. "Dynamic Expression of Small Non-coding RNAs, Including Novel microRNAs and piRNAs/21U-RNAs, During *Caenorhabditis Elegans* Development." *Genome Biology* 10 (5) (January): R54. doi:10.1186/gb-2009-10-5-r54.
- Kee, Younghoon, and Alan D D'Andrea. 2010. "Expanded Roles of the Fanconi Anemia Pathway in Preserving Genomic Stability." *Genes & Development* 24 (16) (August 15): 1680–94. doi:10.1101/gad.1955310.
- Kegel, Andreas, Hanna Betts-Lindroos, Takaharu Kanno, Kristian Jeppsson, Lena Ström, Yuki Katou, Takehiko Itoh, Katsuhiko Shirahige, and Camilla Sjögren. 2011. "Chromosome Length Influences Replication-induced Topological Stress." *Nature* 471 (7338) (March 17): 392–6. doi:10.1038/nature09791.
- Kenyon, Cynthia J. 2010. "The Genetics of Aging." *Nature* 464 (7288) (March 25): 504–12. doi:10.1038/nature08980.
- Ketting, R F, S E Fischer, E Bernstein, T Sijen, G J Hannon, and R H Plasterk. 2001. "Dicer Functions in RNA Interference and in Synthesis of Small RNA Involved in Developmental Timing in *C. Elegans*." *Genes & Development* 15 (20) (October 15): 2654–9. doi:10.1101/gad.927801.
- Kim, Seung-Hwan, and W Matthew Michael. 2008. "Regulated Proteolysis of DNA Polymerase Eta During the DNA-damage Response in *C. Elegans*." *Molecular Cell* 32 (6) (December 26): 757–66. doi:10.1016/j.molcel.2008.11.016.
- Kimble, Judith, and Sarah L. Crittenden. 2005. "Germline Proliferation and Its Control." In *WormBook*.

- Krek, Azra, Dominic Grün, Matthew N Poy, Rachel Wolf, Lauren Rosenberg, Eric J Epstein, Philip MacMenamin, et al. 2005. "Combinatorial microRNA Target Predictions." *Nature Genetics* 37 (5) (May): 495–500. doi:10.1038/ng1536.
- Lagos-Quintana, M, R Rauhut, W Lendeckel, and T Tuschl. 2001. "Identification of Novel Genes Coding for Small Expressed RNAs." *Science (New York, N.Y.)* 294 (5543) (October 26): 853–8. doi:10.1126/science.1064921.
- Lall, Sabbi, Dominic Grün, Azra Krek, Kevin Chen, Yi-Lu Wang, Colin N Dewey, Pranidhi Sood, et al. 2006. "A Genome-wide Map of Conserved microRNA Targets in *C. Elegans*." *Current Biology: CB* 16 (5) (March 7): 460–71. doi:10.1016/j.cub.2006.01.050.
- Lambert, Sarah, Adam Watson, Daniel M Sheedy, Ben Martin, and Antony M Carr. 2005. "Gross Chromosomal Rearrangements and Elevated Recombination at an Inducible Site-specific Replication Fork Barrier." *Cell* 121 (5) (June 3): 689–702. doi:10.1016/j.cell.2005.03.022.
- Lans, Hannes, Jurgen A Marteijn, Björn Schumacher, Jan H J Hoeijmakers, Gert Jansen, and Wim Vermeulen. 2010. "Involvement of Global Genome Repair, Transcription Coupled Repair, and Chromatin Remodeling in UV DNA Damage Response Changes During Development." *PLoS Genetics* 6 (5) (May): e1000941. doi:10.1371/journal.pgen.1000941.
- Lans, Hannes, and Wim Vermeulen. 2011. "Nucleotide Excision Repair in *Caenorhabditis Elegans*." *Molecular Biology International* 2011 (January): 542795. doi:10.4061/2011/542795.
- Lapierre, Louis R, and Malene Hansen. 2012. "Lessons from *C. Elegans*: Signaling Pathways for Longevity." *Trends in Endocrinology and Metabolism: TEM* 23 (12) (December): 637–44. doi:10.1016/j.tem.2012.07.007.
- Lau, N C, L P Lim, E G Weinstein, and D P Bartel. 2001. "An Abundant Class of Tiny RNAs with Probable Regulatory Roles in *Caenorhabditis Elegans*." *Science (New York, N.Y.)* 294 (5543) (October 26): 858–62. doi:10.1126/science.1065062.
- Le, Minh T N, Cathleen Teh, Ng Shyh-Chang, Huangming Xie, Beiyan Zhou, Vladimir Korzh, Harvey F Lodish, and Bing Lim. 2009. "MicroRNA-125b Is a Novel Negative Regulator of P53." *Genes & Development* 23 (7) (April 1): 862–76. doi:10.1101/gad.1767609.
- Le Sage, Carlos, Remco Nagel, David A Egan, Mariette Schrier, Elly Mesman, Annunziato Mangiola, Corrado Anile, et al. 2007. "Regulation of the p27(Kip1) Tumor Suppressor by miR-221 and miR-222 Promotes Cancer Cell Proliferation." *The EMBO Journal* 26 (15) (August 8): 3699–708. doi:10.1038/sj.emboj.7601790.
- Lee, R C, and V Ambros. 2001. "An Extensive Class of Small RNAs in *Caenorhabditis Elegans*." *Science (New York, N.Y.)* 294 (5543) (October 26): 862–4. doi:10.1126/science.1065329.
- Lee, R C, R L Feinbaum, and V Ambros. 1993. "The *C. Elegans* Heterochronic Gene *Lin-4* Encodes Small RNAs with Antisense Complementarity to *Lin-14*." *Cell* 75 (5) (December 3): 843–54.
- Lee, Se-Jin, Anton Gartner, Moonjung Hyun, Byungchan Ahn, and Hyeon-Sook Koo. 2010. "The *Caenorhabditis Elegans* Werner Syndrome Protein Functions Upstream of ATR and ATM in Response to DNA Replication Inhibition and Double-strand DNA Breaks." Edited by Gregory P. Copenhaver. *PLoS Genetics* 6 (1) (January): e1000801. doi:10.1371/journal.pgen.1000801.
- Lehmann, A R, M Walicka, D J Griffiths, J M Murray, F Z Watts, S McCready, and A M Carr. 1995. "The Rad18 Gene of *Schizosaccharomyces Pombe* Defines a New Subgroup of the SMC Superfamily Involved in DNA Repair." *Molecular and Cellular Biology* 15 (12) (December): 7067–80.

- Lehmann, Alan R. 2003. "DNA Repair-deficient Diseases, Xeroderma Pigmentosum, Cockayne Syndrome and Trichothiodystrophy." *Biochimie* 85 (11) (November): 1101–11.
- Lehmann, Alan R. 2011. "DNA Polymerases and Repair Synthesis in NER in Human Cells." *DNA Repair* 10 (7) (July 15): 730–3. doi:10.1016/j.dnarep.2011.04.023.
- Lehmann, Alan R, Atsuko Niimi, Tomoo Ogi, Stephanie Brown, Simone Sabbioneda, Jonathan F Wing, Patricia L Kannouche, and Catherine M Green. 2007. "Translesion Synthesis: Y-family Polymerases and the Polymerase Switch." *DNA Repair* 6 (7) (July 1): 891–9. doi:10.1016/j.dnarep.2007.02.003.
- Leiser, Scott F, Marissa Fletcher, Anisoara Begun, and Matt Kaerberlein. 2013. "Life-Span Extension From Hypoxia in *Caenorhabditis Elegans* Requires Both HIF-1 and DAF-16 and Is Antagonized by SKN-1." *The Journals of Gerontology. Series A, Biological Sciences and Medical Sciences* (February 18). doi:10.1093/gerona/glt016.
- Lemmens, Bennie B L G, and Marcel Tijsterman. 2011. "DNA Double-strand Break Repair in *Caenorhabditis Elegans*." *Chromosoma* 120 (1) (February): 1–21. doi:10.1007/s00412-010-0296-3.
- Leung, Anthony K L, J Mauro Calabrese, and Phillip A Sharp. 2006. "Quantitative Analysis of Argonaute Protein Reveals microRNA-dependent Localization to Stress Granules." *Proceedings of the National Academy of Sciences of the United States of America* 103 (48) (November 28): 18125–30. doi:10.1073/pnas.0608845103.
- Leung, Anthony K L, and Phillip A Sharp. 2010. "MicroRNA Functions in Stress Responses." *Molecular Cell* 40 (2) (October 22): 205–15. doi:10.1016/j.molcel.2010.09.027.
- Lewis, Benjamin P, Christopher B Burge, and David P Bartel. 2005. "Conserved Seed Pairing, Often Flanked by Adenosines, Indicates That Thousands of Human Genes Are microRNA Targets." *Cell* 120 (1) (January 14): 15–20. doi:10.1016/j.cell.2004.12.035.
- Li, W, and D W Melton. 2012. "Cisplatin Regulates the MAPK Kinase Pathway to Induce Increased Expression of DNA Repair Gene ERCC1 and Increase Melanoma Chemoresistance." *Oncogene* 31 (19) (May 10): 2412–22. doi:10.1038/onc.2011.426.
- Li, Xiao, Ran Zhuo, Stanley Tiong, Francesca Di Cara, Kirst King-Jones, Sarah C Hughes, Shelagh D Campbell, and Rachel Wevrick. 2013. "The Smc5/Smc6/MAGE Complex Confers Resistance to Caffeine and Genotoxic Stress in *Drosophila Melanogaster*." *PloS One* 8 (3) (January): e59866. doi:10.1371/journal.pone.0059866.
- Lieber, Michael R. 2010. "The Mechanism of Double-strand DNA Break Repair by the Nonhomologous DNA End-joining Pathway." *Annual Review of Biochemistry* 79 (January): 181–211. doi:10.1146/annurev.biochem.052308.093131.
- Lim, Lee P, Margaret E Glasner, Soraya Yekta, Christopher B Burge, and David P Bartel. 2003. "Vertebrate microRNA Genes." *Science (New York, N.Y.)* 299 (5612) (March 7): 1540. doi:10.1126/science.1080372.
- Lim, Lee P, Nelson C Lau, Earl G Weinstein, Aliaa Abdelhakim, Soraya Yekta, Matthew W Rhoades, Christopher B Burge, and David P Bartel. 2003. "The microRNAs of *Caenorhabditis Elegans*." *Genes & Development* 17 (8) (April 15): 991–1008. doi:10.1101/gad.1074403.
- Lindahl, T, and B Nyberg. 1972. "Rate of Depurination of Native Deoxyribonucleic Acid." *Biochemistry* 11 (19) (September 12): 3610–8.
- Lints, R., and D. Hall. 2009. "Reproductive System, The Germ Line." In *WormAtlas*.

- Loeb, Lawrence A, and Curtis C Harris. 2008. "Advances in Chemical Carcinogenesis: a Historical Review and Prospective." *Cancer Research* 68 (17) (September 1): 6863–72. doi:10.1158/0008-5472.CAN-08-2852.
- Lou, Zhenkun, Katherine Minter-Dykhouse, and Junjie Chen. 2005. "BRCA1 Participates in DNA Decatenation." *Nature Structural & Molecular Biology* 12 (7) (July): 589–93. doi:10.1038/nsmb953.
- Loveless, A., and Jocelyn Stock. 1959. "The Influence of Radiomimetic Substances on Deoxyribonucleic Acid Synthesis and Function Studied in Escherichia Coli Phage System." In *Proceedings of the Royal Society of London. Series B, Biological Sciences*, 129–147.
- Lu, Jun, Gad Getz, Eric A Miska, Ezequiel Alvarez-Saavedra, Justin Lamb, David Peck, Alejandro Sweet-Cordero, et al. 2005. "MicroRNA Expression Profiles Classify Human Cancers." *Nature* 435 (7043) (June 9): 834–8. doi:10.1038/nature03702.
- Lucanic, Mark, Jill Graham, Gary Scott, Dipa Bhaumik, Christopher C Benz, Alan Hubbard, Gordon J Lithgow, and Simon Melov. 2013. "Age-related micro-RNA Abundance in Individual C. Elegans." *Aging* (June 12).
- Manfrini, Nicola, Iliaria Guerini, Andrea Citterio, Giovanna Lucchini, and Maria Pia Longhese. 2010. "Processing of Meiotic DNA Double Strand Breaks Requires Cyclin-dependent Kinase and Multiple Nucleases." *The Journal of Biological Chemistry* 285 (15) (April 9): 11628–37. doi:10.1074/jbc.M110.104083.
- Martin, Julie S, Nicole Winkelmann, Mark I R Petalcorin, Michael J McIlwraith, and Simon J Boulton. 2005. "RAD-51-dependent and -independent Roles of a Caenorhabditis Elegans BRCA2-related Protein During DNA Double-strand Break Repair." *Molecular and Cellular Biology* 25 (8) (April): 3127–39. doi:10.1128/MCB.25.8.3127-3139.2005.
- Martinez-Finley, Ebany J, Daiana Silva Avila, Sudipta Chakraborty, and Michael Aschner. 2011. "Insights from Caenorhabditis Elegans on the Role of Metals in Neurodegenerative Diseases." *Metallomics: Integrated Biometal Science* 3 (3) (March): 271–9. doi:10.1039/c0mt00064g.
- Masutani, C, R Kusumoto, A Yamada, N Dohmae, M Yokoi, M Yuasa, M Araki, S Iwai, K Takio, and F Hanaoka. 1999. "The XPV (xeroderma Pigmentosum Variant) Gene Encodes Human DNA Polymerase Eta." *Nature* 399 (6737) (June 17): 700–4. doi:10.1038/21447.
- McIlwraith, Michael J, Michael J McIlwraith, Alexandra Vaisman, Yilun Liu, Ellen Fanning, Roger Woodgate, and Stephen C West. 2005. "Human DNA Polymerase Eta Promotes DNA Synthesis from Strand Invasion Intermediates of Homologous Recombination." *Molecular Cell* 20 (5) (December 9): 783–92. doi:10.1016/j.molcel.2005.10.001.
- Mets, David G, and Barbara J Meyer. 2009. "Condensins Regulate Meiotic DNA Break Distribution, Thus Crossover Frequency, by Controlling Chromosome Structure." *Cell* 139 (1) (October 2): 73–86. doi:10.1016/j.cell.2009.07.035.
- Miska, Eric A, Ezequiel Alvarez-Saavedra, Allison L Abbott, Nelson C Lau, Andrew B Hellman, Shannon M McGonagle, David P Bartel, Victor R Ambros, and H Robert Horvitz. 2007. "Most Caenorhabditis Elegans microRNAs Are Individually Not Essential for Development or Viability." *PLoS Genetics* 3 (12) (December): e215. doi:10.1371/journal.pgen.0030215.
- Mizuno, Ken'Ichi, Izumi Miyabe, Stephanie A Schalbetter, Antony M Carr, and Johanne M Murray. 2013. "Recombination-restarted Replication Makes Inverted Chromosome Fusions at Inverted Repeats." *Nature* 493 (7431) (January 10): 246–9. doi:10.1038/nature11676.

- Motameny, Susanne, Stefanie Wolters, Peter Nürnberg, and Björn Schumacher. 2010. "Next Generation Sequencing of miRNAs – Strategies, Resources and Methods." *Genes* 1 (1) (June 3): 70–84. doi:10.3390/genes1010070.
- Mourelatos, Zissimos, Josée Dostie, Sergey Paushkin, Anup Sharma, Bernard Charroux, Linda Abel, Juri Rappsilber, Matthias Mann, and Gideon Dreyfuss. 2002. "miRNPs: a Novel Class of Ribonucleoproteins Containing Numerous microRNAs." *Genes & Development* 16 (6) (March 15): 720–8. doi:10.1101/gad.974702.
- Nasim, A, and B P Smith. 1975. "Genetic Control of Radiation Sensitivity in *Schizosaccharomyces Pombe*." *Genetics* 79 (4) (April): 573–82.
- Nasmyth, Kim, and Christian H. Haering. 2009. "Cohesin: Its Roles and Mechanisms" (November 17).
- Oh, Steve D, Jessica P Lao, Andrew F Taylor, Gerald R Smith, and Neil Hunter. 2008. "RecQ Helicase, Sgs1, and XPF Family Endonuclease, Mus81-Mms4, Resolve Aberrant Joint Molecules During Meiotic Recombination." *Molecular Cell* 31 (3) (August 8): 324–36. doi:10.1016/j.molcel.2008.07.006.
- Ohkumo, Tsuyoshi, Chikahide Masutani, Toshihiko Eki, and Fumio Hanaoka. 2006. "Deficiency of the *Caenorhabditis Elegans* DNA Polymerase Eta Homologue Increases Sensitivity to UV Radiation During Germ-line Development." *Cell Structure and Function* 31 (1) (January): 29–37.
- Okamura, Katsutomo, Michael D Phillips, David M Tyler, Hong Duan, Yu-ting Chou, and Eric C Lai. 2008. "The Regulatory Activity of microRNA\* Species Has Substantial Influence on microRNA and 3' UTR Evolution." *Nature Structural & Molecular Biology* 15 (4) (April): 354–63. doi:10.1038/nsmb.1409.
- Olive, Virginie, Iris Jiang, and Lin He. 2010. "Mir-17-92, a Cluster of miRNAs in the Midst of the Cancer Network." *The International Journal of Biochemistry & Cell Biology* 42 (8) (August): 1348–54. doi:10.1016/j.biocel.2010.03.004.
- Olsen, P H, and V Ambros. 1999. "The Lin-4 Regulatory RNA Controls Developmental Timing in *Caenorhabditis Elegans* by Blocking LIN-14 Protein Synthesis after the Initiation of Translation." *Developmental Biology* 216 (2) (December 15): 671–80. doi:10.1006/dbio.1999.9523.
- Ota, A. 2004. "Identification and Characterization of a Novel Gene, C13orf25, as a Target for 13q31-q32 Amplification in Malignant Lymphoma." *Cancer Research* 64 (9) (May 1): 3087–3095. doi:10.1158/0008-5472.CAN-03-3773.
- Palecek, Jan, Susanne Vidot, Min Feng, Aidan J Doherty, and Alan R Lehmann. 2006. "The Smc5-Smc6 DNA Repair Complex. Bridging of the Smc5-Smc6 Heads by the KLEISIN, Nse4, and non-Kleisin Subunits." *The Journal of Biological Chemistry* 281 (48) (December 1): 36952–9. doi:10.1074/jbc.M608004200.
- Paraskevopoulou, Maria D, Georgios Georgakilas, Nikos Kostoulas, Ioannis S Vlachos, Thanasis Vergoulis, Martin Reczko, Christos Filippidis, Theodore Dalamagas, and A G Hatzigeorgiou. 2013. "DIANA-microT Web Server V5.0: Service Integration into miRNA Functional Analysis Workflows." *Nucleic Acids Research* 41 (W1) (July 1): W169–W173. doi:10.1093/nar/gkt393.
- Pathania, Shailja, Jenna Nguyen, Sarah J Hill, Ralph Scully, Guillaume O Adelmant, Jarrod A Marto, Jean Feunteun, and David M Livingston. 2011. "BRCA1 Is Required for Postreplication Repair after UV-induced DNA Damage." *Molecular Cell* 44 (2) (October 21): 235–51. doi:10.1016/j.molcel.2011.09.002.
- Petalcorin, Mark I R, Vitold E Galkin, Xiong Yu, Edward H Egelman, and Simon J Boulton. 2007. "Stabilization of RAD-51-DNA Filaments via an Interaction Domain in *Caenorhabditis Elegans* BRCA2." *Proceedings of the*

- National Academy of Sciences of the United States of America* 104 (20) (May 15): 8299–304.  
doi:10.1073/pnas.0702805104.
- Petermann, Eva, and Thomas Helleday. 2010. “Pathways of Mammalian Replication Fork Restart.” *Nature Reviews. Molecular Cell Biology* 11 (10) (October): 683–7. doi:10.1038/nrm2974.
- Petermann, Eva, Manuel Luís Orta, Natalia Issaeva, Niklas Schultz, and Thomas Helleday. 2010. “Hydroxyurea-stalled Replication Forks Become Progressively Inactivated and Require Two Different RAD51-mediated Pathways for Restart and Repair.” *Molecular Cell* 37 (4) (February 26): 492–502.  
doi:10.1016/j.molcel.2010.01.021.
- Pfaffl, M W. 2001. “A New Mathematical Model for Relative Quantification in Real-time RT-PCR.” *Nucleic Acids Research* 29 (9) (May 1): e45.
- Pinder, Jordan B, Kathleen M Attwood, and Graham Dellaire. 2013. “Reading, Writing, and Repair: The Role of Ubiquitin and the Ubiquitin-like Proteins in DNA Damage Signaling and Repair.” *Frontiers in Genetics* 4 (January): 45. doi:10.3389/fgene.2013.00045.
- Pothof, Joris, Nicole S Verkaik, Wilfred van IJcken, Erik A C Wiemer, Van T B Ta, Gijsbertus T J van der Horst, Nicolaas G J Jaspers, Dik C van Gent, Jan H J Hoeijmakers, and Stephan P Persengiev. 2009. “MicroRNA-mediated Gene Silencing Modulates the UV-induced DNA-damage Response.” *The EMBO Journal* 28 (14) (June 18): 2090–2099. doi:10.1038/emboj.2009.156.
- Potts, Patrick Ryan, Matthew H Porteus, and Hongtao Yu. 2006. “Human SMC5/6 Complex Promotes Sister Chromatid Homologous Recombination by Recruiting the SMC1/3 Cohesin Complex to Double-strand Breaks.” *The EMBO Journal* 25 (14) (July 26): 3377–88. doi:10.1038/sj.emboj.7601218.
- Potts, Patrick Ryan, and Hongtao Yu. 2005. “Human MMS21/NSE2 Is a SUMO Ligase Required for DNA Repair.” *Molecular and Cellular Biology* 25 (16) (August): 7021–32. doi:10.1128/MCB.25.16.7021-7032.2005.
- Ravanat, J L, T Douki, and J Cadet. 2001. “Direct and Indirect Effects of UV Radiation on DNA and Its Components.” *Journal of Photochemistry and Photobiology. B, Biology* 63 (1-3) (October): 88–102.
- Raymond, Christopher K, Brian S Roberts, Phillip Garrett-Engele, Lee P Lim, and Jason M Johnson. 2005. “Simple, Quantitative Primer-extension PCR Assay for Direct Monitoring of microRNAs and Short-interfering RNAs.” *RNA (New York, N.Y.)* 11 (11) (November): 1737–44. doi:10.1261/rna.2148705.
- Reczko, Martin, Manolis Maragkakis, Panagiotis Alexiou, Ivo Grosse, and Artemis G Hatzigeorgiou. 2012. “Functional microRNA Targets in Protein Coding Sequences.” *Bioinformatics (Oxford, England)* 28 (6) (March 15): 771–6. doi:10.1093/bioinformatics/bts043.
- Reinhart, B J, F J Slack, M Basson, A E Pasquinelli, J C Bettinger, A E Rougvie, H R Horvitz, and G Ruvkun. 2000. “The 21-nucleotide Let-7 RNA Regulates Developmental Timing in *Caenorhabditis Elegans*.” *Nature* 403 (6772) (February 24): 901–6. doi:10.1038/35002607.
- Roerink, Sophie F, Wouter Koole, L Carine Stapel, Ron J Romeijn, and Marcel Tijsterman. 2012. “A Broad Requirement for TLS Polymerases  $\eta$  and  $\kappa$ , and Interacting Sumoylation and Nuclear Pore Proteins, in Lesion Bypass During *C. Elegans* Embryogenesis.” *PLoS Genetics* 8 (6) (June): e1002800.  
doi:10.1371/journal.pgen.1002800.
- Rosen, Eliot M. 2013. “BRCA1 in the DNA Damage Response and at Telomeres.” *Frontiers in Genetics* 4 (January): 85. doi:10.3389/fgene.2013.00085.

- Roush, Sarah, and Frank J Slack. 2008. "The Let-7 Family of microRNAs." *Trends in Cell Biology* 18 (10) (October 1): 505–16. doi:10.1016/j.tcb.2008.07.007.
- Rowley, R, J Hudson, and P G Young. 1992. "The Wee1 Protein Kinase Is Required for Radiation-induced Mitotic Delay." *Nature* 356 (6367) (March 26): 353–5. doi:10.1038/356353a0.
- Rual, Jean-François, Julian Ceron, John Koreth, Tong Hao, Anne-Sophie Nicot, Tomoko Hirozane-Kishikawa, Jean Vandenhaute, et al. 2004. "Toward Improving Caenorhabditis Elegans Phenome Mapping with an ORFeome-based RNAi Library." *Genome Research* 14 (10B) (October): 2162–8. doi:10.1101/gr.2505604.
- Ruby, J Graham, Calvin H Jan, and David P Bartel. 2007. "Intronic microRNA Precursors That Bypass Drosha Processing." *Nature* 448 (7149) (July 5): 83–6. doi:10.1038/nature05983.
- Ryu, Jin-Sun, Sang Jo Kang, and Hyeon-Sook Koo. 2013. "The 53BP1 Homolog in C. Elegans Influences DNA Repair and Promotes Apoptosis in Response to Ionizing Radiation." *PloS One* 8 (5) (January): e64028. doi:10.1371/journal.pone.0064028.
- Saito, Takamune T, Jillian L Youds, Simon J Boulton, and Monica P Colaiácovo. 2009. "Caenorhabditis Elegans HIM-18/SLX-4 Interacts with SLX-1 and XPF-1 and Maintains Genomic Integrity in the Germline by Processing Recombination Intermediates." *PLoS Genetics* 5 (11) (November): e1000735. doi:10.1371/journal.pgen.1000735.
- Sale, Julian E, Alan R Lehmann, and Roger Woodgate. 2012. "Y-family DNA Polymerases and Their Role in Tolerance of Cellular DNA Damage." *Nature Reviews. Molecular Cell Biology* 13 (3) (March): 141–52. doi:10.1038/nrm3289.
- Saleh, Anthony D, Jason E Savage, Liu Cao, Benjamin P Soule, David Ly, William DeGraff, Curtis C Harris, James B Mitchell, and Nicole L Simone. 2011. "Cellular Stress Induced Alterations in microRNA Let-7a and Let-7b Expression Are Dependent on P53." Edited by Natasha Kyprianou. *PloS One* 6 (10) (January): e24429. doi:10.1371/journal.pone.0024429.
- Sarin, Sumeet, Vincent Bertrand, Henry Bigelow, Alexander Boyanov, Maria Doitsidou, Richard J Poole, Surinder Narula, and Oliver Hobert. 2010. "Analysis of Multiple Ethyl Methanesulfonate-mutagenized Caenorhabditis Elegans Strains by Whole-genome Sequencing." *Genetics* 185 (2) (June 1): 417–30. doi:10.1534/genetics.110.116319.
- Schauber, C, L Chen, P Tongaonkar, I Vega, D Lambertson, W Potts, and K Madura. 1998. "Rad23 Links DNA Repair to the Ubiquitin/proteasome Pathway." *Nature* 391 (6668) (February 12): 715–8. doi:10.1038/35661.
- Schleiffer, Alexander, Susanne Kaitna, Sebastian Maurer-Stroh, Michael Glotzer, Kim Nasmyth, and Frank Eisenhaber. 2003. "Kleisins: a Superfamily of Bacterial and Eukaryotic SMC Protein Partners." *Molecular Cell* 11 (3) (March): 571–5.
- Schmittgen, Thomas D, Eun Joo Lee, Jinmai Jiang, Anasuya Sarkar, Liuqing Yang, Terry S Elton, and Caifu Chen. 2008. "Real-time PCR Quantification of Precursor and Mature microRNA." *Methods (San Diego, Calif.)* 44 (1) (January): 31–8. doi:10.1016/j.ymeth.2007.09.006.
- Schott, Daniel H, David K Cureton, Sean P Whelan, and Craig P Hunter. 2005. "An Antiviral Role for the RNA Interference Machinery in Caenorhabditis Elegans." *Proceedings of the National Academy of Sciences of the United States of America* 102 (51) (December 20): 18420–4. doi:10.1073/pnas.0507123102.
- Shao, Genze, Dana R Lilli, Jeffrey Patterson-Fortin, Kara A Coleman, Devon E Morrissey, and Roger A Greenberg. 2009. "The Rap80-BRCC36 De-ubiquitinating Enzyme Complex Antagonizes RNF8-Ubc13-dependent

- Ubiquitination Events at DNA Double Strand Breaks.” *Proceedings of the National Academy of Sciences of the United States of America* 106 (9) (March 3): 3166–71. doi:10.1073/pnas.0807485106.
- Shaw, W Robert, Javier Armisen, Nicolas J Lehrbach, and Eric A Miska. 2010. “The Conserved miR-51 microRNA Family Is Redundantly Required for Embryonic Development and Pharynx Attachment in *Caenorhabditis Elegans*.” *Genetics* 185 (3) (July): 897–905. doi:10.1534/genetics.110.117515.
- Sheedy, Daniel M, Dora Dimitrova, Jessica K Rankin, Kirstin L Bass, Karen M Lee, Claudia Tapia-Alveal, Susan H Harvey, Johanne M Murray, and Matthew J O’Connell. 2005. “Brc1-mediated DNA Repair and Damage Tolerance.” *Genetics* 171 (2) (October 1): 457–68. doi:10.1534/genetics.105.044966.
- Shiloh, Yosef. 2003. “ATM and Related Protein Kinases: Safeguarding Genome Integrity.” *Nature Reviews. Cancer* 3 (3) (March): 155–68. doi:10.1038/nrc1011.
- Si, M-L, S Zhu, H Wu, Z Lu, F Wu, and Y-Y Mo. 2007. “miR-21-mediated Tumor Growth.” *Oncogene* 26 (19) (April 26): 2799–803. doi:10.1038/sj.onc.1210083.
- Sijen, Titia, and Ronald H A Plasterk. 2003. “Transposon Silencing in the *Caenorhabditis Elegans* Germ Line by Natural RNAi.” *Nature* 426 (6964) (November 20): 310–4. doi:10.1038/nature02107.
- Stergiou, L, K Doukometzidis, A Sendoel, and M O Hengartner. 2007. “The Nucleotide Excision Repair Pathway Is Required for UV-C-induced Apoptosis in *Caenorhabditis Elegans*.” *Cell Death and Differentiation* 14 (6) (June): 1129–38. doi:10.1038/sj.cdd.4402115.
- Sun, Yuxiao, Martin Kucej, Heng-Yu Fan, Hong Yu, Qing-Yuan Sun, and Hui Zou. 2009. “Separase Is Recruited to Mitotic Chromosomes to Dissolve Sister Chromatid Cohesion in a DNA-dependent Manner.” *Cell* 137 (1) (April 3): 123–32. doi:10.1016/j.cell.2009.01.040.
- Tan, Guangyun, Jixiao Niu, Yuling Shi, Hongsheng Ouyang, and Zhao-Hui Wu. 2012. “NF-κB-dependent microRNA-125b Up-regulation Promotes Cell Survival by Targeting P38α Upon Ultraviolet Radiation.” *The Journal of Biological Chemistry* 287 (39) (September 21): 33036–47. doi:10.1074/jbc.M112.383273.
- Taniguchi, Toshiyasu, Irene Garcia-Higuera, Paul R Andreassen, Richard C Gregory, Markus Grompe, and Alan D D’Andrea. 2002. “S-phase-specific Interaction of the Fanconi Anemia Protein, FANCD2, with BRCA1 and RAD51.” *Blood* 100 (7) (October 1): 2414–20. doi:10.1182/blood-2002-01-0278.
- Tavazoie, Sohail F, Claudio Alarcón, Thordur Oskarsson, David Padua, Qiongqing Wang, Paula D Bos, William L Gerald, and Joan Massagué. 2008. “Endogenous Human microRNAs That Suppress Breast Cancer Metastasis.” *Nature* 451 (7175) (January 10): 147–52. doi:10.1038/nature06487.
- Taylor, Elaine M, Alice C Copsey, Jessica J R Hudson, Susanne Vidot, and Alan R Lehmann. 2008. “Identification of the Proteins, Including MAGEG1, That Make up the Human SMC5-6 Protein Complex.” *Molecular and Cellular Biology* 28 (4) (February): 1197–206. doi:10.1128/MCB.00767-07.
- Timmons, L, and A Fire. 1998. “Specific Interference by Ingested dsRNA.” *Nature* 395 (6705) (October 29): 854. doi:10.1038/27579.
- Timmons, Lisa, Hiroaki Tabara, Craig C Mello, and Andrew Z Fire. 2003. “Inducible Systemic RNA Silencing in *Caenorhabditis Elegans*.” *Molecular Biology of the Cell* 14 (7) (July): 2972–83. doi:10.1091/mbc.E03-01-0858.

- Tong, Lei, Lexun Lin, Shuo Wu, Zhiwei Guo, Tianying Wang, Ying Qin, Ruixue Wang, et al. 2013. "MiR-10a\* Up-regulates Coxsackievirus B3 Biosynthesis by Targeting the 3D-coding Sequence." *Nucleic Acids Research* 41 (6) (April 1): 3760–71. doi:10.1093/nar/gkt058.
- Torres-Rosell, Jordi, Félix Machín, Sarah Farmer, Adam Jarmuz, Trevor Eydmann, Jacob Z Dalgaard, and Luis Aragón. 2005. "SMC5 and SMC6 Genes Are Required for the Segregation of Repetitive Chromosome Regions." *Nature Cell Biology* 7 (4) (April): 412–9. doi:10.1038/ncb1239.
- Van Laar, Theo, Alex J van der Eb, and Carrol Terleth. 2002. "A Role for Rad23 Proteins in 26S Proteasome-dependent Protein Degradation?" *Mutation Research* 499 (1) (January 29): 53–61.
- Vastenhouw, Nadine L, Karin Brunschwig, Kristy L Okihara, Fritz Müller, Marcel Tijsterman, and Ronald H A Plasterk. 2006. "Gene Expression: Long-term Gene Silencing by RNAi." *Nature* 442 (7105) (August 24): 882. doi:10.1038/442882a.
- Verkade, H M, S J Bugg, H D Lindsay, A M Carr, and M J O'Connell. 1999. "Rad18 Is Required for DNA Repair and Checkpoint Responses in Fission Yeast." *Molecular Biology of the Cell* 10 (9) (September): 2905–18.
- Vora, M Mehul. 2011. "MicroRNA Modulation of Caenorhabditis Elegans Dietary Restriction and Longevity". State University of New Jersey.
- Wang, Bin, Shuhei Matsuo, Phillip B Carpenter, and Stephen J Elledge. 2002. "53BP1, a Mediator of the DNA Damage Checkpoint." *Science (New York, N.Y.)* 298 (5597) (November 15): 1435–8. doi:10.1126/science.1076182.
- Wang, Jin, Martin Haubrock, Kun-Ming Cao, Xu Hua, Chen-Yu Zhang, Edgar Wingender, and Jie Li. 2011. "Regulatory Coordination of Clustered microRNAs Based on microRNA-transcription Factor Regulatory Network." *BMC Systems Biology* 5 (1) (January): 199. doi:10.1186/1752-0509-5-199.
- Ward, Jordan D, Louise J Barber, Mark Ir Petalcorin, Judith Yanowitz, and Simon J Boulton. 2007. "Replication Blocking Lesions Present a Unique Substrate for Homologous Recombination." *The EMBO Journal* 26 (14) (July 25): 3384–96. doi:10.1038/sj.emboj.7601766.
- Ward, Jordan D, Diego M Muzzini, Mark I R Petalcorin, Enrique Martinez-Perez, Julie S Martin, Paolo Plevani, Giuseppe Cassata, Federica Marini, and Simon J Boulton. 2010. "Overlapping Mechanisms Promote Postsynaptic RAD-51 Filament Disassembly During Meiotic Double-strand Break Repair." *Molecular Cell* 37 (2) (January 29): 259–72. doi:10.1016/j.molcel.2009.12.026.
- Warf, M Bryan, W Evan Johnson, and Brenda L Bass. 2011. "Improved Annotation of C. Elegans microRNAs by Deep Sequencing Reveals Structures Associated with Processing by Drosha and Dicer." *RNA (New York, N.Y.)* 17 (4) (April): 563–77. doi:10.1261/rna.2432311.
- Wee, Liang Meng, C Fabián Flores-Jasso, William E Salomon, and Phillip D Zamore. 2012. "Argonaute Divides Its RNA Guide into Domains with Distinct Functions and RNA-binding Properties." *Cell* 151 (5) (November 21): 1055–67. doi:10.1016/j.cell.2012.10.036.
- Weidhaas, Joanne B, Imran Babar, Sunitha M Nallur, Phong Trang, Sarah Roush, Michelle Boehm, Erin Gillespie, and Frank J Slack. 2007. "MicroRNAs as Potential Agents to Alter Resistance to Cytotoxic Anticancer Therapy." *Cancer Research* 67 (23) (December 1): 11111–6. doi:10.1158/0008-5472.CAN-07-2858.
- Weidhaas, Joanne B, David M Eisenmann, Justin M Holub, and Sunitha V Nallur. 2006. "A Conserved RAS/mitogen-activated Protein Kinase Pathway Regulates DNA Damage-induced Cell Death Postirradiation in Radelegans." *Cancer Research* 66 (21) (November 1): 10434–8. doi:10.1158/0008-5472.CAN-06-2182.

- Weinert, T, and L Hartwell. 1989. "Control of G2 Delay by the Rad9 Gene of *Saccharomyces Cerevisiae*." *Journal of Cell Science. Supplement* 12 (January): 145–8.
- Wightman, B, I Ha, and G Ruvkun. 1993. "Posttranscriptional Regulation of the Heterochronic Gene Lin-14 by Lin-4 Mediates Temporal Pattern Formation in *C. Elegans*." *Cell* 75 (5) (December 3): 855–62.
- Wilkins, Courtney, Ryan Dishongh, Steve C Moore, Michael A Whitt, Marie Chow, and Khaled Machaca. 2005. "RNA Interference Is an Antiviral Defence Mechanism in *Caenorhabditis Elegans*." *Nature* 436 (7053) (August 18): 1044–7. doi:10.1038/nature03957.
- Wolters, Stefanie, and Björn Schumacher. 2013. "Genome Maintenance and Transcription Integrity in Aging and Disease." *Frontiers in Genetics* 4 (January 25): 19. doi:10.3389/fgene.2013.00019.
- Woodward, Anna M, Thomas Göhler, M Gloria Luciani, Maren Oehlmann, Xinquan Ge, Anton Gartner, Dean A Jackson, and J Julian Blow. 2006. "Excess Mcm2-7 License Dormant Origins of Replication That Can Be Used Under Conditions of Replicative Stress." *The Journal of Cell Biology* 173 (5) (June 5): 673–83. doi:10.1083/jcb.200602108.
- Wu, Jiaxue, Chao Liu, Junjie Chen, and Xiaochun Yu. 2012. "RAP80 Protein Is Important for Genomic Stability and Is Required for Stabilizing BRCA1-A Complex at DNA Damage Sites in Vivo." *The Journal of Biological Chemistry* 287 (27) (June 29): 22919–26. doi:10.1074/jbc.M112.351007.
- Wu, Nan, and Hongtao Yu. 2012. "The Smc Complexes in DNA Damage Response." *Cell & Bioscience* 2 (January): 5. doi:10.1186/2045-3701-2-5.
- Xia, Yan, Gerald M Pao, Hong-Wu Chen, Inder M Verma, and Tony Hunter. 2003. "Enhancement of BRCA1 E3 Ubiquitin Ligase Activity through Direct Interaction with the BARD1 Protein." *The Journal of Biological Chemistry* 278 (7) (February 14): 5255–63. doi:10.1074/jbc.M204591200.
- Xu, B, Kim St, and M B Kastan. 2001. "Involvement of Brca1 in S-phase and G(2)-phase Checkpoints after Ionizing Irradiation." *Molecular and Cellular Biology* 21 (10) (May): 3445–50. doi:10.1128/MCB.21.10.3445-3450.2001.
- Xu, Bo, Anne H O'Donnell, Seong-Tae Kim, and Michael B Kastan. 2002. "Phosphorylation of Serine 1387 in Brca1 Is Specifically Required for the Atm-mediated S-phase Checkpoint after Ionizing Irradiation." *Cancer Research* 62 (16) (August 15): 4588–91.
- Yacoub, A, J S Park, L Qiao, P Dent, and M P Hagan. 2001. "MAPK Dependence of DNA Damage Repair: Ionizing Radiation and the Induction of Expression of the DNA Repair Genes XRCC1 and ERCC1 in DU145 Human Prostate Carcinoma Cells in a MEK1/2 Dependent Fashion." *International Journal of Radiation Biology* 77 (10) (October): 1067–78. doi:10.1080/09553000110069317.
- Yager, James D, and Nancy E Davidson. 2006. "Estrogen Carcinogenesis in Breast Cancer." *The New England Journal of Medicine* 354 (3) (January 19): 270–82. doi:10.1056/NEJMra050776.
- Yang, Jr-Shiuan, Michael D Phillips, Doron Betel, Ping Mu, Andrea Ventura, Adam C Siepel, Kevin C Chen, and Eric C Lai. 2011. "Widespread Regulatory Activity of Vertebrate microRNA\* Species." *RNA (New York, N.Y.)* 17 (2) (February): 312–26. doi:10.1261/rna.2537911.
- Zhang, Junran. 2013. "The Role of BRCA1 in Homologous Recombination Repair in Response to Replication Stress: Significance in Tumorigenesis and Cancer Therapy." *Cell & Bioscience* 3 (1) (January): 11. doi:10.1186/2045-3701-3-11.

- Zhang, Xiaochang, Rebecca Zabinsky, Yudong Teng, Mingxue Cui, and Min Han. 2011. "microRNAs Play Critical Roles in the Survival and Recovery of *Caenorhabditis Elegans* from Starvation-induced L1 Diapause." *Proceedings of the National Academy of Sciences of the United States of America* 108 (44) (November 1): 17997–8002. doi:10.1073/pnas.1105982108.
- Zhao, H, and H Piwnica-Worms. 2001. "ATR-mediated Checkpoint Pathways Regulate Phosphorylation and Activation of Human Chk1." *Molecular and Cellular Biology* 21 (13) (July): 4129–39. doi:10.1128/MCB.21.13.4129-4139.2001.
- Zhao, Xiaolan, and Günter Blobel. 2005. "A SUMO Ligase Is Part of a Nuclear Multiprotein Complex That Affects DNA Repair and Chromosomal Organization." *Proceedings of the National Academy of Sciences of the United States of America* 102 (13) (March 29): 4777–82. doi:10.1073/pnas.0500537102.
- Zuryn, Steven, Stéphanie Le Gras, Karine Jamet, and Sophie Jarriault. 2010. "A Strategy for Direct Mapping and Identification of Mutations by Whole-genome Sequencing." *Genetics* 186 (1) (September): 427–30. doi:10.1534/genetics.110.119230.

Ich versichere, dass ich die von mir vorgelegte Dissertation selbständig angefertigt, die benutzten Quellen und Hilfsmittel vollständig angegeben und die Stellen der Arbeit – einschließlich Tabellen, Karten und Abbildungen –, die anderen Werken im Wortlaut oder dem Sinn nach entnommen sind, in jedem Einzelfall als Entlehnung kenntlich gemacht habe; dass diese Dissertation noch keiner anderen Fakultät oder Universität zur Prüfung vorgelegen hat; dass sie – abgesehen von angegebenen Teilpublikationen – noch nicht veröffentlicht worden ist sowie, dass ich eine solche Veröffentlichung vor Abschluss des Promotionsverfahrens nicht vornehmen werde. Die Bestimmungen der Promotionsordnung sind mir bekannt. Die von mir vorgelegte Dissertation ist von Dr. Björn Schumacher betreut worden.

.....